Manipulation of the dopaminergic system in the fruit fly *Drosophila melanogaster* as a tool to model Parkinson's disease

Dissertation

in fulfilment of the requirements for the degree "Dr. rer. nat."

of the Faculty of Mathematics and Natural Sciences

at Kiel University

submitted by

Flora Stephano

Kiel, 2013

First referee:	Prof. Dr. Thomas Roeder
Second referee:	Prof. Dr. Holger Heine
Date of the oral examination:	19.9.2013
Approved for publication:	19.9.2013
Dean:	Prof. Dr. Wolfgang J. Duschl

To Almighty God, to whom nothing is impossible

and

to my late grandfather Stephano Nyaki in his loving memory and late Prof. A.M. Nikundiwe my first mentor

TABLE OF CONTENTS

Table of contents

Table of contents

Table of contents

LIST OF TABLES

LIST OF FIGURES

List of figures

SUMMARY

Dopamine is an intercellular messenger in both vertebrates and invertebrates. It exerts its physiological functions by binding to specific dopamine receptors. Dopaminergic systems in mammals control several important physiological functions ranging from voluntary movement and reward to general aspects of hormonal regulation and the regulation of blood pressure to name only few. Alterations in the dopaminergic system have been associated with several psychiatric and neurological disorders such as Schizophrenia and Parkinson's disease (PD). On the contrary, the dopaminergic system in *Drosophila* is not well characterized. For this, characterization of the dopaminergic system in normal flies before further analyses was a basis of this study. The aim was to elucidate the expression patterns of dopamine receptors in the central nervous system (CNS) and the digestive tract and to analyze the function of these receptors at cellular and/or behavioral level in *Drosophila*. With this respect, I used immunohistochemical, RNAi, overexpression and pharmacological approaches. The findings from this part of study were striking. A wide distribution of four dopamine receptors present in *Drosophila* was apparent in the CNS and in the digestive tract. In the CNS, one receptor, DopR, was localized in dopamine producing cells, which suggests an auto-receptor function of this receptor at least in this subset of dopamine producing cells. More importantly, two receptors; DopR and DopR2 where localized in a subset of clock neurons that expresses the neuropeptide PDF (pigment dispersing factor) indicative for the hypothesis that these receptors control circadian rhythms in *Drosophila melanogaster*. Localization was also observed in higher order brain structures such as mushroom bodies and the central complex, regions that are implicated in controlling of learning/memory and locomotion, respectively. In the digestive tract, dopamine receptors were distributed differently in the major cells of the midgut. The wide distribution of dopamine receptors in neurons and non-neuronal tissues provides insights into the roles played by these receptors in controlling different physiological functions and behaviors in the fruit fly.

Advanced age is a major risk factor for many neurodegenerative disorders including Parkinson's disease Preventing or stopping the development of this neurological disorder and the search for alternative treatment strategies is a major scientific challenge. Both genetic and environmental factors seem to contribute to PD development. Unfortunately, clinically relevant symptoms of PD appear when degeneration of the nigrostriatal dopamine producing (DA) neurons is at an advanced stage. For this reason, the second aim of this study focused on elucidating molecular responses involved during the asymptomatic phase of PD in-order to identify potential targets for therapeutic intervention. I used the pesticide rotenone to induce Parkinsonism in *Drosophila melanogaster.* Moreover, rotenone-induced Parkinsonism was combined with a focused transcriptomic analysis of DA neurons. This study provides evidences that the outcome of various highly relevant signaling pathways is modified in the dopamine producing neurons that are in an early stage of PD. Amongst these affected systems are the Wnt-, MAPK/EGFR-, TGF-β-, and TOR-signaling pathways, which are known to be important for cell survival and/or cell death in the CNS. Thus, further studies involving these pathways may provide new insights into the molecular events underlying pathogenesis and, hopefully, lead to the identification of new potential targets for neuroprotective interventions for PD.

Lastly, this study focused on the development of alternative therapeutic strategies for treatment of PD. In this, I tested whether modulation of intracellular second messenger systems by employing so-called DREADD (Designer Receptors Exclusively Activated by Designer Drugs) receptors in DA-producing neurons during rotenone treatment can prevent or delay development of the disease phenotype. Manipulation of these second messenger systems (cAMP or Ca^{2+}) in DA-producing neurons did not prevent development of the disease phenotype induced by rotenone in the *Drosophila* model of PD.

ZUSAMMENFASSUNG

Dopaminerge Systeme steuern verschiedene wichtige physiologische Funktionen in Säugetieren wie die spontane Bewegung, Belohnung sowie generelle Aspekte der hormonellen Regulation und der Steuerung des Blutdrucks. Funktionsstörungen des dopaminergen Systems wurden mit verschiedenen psychatrischen und neurologischen Störungen wie Schizophrenie und Parkinson in Verbindung gebracht.

Da das dopaminerge System von *Drosophila* noch nicht sehr gut erforscht ist, war das grundlegende Ziel dieser Arbeit, das Expressionsmuster der Dopaminrezeptoren im Zentralnervensystem (ZNS) und im Gastrointestinaltrakt sowie deren Funktionen auf zellulärer und/oder verhaltensbiologischer Ebene zu untersuchen. Hierfür habe ich immunhistochemische und pharmakologische Ansätze sowie RNA-Interferenz und Überexpression verwendet. Die Ergebnisse dieser Untersuchungen waren beachtlich. Die vier Dopaminrezeptoren von *Drosophila* zeigten eine weite Verbreitung im ZNS und im Gastrointestinaltrakt. Im ZNS wird der Rezeptor DopR in DA-Neuronen exprimiert, was auf eine Autorezeptorfunktion schließen lässt. Darüber hinaus wurden DopR und DopR2 in einer Gruppe von Zeitgeber-Neuronen gefunden, die das Neuropeptid PDF (*pigment dispersing factor*) exprimieren. Dies deutet daraufhin, dass diese Rezeptoren den circadianen Rhythmus von *Drosophila* melanogaster steuern. Die Rezeptoren wurden außerdem in übergeordneten Strukturen wie den Pilzkörpern bzw. dem Zentralkomplex, Regionen, die an der Steuerung von Lernen und Gedächtnis bzw. der Bewegung beteiligt sind, detektiert. Im Gastrointestinaltrakt zeigten die Rezeptoren unterschiedliche Expressionsmuster in den verschiedenen Zelltypen des Mitteldarms. Die weite Verbreitung der Dopaminrezeptoren in Neuronen und nicht neuronalen Geweben liefert Hinweise auf die Beteiligung dieser Rezeptoren an der Steuerung physiologischer Funktionen und Verhaltensweisen in der Taufliege.

Der größte Risikofaktor für Parkinson und viele andere neurodegenerative Erkrankungen ist fortgeschrittenes Alter. Es stellt eine große Herausforderung für die Wissenschaft dar, das Auftreten dieser neurologischen Störung mithilfe alternativer Behandlungsmethoden zu verhindern oder deren Entwicklung aufzuhalten.

An der Ätiologie von Parkinson scheinen genetische sowie Umweltfaktoren beteiligt zu sein. Leider treten die klinischen Symptome der Erkrankung erst auf, wenn die Degeneration der nigrostriatalen Dopamin-produzierenden Neurone (DA-Neurone) bereits fortgeschritten ist. Deshalb war das nächste Ziel dieser Arbeit, die molekularen Mechanismen aufzuklären, die während der asymptomatischen Phase zur Entwicklung von Parkinson beitragen, um potentielle Zielstrukturen für therapeutische Interventionen zu identifizieren. Ich habe das Pestizid Rotenon verwendet, um in *Drosophila melanogaster* Parkinson zu induzieren. Mithilfe dieses Modells war es möglich, das Tanskriptom der DA-Neurone zu analysieren. Die Ergebnisse dieser Untersuchung zeigen, dass verschiedene relevante Signalwege in der frühen Phase der Erkrankung moduliert werden. Unter diesen finden sich der Wnt-, MAPK/EGFR-, TGF-β- sowie der TOR-Signalweg, die wichtige Funktionen bei der Steuerung von Zellüberleben und -tod im Zentralnervensystem (ZNS) haben. Die genauere Untersuchung der identifizierten Signalwege kann neue Einblicke in die molekularen Ereignisse, die der Pathogenese zugrunde liegen, geben und helfen, neue potentielle Ziele für therapeutische Interventionen zu identifizieren.

Ein dritter Hauptaspekt der Arbeit beschäftigte sich mit der Entwicklung alternativer Therapiestrategien von Parkinson. Hierbei habe ich untersucht, ob die Modulation verschiedener intrazellulärer *second messenger*-Systeme in DA-Neuronen die Entwicklung des Krankheitsbildes verhindern oder verzögern kann. Die *second messenger*-Systeme wurden mithilfe von sogenannten DREADD-Rezeptoren *(Designer Receptors Exclusively Activated by Designer Drugs)* während der Rotenon-Behandlung manipuliert. Die Modulation der *second messenger*-Systeme (cAMP oder Ca^{2+}) in DA-Neuronen verhinderte die Entwicklung des Krankheits-Phänotyps im *Drosophila*-Modell von Parkinson nicht.

.

LIST OF ABBREVIATIONS

AC	Adenylate cyclase
bp	base pairs
CaMKII	Ca^{2+}/Calmodulin-dependent protein kinase II
cAMP	Cyclic adenosine monophosphate
cc	central complex
Cdk5	Cyclin-dependent kinase 5
cDNA	complementary Deoxyribonucleic acid
CNO	Cloxapine-N-Oxide
CNS	central nervous system
CREB	cylic AMP response element binding protein
DA	Dopamine
DAG	Diacylglycerol
DAM	Drosophila Activity Monitor
DARPP-32	Dopamine and cyclic AMP-regulated phosphoprotein
DAVID	Database for Annotation, Visualization and Intergrated Discovery
DD	constant darkness
DMSO	Dimethyl sulfoxide
DNA	Deoxyribonucleic acid
dNTP	Deoxyribonucleotide triphosphate
DREADD	Designer Receptors Exclusively Activated by a Designer Drug
Epac	exchange proteins activated by cAMP
ERK	Extracellular regulatory kinase
F1	First generation
Fig.	Figure

fwd	Forward
g	gram
GFP	Green Fluorescent Protein
GPCR	G-protein-coupled receptor
Gαi	Gi-alpha subunit
Gαs/olf	G_s-alpha subunit
H_2O	Water
HL3	hemolymph-like 3 saline
HPLC	high pressure liquid chromatography
hrs	hours
IP3	Inositol-1,4,5-triphosphate
JNK	c-Jun amino-terminal kinase
KEGG	Kyoto Encyclopedia of Genes and Genomes
LD	Light/Dark
L-DOPA	Levodopamine
LRRK2	Leucine-rich repeat kinase 2
MAPK	Mitogen-activated protein kinase
mb	mushroom bodies
ml	milliliter
NMDA	N-methyl-D-aspartate
ns	not significant
PBS	Phosphate buffered saline
PCR	Polymerase Chain Reaction
PINK1	PTEN-induced-putative kinase 1
PIP2	Phosphotidylinositol-4,5-biphosphate
PKA	Protein kinase A

PKC	Protein kinase C
PMAT	Plasma membrane monoamine transporter
PP1	Protein phosphatase 1
PP2B	Protein phosphatase 2B
qRT-PCR	Quantitative real time PCR
rev	Reverse
RNA	Ribonucleic acid
RNAi	Ribonucleic acid interference
RT	Room Temperature
sec	second
TBE	Tris/Borate/EDTA
TH	Tyrosine hydroxylase
TRITC	Tetramethyl rhodamine isothiocyanate
UAS	Upstream Activation Sequence
UCH-L1	Ubiquitin carboxyl-terminal esterase L1
VMAT2	Vesicular monoamine transporter 2
x-g	x-fold gravity
ZT	*Zeitgeber*

1 INTRODUCTION

1.1 OVERVIEW OF THE DOPAMINERGIC SYSTEM IN MAMMALS

1.1.1 DOPAMINE NEUROTRANSMISSION

Dopamine (DA) is a catecholamine neurotransmitter, which controls several important physiological functions ranging from voluntary movement and reward to hormonal regulation and hypertension. DA was first synthesized in 1910 by George Borger and James Ewens at the Wellcome Laboratories in London, England. It was named dopamine because it is a monoamine whose precursor is levodopamine (L-DOPA). In 1958, Arvid Carlsson and Nils-AkeHillarp were the first to recognize DA functions as a neurotransmitter. Carlsson was awarded the 2000 Nobel Prize in Physiology or Medicine for showing that dopamine is not only a precursor of norepinephrine (noradrenaline) and epinephrine (adrenaline), but also a neurotransmitter.

Dopamine is produced in several areas of the brain including the *Substantia nigra* and the ventral tegmental area. It is also synthesized in non-neuronal cells such as the adrenal glands' medulla. DA is synthesized from the amino acid L-Tyrosine, which is consumed from dietary proteins. L-Tyrosine is converted into L-DOPA by the enzyme tyrosine hydroxylase (TH) with tetrahydrobiopterin, O_2, and ferrous ion (Fe^{2+}) as cofactors. In turn, L-DOPA is converted into dopamine by the enzyme aromatic amino acid decarboxylase (AAAD also known as DOPA decarboxylase (DDC) with pyridoxal phosphate as cofactor. Upon synthesis, DA is transported into synaptic vesicles by the vesicular monoamine transporter 2 (VMAT2). In these vesicles DA is stored until an action potential occurs and forces them to merge with the cell membrane by exocytosis, thereby releasing DA into synapses. Once in the synaptic cleft, DA binds and activates postsynaptic dopamine receptors to propagate a pre-synaptic signal to the postsynaptic neuron. DA also binds to pre-synaptically located dopamine receptors called autoreceptors, which inhibit neurotransmitter synthesis and release. They serve to keep DA levels normalized. Following the transmission of the signal, DA is transported back either through high affinity DA transporter (DAT) or low-affinity plasma membrane monoamine transporter (PMAT).

1.1.2 DOPAMINE RECEPTORS CLASSIFICATION AND EXPRESSION

DA exerts its physiological action by binding to specific dopamine receptors. These receptors are G-protein coupled receptors (GPCRs), whose signaling is primarily mediated by interaction with, and activation of heterotrimeric GTP-binding proteins (G-proteins) (Neve et al., 2004). The contributions of Kobilka and Lefkowitz, the winners of Nobel prize in Chemistry 2012, on studies of GPCR signaling provided evidences that GPCRs signal in a G-protein dependent manner and/or a G-protein independent manner. The latter mechanism depends on other regulatory proteins such as arrestins (Lefkowitz and Shenoy, 2005).

In mammals, five distinct subtypes of DA receptors have been isolated, characterized and subdivided into two major classes; D1- and D2-like, on the basis of their structural, pharmacological and biochemical properties. D1-class receptors comprise of D1 and D5, which stimulate Gαs/olf proteins to stimulate cAMP production by adenylate cyclase (AC) (Herve et al., 1993). In contrast, D2-class receptors (D2, D3 and D4) couple to Gαi and thus induce inhibition of AC (Missale et al., 1998, Vallone et al., 2000, Neve et al., 2004, Beaulieu and Gainetdinov, 2011).

Dopamine receptors have broad expression patterns in the brain and in the periphery. In the brain, D1-dopamine receptors are expressed at highest levels in the nigrostriatal, mesolimbic, mesocortical areas such as caudate-putamen (striatum), *Nucleus accumbens*, olfactory bulb, frontal cortex, cerebellum, thalamic and hypothalamic areas. On the other hand, D2-dopamine receptors are abundant in the striatum, the *Nucleus accumbens*, and the olfactory tubercle. D2 receptors are also expressed at significant levels in the *Substantia nigra*, ventral tegmental area, cortical areas, amyglada and hippocampus. In the periphery, all subtypes of DA receptors have been observed in the kidney, adrenal glands, gastrointestinal tract, blood vessels and heart (Missale et al., 1998, Sokoloff et al., 2006, Iversen and Iversen, 2007, Rondou et al., 2010, Beaulieu and Gainetdinov, 2011).

1.1.3 DOPAMINE RECEPTOR SIGNALING MECHANISMS

As pointed out earlier, the D1-class receptors couple primarily to the stimulatory G-protein, Gαs/olf and stimulate the production of the second messenger cAMP. At its active state, Gαs/olf binds and activates AC, the enzyme, which catalyzes the conversion of ATP to cAMP, which in turn activates the protein kinase A (PKA). Protein kinase A then phosphorylates and regulates the downstream substrates including the 32-kDA dopamine and cAMP regulated phosphoprotein (DARPP-32), the transcription factor CREB, the ionotropic glutamate receptors (AMPA and NMDA) and certain voltage gated ion channels. The DARPP-32 is a multifunctional signal transduction molecule enriched in medium spiny neurons in the striatum (Missale et al., 1998, Neve et al., 2004, Beaulieu and Gainetdinov, 2011). It inhibits PP1 (protein phosphatase 1) activity when phosphorylated at threonine 34 by PKA and is converted to a PKA inhibitor when phoshorylated at threonine 75 by cyclin-dependent kinase 5 (Cdk5) (Bibb et al., 1999).

Several reports have described D1-class receptors activation of mitogen-activated protein (MAP) kinases including ERK (extracellular regulatory kinase) (Gerfen, 2003), p38 MAP kinase and c-Jun amino-terminal kinase (JNK) (Zhen et al., 1998). Regulation of the latter two MAP kinase pathways are mediated by PKA, whereas D1-like receptor activation of ERK may be partially independent of PKA or cAMP. One possible PKA-independent but cAMP-dependent mechanism for activation of ERK by D1-class receptors is activation of Rap GTPase by guanine nucleotide exchange factor directly activated by cAMP, Epac (de Rooij et al., 1998, Neve et al., 2004).

In contrast to D1-class receptors, D2-class receptors are coupled to Gαi that negatively regulate the production of cAMP resulting in decrease in PKA activity (Kebabian and Greengard, 1971, Kebabian and Calne, 1979, Beaulieu and Gainetdinov, 2011) (Fig. 1)

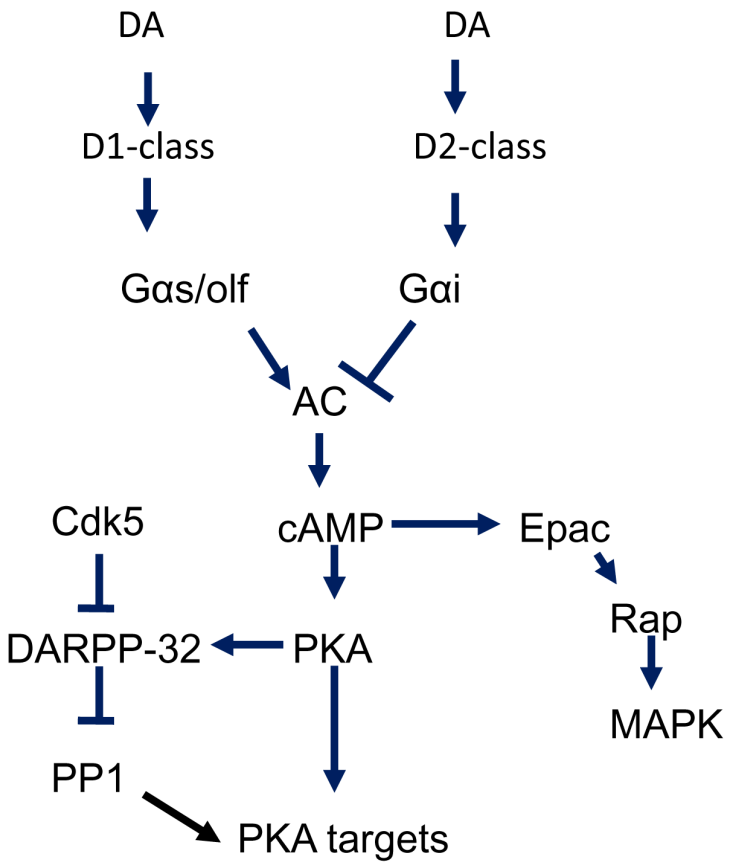

Figure 1: Signaling networks regulated by dopamine in D1 and D2-class dopamine receptor responding neurons. D1-class through Gαs/olf stimulates cAMP/PKA signaling while D2-class through Gαi inhibits it. Blue arrows indicate activation, blue-T arrows indicate inhibition, and black arrow indicates actions that can be either activating or inhibitory on the function of specific substrates. Based on Neve et al., 2004, Beaulieu and Gainetdinov, 2011.

In addition to their effects on cAMP-regulated signaling, D1-like receptors, particularly the D5 receptor couples to Gαq to regulate phospholipase C (PLC) (Fig. 2). Upon activation, PLC cleaves phosphotidylinositol-4,5-biphosphate (PIP_2) into two second messengers, inositol triphosphate (IP_3) and diacylglycerol (DAG). The latter remains on the plasma membrane and activates protein kinase C (PKC) that phosphorylates downstream substrates. On the other hand, IP_3 diffuses into the cytoplasm and binds to the IP_3 receptor in the endoplamic reticulum thereby mobilizing intracellular calcium. Calcium in turn activates calcium-dependent proteins such as protein phosphatase 2B (calcineurin) and Ca^{2+}/calmodulin-dependent protein kinase II (CaMKII) and PKC (Fig. 2).

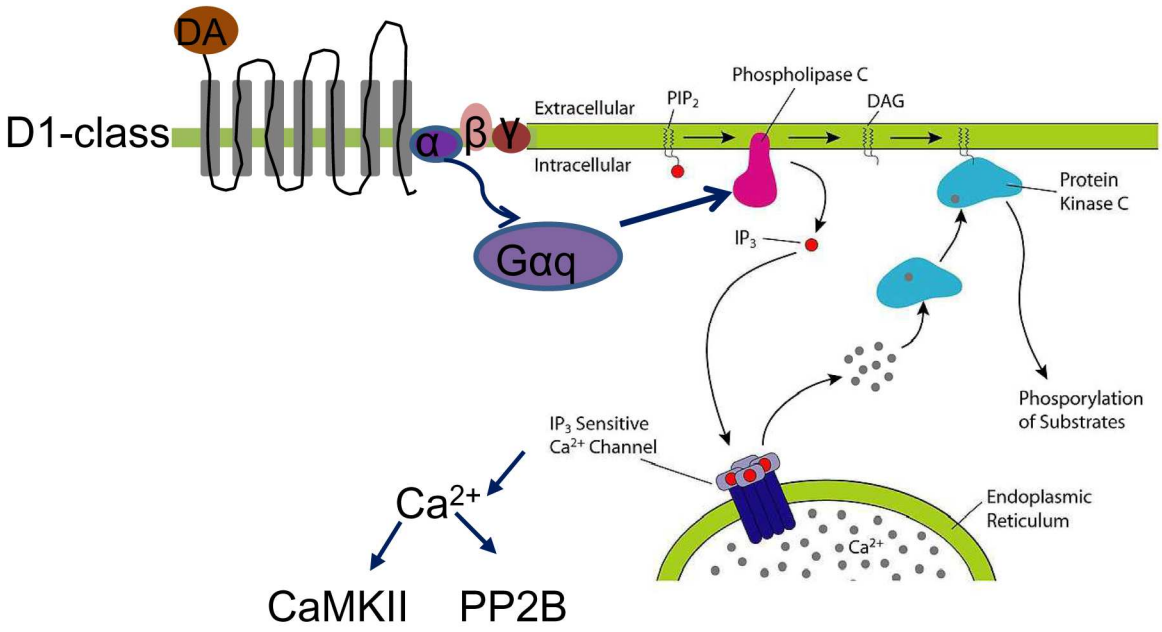

Figure 2: Regulation of Gαq/PLC signaling by D1-class dopamine receptors. Upon activation, PLC cleaves PIP_2 to IP_3 and DAG that initiate intracellular calcium release and PKC activation. Blue and black arrows indicate activation. Modified from: http://eb.wikipedia.org/wiki/Inositol-1,4,5-triphosphate.

The D2-like receptors also regulate PLC-pathways through Gβγ-subunits. Several evidences have shown that activation of D2-like receptors through Gβγ stimulate MAP kinase pathways such as ERK. These mechanisms are at least mediated by transactivation of a receptor tyrosine kinase (RTK), thus recruiting the RTK-signaling cascade in response to DA (Neve et al., 2004).

1.1.4 FUNCTIONS OF DOPAMINE RECEPTORS

The functional roles of the different DA receptors have been extensively characterized. The most studied role involves the effects of DA on locomotor activity. Several lines of evidence indicate that locomotor activity is primarily controlled by D1, D2, and D3 dopamine receptors. Activation of D1 dopamine receptors that are exclusively expressed on the postsynaptic neurons has a moderate stimulatory effect on locomotor activity. On the contrary, presynaptically localized autoreceptors, D2-class, generally provide an important negative feedback mechanism that adjusts neuronal firing rate, synthesis and release of the neurotransmitter levels in response

to changes in extracellular neurotransmitter levels. Generally, activation of D2-class autoreceptors causes a decrease in DA release that results in decreased locomotor activity, whereas activation of postsynaptic receptors stimulates locomotion. D2 in particular, is present in two splice variants, D2-long (D2L) and D2-short (D2S) (Giros et al., 1989, Monsma et al., 1989). D2S is predominantly found presynaptically and D2L postsynaptically. D3 dopamine receptors seem to exert a moderate inhibitory action on locomotion either by acting as autoreceptors or through the involvement of postsynaptic receptor populations. The roles of D4 and D5 dopamine receptors, which have a limited expression pattern in the primary motor regions of the brain, are involved in control of movement to much lesser extents. Therefore, activation of both the postsynaptic D1 and D2-class DA receptors is necessary for the full manifestation of dopamine induced locomotor activity (Missale et al., 1998, Sokoloff et al., 2006, Rondou et al., 2010, Beaulieu and Gainetdinov, 2011).

Dopamine receptors are also involved in other vital functions. D1, D2 and, to lesser extent, D3 are critically involved in reward and reinforcement mechanisms. Alterations of DA receptors by pharmacological and genetic approaches have shown a significant modulation of the responses to natural rewards and addictive drugs (Missale et al., 1998, Sokoloff et al., 2006, Beaulieu and Gainetdinov, 2011, Blum et al., 2012). Moreover, both D1 and D2 dopamine receptors have been shown to be critical for learning and memory. Parallel with this, D3 and D4 and potentially D5 receptors seem to have a minor modulatory influence on some aspects of cognitive functions that are mediated within the hippocampus (Missale et al., 1998, Beaulieu and Gainetdinov, 2011, Xu et al., 2012). Other functions mediated by DA receptors that are localized outside the CNS include: olfaction, vision, and hormonal regulation such as pituitary D2 dopamine receptor-mediated regulation of prolactin secretion; kidney D1 dopamine receptor-mediated rennin secretion; adrenal gland D2 regulation of aldosterone secretion; the regulation of sympathetic tone; D1, D2 and D4 receptors-mediated regulation of vasodilation; renal function; blood pressure regulation; and gastrointestinal motility (Aperia, 2000, Witkovsky, 2004, Li et al., 2006, Beaulieu and Gainetdinov, 2011). The fact that dopamine and its receptors are involved in a variety of critical functions, it is not surprising that multiple human disorders such as Schizophrenia, Attention Deficit Hyperactivity Disorder, drug

addiction and PD have been related to dopaminergic dysfunctions. The most recognized dopamine-related disorder is PD.

1.2 PARKINSON'S DISEASE

Parkinson's disease is the second most prevalent neurodegenerative disorder with an incidence of about 1% in people older than 65 years (Whitworth, 2011). Pathologically, the disease is characterized by a selective and progressive loss of dopaminergic (DA) neurons and the presence of Lewy bodies in the neurons of the *Substantia nigra pars compacta* (Forno, 1996). PD is typically recognized by the classical motor system disturbances such as bradykinesia, resting tremor, rigidity and postural instability. In addition to motor dysfunction, PD patients also suffer from non-motor symptoms such as constipation, sleep disorder and at an advanced stage, dementia and cognitive dysfunction (Whitworth, 2011, Xu et al., 2012). There are two forms of PD; a rare heritable form due to mutations in certain genes and a sporadic form mainly of idiopathic causes. Unfortunately, the majority of cases occur sporadically. Generally, it is considered that both genetic susceptibility and environmental factors play a role in pathogenesis. Despite of extensive studies, there is currently no cure or treatment that can stop disease progression. While the precise pathologic mechanisms remain unclear, epidemiological and genetic studies have begun to obtain insights into causes underlying pathogenesis. Currently, the favored mechanisms include mitochondrial dysfunction, calcium imbalance, aberrant protein degradation and inflammation. In addition, oxidative stress is a prominent and common feature in all forms of PD and likely represents a convergent toxin event leading to neuronal cell death (Gupta et al., 2008).

Due to ethical and technical reasons in using human as experimental system, animal models are the major tools for studying PD pathogenesis. Vertebrate models have been used in the PD field for many years. They include non-human primates, rodents (mice and rats), zebrafish, frogs, and chickens with rodent models predominating the field. However, rodent models, especially murine ones do not recapitulate the human disease pathology, especially regarding the final aspects of the pathology, the dying of dopaminergic cells (Dawson et al., 2010). Thus,

alternative models, including very simple ones may have a substantial relevance for future research.

A *Drosophila* model to study basic aspects of PD was introduced more than a decade ago (Feany and Bender, 2000). Targeted overexpression of normal and mutant forms of the human protein alpha synuclein induces symptoms typically seen in human PD patients. These include the development of Lewy-body like filamentous intraneuronal inclusions and the adult-onset loss of DA neurons. Not only alpha-synuclein, but also other PD susceptibility genes have been characterized in *Drosophila* models of the disease (Bilen and Bonini, 2005, Lessing and Bonini, 2009, Whitworth, 2011). In addition, a very simple, pharmacologically induced PD model, dependent on the pesticide rotenone has been introduced in flies and triggers DA neuron degeneration leading to a drastically impaired climbing ability (Coulom and Birman, 2004). Surprisingly to some, *Drosophila* models have replicated many pathological processes related to human neurological disorders (Zoghbi and Warren, 2010, Guo, 2012).

1.3 ADVANTAGES OF USING DROSOPHILA AS A MODEL ORGANISM

D. melanogaster, commonly referred to as fruit fly, was first used for genetic experiments more than a century ago by William Ernest Castle and his colleagues, who studied inbreeding and selection, the work which was published in 1906. It was through Castle's influence that *D. melanogaster* became known to geneticists, most notably to T. H. Morgan, and work with this species became the basis of Morgan's 1933 Nobel Prize in Medicine for identifying chromosomes as the vector of inheritance for genes (Snell and Reed, 1993). Since that, *Drosophila* has been used extensively for investigating fundamental biological processes such as cell proliferation, growth, cell death and migration. In addition, behavioral studies have shown that *Drosophila* can perform complex behaviors such as learning and memory, circadian rhythms, sleep and aggression (Bellen et al., 2010), some of which were first assumed to be exclusively performed by mammals/humans. Therefore, these studies from more than a century coupled with the versatility and rapidity of techniques have left the modern fly field with powerful molecular genetics

tools (Adams and Sekelsky, 2002, Venken and Bellen, 2005, Venken and Bellen, 2007).

Drosophila has a short generation time of approx. 10-12 days at 25 °C and an average life span of 50-60 days. The fly genome has been completely sequenced and annotated (Adams et al., 2000). It requires little labor and is cost effective to maintain fly stocks. Mutant flies and transgenic ones are available from public stock centers at low cost and only small space is required for their maintenance. Importantly, it has been estimated that nearly 75 % of all human disease associated genes are conserved in *D. melanogaster* (Bier, 2005). In particular, the *Drosophila* genome encodes the currently identified PD-related genes *LRRK2/Dardarin, parkin, PINK1, Omi/HtrA2, DJ-1, UCH-L1, GIGYF2, PLA2G6, and GBA* (Whitworth et al., 2006, Gupta et al., 2008, Whitworth, 2011). This set of features makes *D. melanogaster* an excellent model system to study the functions of disease genes *in vivo* including those involved in neurodegenerative disorders such as PD and to dissect genetic pathways related to these disease genes.

There are several tools available in *Drosophila* but I will only mention those that are relevant to disease models particularly to PD and that were used in this study. One particularly powerful approach is the transposon-mediated transgenesis (Rubin and Spradling, 1982). The fly community has generated a number of transposon insertion lines that can be used for insertional mutagenesis in *Drosophila*. Another powerful and versatile approach in *Drosophila* is the GAL4/UAS system. It is a bipartite transcription activation system (Brand and Perrimon, 1993), which allows a gene of choice to be expressed in a defined set of cells or tissue of interest. In this system, one transgene consists of a yeast transcriptional factor (GAL4), driven by a tissue specific promoter such as the dopaminergic neuron-specific tyrosine hydroxylase (TH) one. The second transgene consists of a gene of interest that is under the control of the UAS (upstream activation sequence), which drives transcription in response to GAL4 binding. This could be for example a reporter gene such as green fluorescent protein (GFP) or an RNAi gene (Fig. 3). RNAi stands for RNA interference. This is another highly favorable approach in *Drosophila* to knock down the gene of interest (Kalidas and Smith, 2002). This approach capitalizes on the finding that double stranded RNA (ds-RNA) molecules corresponding in sequence to

endogenous transcripts can trigger the degradation of the endogenous transcripts. It requires the construction of a transgenic construct bearing an inverted repeat sequence corresponding to the target transcript (Whitworth, 2011, Guo, 2012). This, in combination with the GAL4/UAS system to target expression of the dsRNA to the desired tissue, can simply be achieved by performing the appropriate cross (Fig. 3).

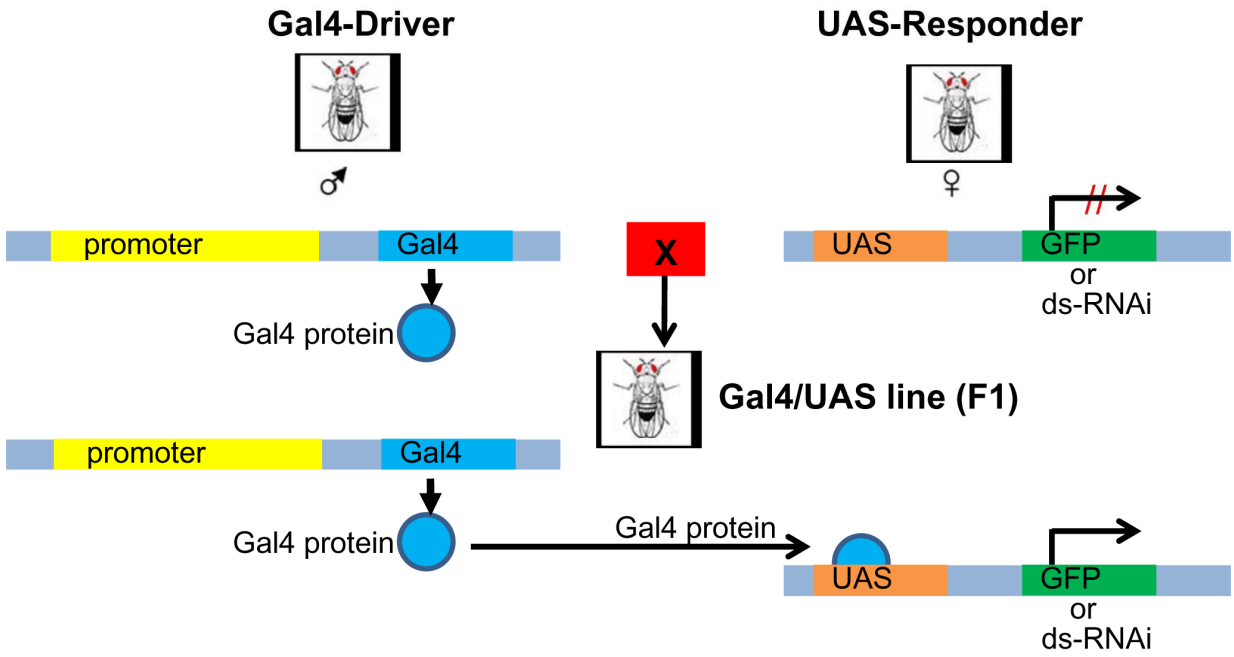

Figure 3: GAL4/UAS system. The system is used for overexpression or silencing of a gene of interest in *Drosophila*.The transcript of the targeted gene will be expressed in the F1 generation (GAL4/UAS progeny) only in those tissues/cells where GAL4 is present.

1.4 THE DOPAMINERGIC SYSTEM IN DROSOPHILA

The *Drosophila* nervous system contains approximately 100,000 neurons including a subset of approximately 200 DA neurons. Although the anatomy of the fly brain and distribution of DA neurons in the *Drosophila* CNS differs from that of the vertebrate brain, previous work indicated that many fundamental cellular and molecular biological features of neuronal development and function are conserved between vertebrates and invertebrates (Whitworth, 2011). Thus, this conservation again makes *Drosophila* a powerful system for cell biological studies of neuronal dysfunction.

In *Drosophila,* likewise, four dopamine receptors have been isolated and pharmacologically characterized, leading to a subdivision into the two subtypes D1- and D2-like receptors. D1-like receptors that activate cAMP comprise the DopR, the DopR2 and the dopamine/ecdysteroid receptor-DopEcR (Gotzes et al., 1994, Sugamori et al., 1995, Feng et al., 1996, Han et al., 1996, Srivastava et al., 2005), while the D2-like subtype consists of only one member, the D2R/DD2R (Hearn et al., 2002).

Spatial expression patterns in the CNS have been described (Kim et al., 2003, Draper et al., 2007) based on immunoreactivity using the antibodies against DopR, DopR2 and D2R. Comparison of DopR and DopR2 immunoreactivities showed overlapping, yet distinct, expression patterns in the mushroom bodies (mb) and the central complex (cc) (Kim et al., 2003). Studies using genetic and pharmacological manipulations revealed the mb to be involved in higher order brain function such as learning and memory as reviewed in Kim and colleagues (Kim et al., 2003, Rahn et al., 2013). In addition, appetitive and olfactory learning was impaired in dopamine receptor mutants (Selcho et al., 2009). The cc has been implicated in controlling motor functions such as movement (Strauss, 2002) and functional ethanol tolerance (Scholz et al., 2000, Kong et al., 2010). Lebestky and colleagues reported that a loss-of-function mutation in DopR leads to a decrease in sleep-wake arousal (Lebestky et al., 2009). It has also been reported that DopR is essential to control temperature preference behaviors through αβ lobes of mb (Bang et al., 2011). The

D2R was shown to be expressed in the cell groups that include the Ap-let cohort of peptidergic neurons (Draper et al., 2007) and more recently, qPCR analysis revealed that DopR, D2R and DopEcR are expressed in the Gr5a Gustatory Receptor Neurons (Inagaki et al., 2012b).

1.5 BASIC ANATOMY OF LARVAL AND ADULT DROSOPHILA CNS

The anatomy of the larval and adult fly CNS has been analyzed and several nomenclature systems exist. In this study, I used a simplified larval nomenclature system as described by Selcho and colleagues (Selcho et al., 2009). To locate the different types of neurons and their processes in the brain, they divided each hemisphere into four subregions; dorsomedial protocerebrum, dorsolateral protocerebrum, basomedial protocerebrum and basolateral protocerebrum separated by the mb region (Fig. 4A). To ease comparison with the adult brain this nomenclature is based on the body-axis of the larva. This terminology does not reflect the flattening of the CNS during mounting and therefore ignores its 90° rotation near the intersection between subesophageal ganglion (sog) and ventral nerve cord (vnc) (dashed line in Fig. 4A). Cell clusters are delineated according to the position they occupy in the CNS, e.g. in the larval brain hemispheres, DM (dorsomedial), DL1 (dorsolateral 1), and DL2 (dorsolateral 2). In the sog, the two anteromedial clusters are SM1 and SM2, respectively and a more lateral cluster SL (Fig. 4B).

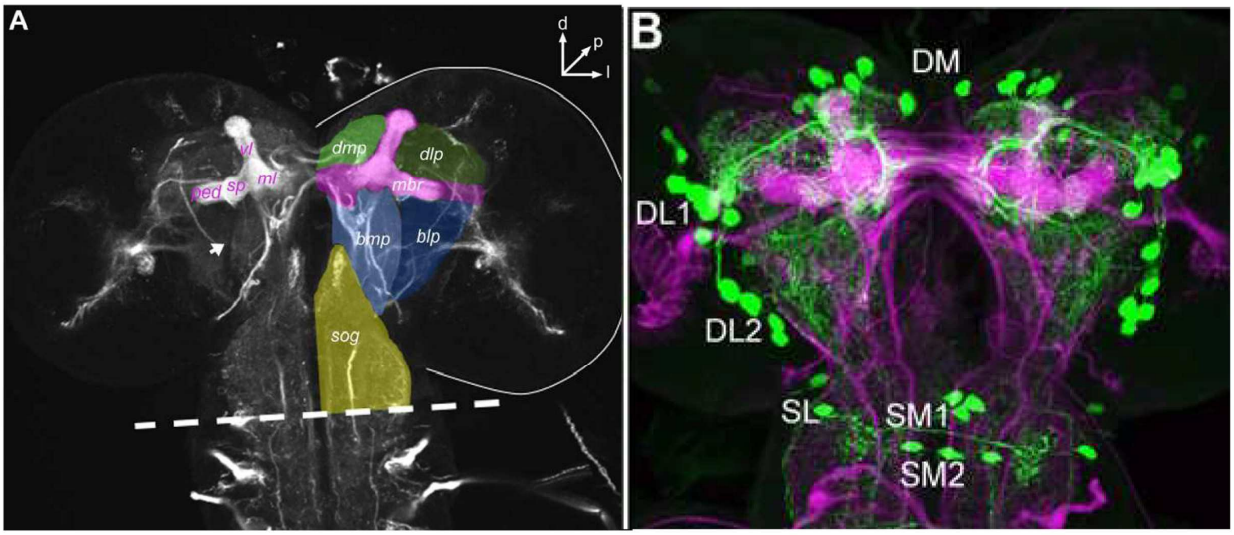

Figure 4: Anatomy and nomenclature of the larval brain regions and cell clusters. The orientation refers to the body axis (A: d: dorsal; l: lateral; p: posterior). (A) Shows the brain at a middle anteroposterior level. (B) Shows the anatomy of the dopaminergic system in the larval CNS based on the TH-GAL4 driver. Source: Selcho et al., 2009.

As pointed out earlier, the adult *Drosophila* brain contains approximately 100,000 neurons, whose projections cluster in internal neuropil structures, while cell bodies are found in the outer brain regions. To better understand the connection between these neurons and their projections at the single-cell level resolution, Chiang and colleagues (Chiang et al., 2011) generated a standard model brain, which was segmented into 58 morphologically distinguishable neuropil regions (see figure 5 for names).

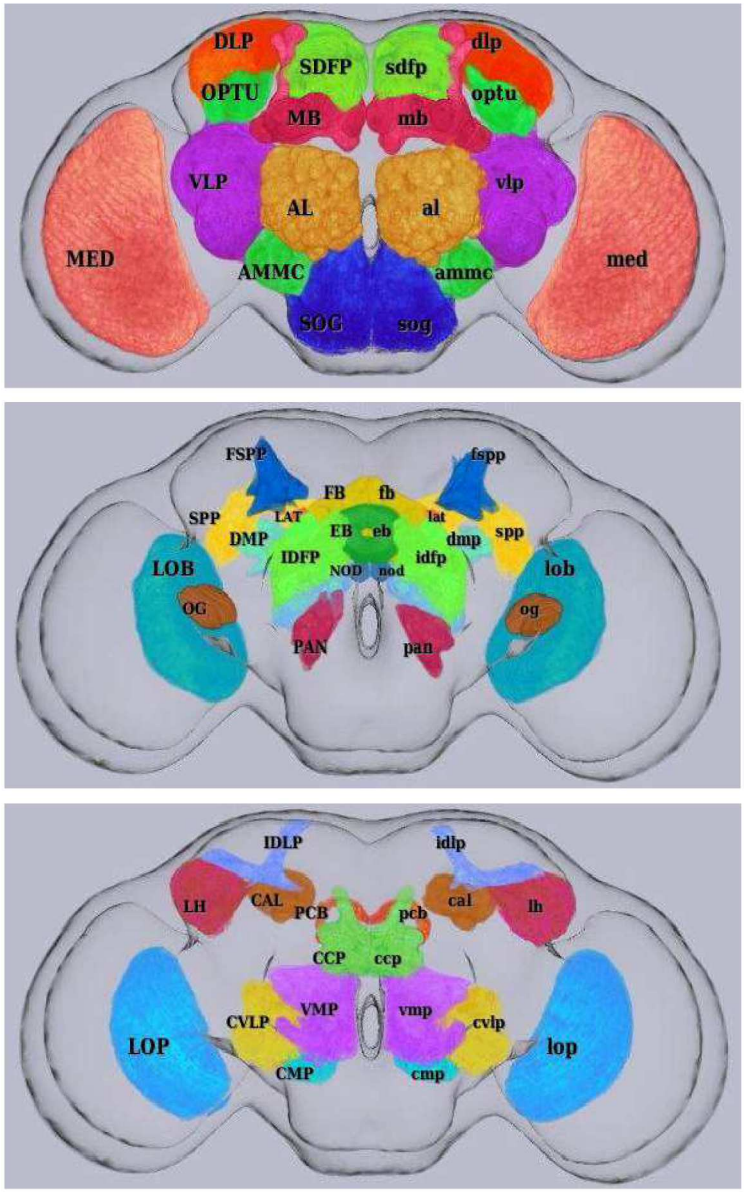

Figure 5: Nomenclature of the adult fly brain regions. AL, Antennal Lobe; AMMC, Antennal Mechanosensory and Motor Center; Cal, Calyx; CCP, Caudalcentral Protocerebrum; CMP, Caudalmedial Protocerebrum; CVLP, Caudal Ventrallateral Protocerebrum; DLP, Dorsolateral Protocerebrum; DMP, Dorsomedial Protocerebrum; EB, Ellipsoid Body; FP, Fanshaped Body; FSPP, Frontal Superpeduncular Protocerebrum; IDFP, Inferior Dorsofrontal Protocerebrum; IDLP, Inner Dorsolateral Protocerebrum; LH, Lateral Horn; Lob, Lobula; LoP, Lobula Plate; LatTri, Lateral Triangle; MB, Mushroom Body; Med, Medulla; Nod, Noduli; OG, Optic Glomerulus; OPTU, Optic Tubercle; PAN, Proximal Antennal Protocerebrum; SOG, Subesophageal Ganglion; SPP, Superpeduncular Protocerebrum; VLP, Ventrolateral Protocerebrum; VMP, Ventromedial Protocerebrum. Source: Chiang et al., 2011.

1.6 AIMS OF THE STUDY

The aim of this study was to elucidate the expression patterns of dopamine receptors in the central nervous system and periphery system particulary, the digestive tract and to analyze the function of these receptors in *Drosophila melanogaster*.

The second major aim of this study was to understand the changes in dopaminergic cells in the fruit fly *Drosophila melanogaster* during induced Parkinsonism. For this, rotenone-induced Parkinsonism in the dopaminergic system should be analyzed using genetic and pharmacological manipulations, transcriptomic analyses of the targeted DA neurons as well as behavioral assays. This relies on two major research questions:

1. What are the target genes/pathways induced during disease development?
2. Does modulation of the intracellular signaling in dopaminergic neurons alters disease progression?

.

1.7 SIGNIFICANCE OF THE STUDY

Dopaminergic system in *Drosophila* is not well characterized. In this study I have analyzed the distribution of four *Drosophila* dopamine receptors using immunohistochemistry to elucidate the morphological architecture of dopaminergic signaling. This information is the basis to understand the role played by these receptors in controlling different physiological functions and behaviors in the fruit fly.

Parkinson's disease in humans is a gradual progressive neurodegenerative disease that becomes clinically apparent after an estimated 70 % of vulnerable DA neurons in the *Substantia nigra* have already died. Postmortem studies are limited by tissue availability and hardly ever allow identification of the initial pathological events during pre-symptomatic stages. Hence, modeling PD at pre-symptomatic phase *in vivo* is essential for understanding the development of the disease and possibly identifies potential targets for neuroprotection measures for PD at pre-clinical stages. The gene expression analysis carried out in this study is, to my knowledge, the first of its own kind in rotenone-induced Parkinsonism in *Drosophila* that performed specifically

on sorted DA neurons. Moreover, the molecular mechanisms underlying the cause of PD remain largely unknown. The current treatment relying more on the symptoms of the disease, which most of them have got devastating side effects. Thus, identifying novel molecular pathways that may enhance the survival of DA neurons may provide future alternatives for causal therapies..

2 MATERIALS AND METHODS

2.1 MATERIALS

2.1.1 CHEMICALS

Table 1: Name and source of chemicals

Chemicals from Carl-Roth GmbH	**Chemicals from other Sources**
Agar-Agar, Chloroform	Bovine serum albumin-Sigma Aldrich
Calcium chloride, Ethanol (≥ 99.8 %)	Normal goat serum-Sigma Aldrich
Ethidium bromine, Glucose	Rotenone-Sigma Aldrich
HEPES, Isopropanol	Clozapine-N-Oxide- C.D Nichols, LSU
Magnesium chloride hydrated ($Mgcl_2.6H_2O$	RNA Magic-Bio-Budget
Nipagin (Methyl-4-Hydroxybenzoate	SureClean-Bioline
Propionic acid, Pottasium chloride (Kcl)	Yeast-Leiber
Potassium dihydrogen phosphate (KH_2PO_4)	Paraformaldehyde-Polysciences
Sodium chloride (Nacl), Sucrose	dNTPs-Promega
Sodium bicabornate ($NaHCO_3$)	Agarose-Biozym
Sodium dihydrogen phosphate ($NaH_2PO_{4)}$	Beet syrup-Reform house
Trehalose, Triton X-100	Maize meal-Reform house
Roti-Mount FluorCare DAPI	Melasse-Reform house
	FocusClear- CelExplorer Labs.Co
	RiboLock Ribonuclease- Inhibitor-Fermentas

2.1.2 DNA LADDER

1kb-GeneRuler	Fermentas GmbH, St. Leon-Rot
50bp GeneRuler	Fermentas GmbH, St. Leon-Rot

2.1.3 ANTIBODIES

2.1.3.1 PRIMARY ANTIBODIES

Rabbit α-delta	Developmental Studies Hybridoma Bank, Iowa
Rabbit α-dopa decarboxylase	Gift from Uwe Homberg, University of Marburg
Rabbit α-DILP2	Gift from Manfred Schmid, ETH

Rabbit α-GFP	Invitrogen, Karlsruhe
Rat α-GFP	Santa Cruz Biotechnology, Heidelberg
Mouse α-Nc82	Developmental Studies Hybridoma Bank, Iowa
Rabbit α-Notch	Developmental Studies Hybridoma Bank Iowa
Mouse α-Prospero (MR1A)	Developmental Studies Hybridoma Bank, Iowa
Mouse α-PDF C7	Developmental Studies Hybridoma Bank, Iowa

2.1.3.2 SECONDARY ANTIBODIES:

Goat α-rabbit Dylight 488	Jackson ImmunoResearch
Donkey α-rat Dylight 488	Jackson ImmunoResearch
Goat α-mouse Dylight 549	Jackson ImmunoResearch
Goat α-rabbit Dylight 549	Jackson ImmunoResearch
Rat α-mouse CD8a Biotin	eBioscience
Phalloidin-TRITC	Life technologies

2.1.4 ENZYMES

Taq DNA polymerase	Fermentas, St. Leon-Rot
Pwo DNA polymerase	Peqlab Biotechnologie
PrimerScript Reverse Transcriptase	Takara Bio Europe SAS, St. Germain-en-Laye

2.1.5 REAGENT SYSTEM

T7 Megascript	Ambion, Austin
Nucleospin RNA II Kit	Macherey Nagel, Düren

2.1.6 BUFFER AND SOLUTIONS

- Hemolymph-like 3-Saline (HL3): 70 mM Nacl, 5 mM Kcl, 1.5 mM $Cacl_2.2H_20$, 20 mM $Mgcl_{2.}H_2O$, 10 mM $NaHCO_{3,}$ 5 mM Trehalose, 115 mm Sucrose, 5 mM HEPES (pH 7.1).
- Phosphate-Buffered Saline (PBS) (10X): 80 g Nacl, 2 g Kcl, 14.4 g, $Na_2HPO_4.H_2O$, 2.4 g KH_2PO_4 in 1 l ddH_2O, (pH 7.4)
- Washing buffer for microarray: 20XSSC: 175.3 g Nacl, and 88.2 g Sodium citrate in 1 L ddH_2O

  L1 = 1 X SSC

  L2 = 1 X SSC + 0.1% Triton X-100

  L3 = 0.1 X SSC + 0.1% Triton X-100

  L4 = 0.1 X SSC

- Paraformaldehyde (4% PFA): 4 g in 100 ml of 1x PBS+0.3% Triton X-100

2.1.7 DROSOPHILA STOCKS/LINES

Table 2: Name, function and source of fly lines.

Name	Function	Source
W^{1118}	Wild type	Bloomington Drosophila Stock Center
Canton S (CS)	Wild type	Bloomington Drosophila Stock Center
DopR1-Gal4	Expresses Gal4 in the pattern of DopR1 (Dopamine receptor 1)	BestGene Inc
DopR2-Gal4	Expresses Gal4 in the pattern of DopR2 Dopamine receptor 2)	BestGene Inc
D2R-Gal4	Expresses Gal4 in the pattern of D2R Dopamine receptor 2- like)	BestGene Inc
DopEcR-Gal4	Expresses Gal4 in the pattern of Dopamine/ecdysteroid receptor	Bloomington Drosophila Stock Center
$DopR^{f02676}$	DopR1 deficient in CS background	Gift from David Anderson HHMI
TH-Gal4	Expresses Gal4 in dopaminergic neurons	Bloomington Drosophila Stock Center
NP1-Gal4	Expresses Gal4 in enterocytes	Gift from D. Ferrandon
nsyb-Gal4 (Synaptobrevin)	Expresses Gal4 to all neurons	Gift from Julia Simpson
DopR2-RNAi	Expresses dsRNA for RNAi of DopR2 under UAS control	VDRC
DopR-RNAi	Expresses dsRNA for RNAi of DopR under UAS control	VDRC
D2R-RNAi	Expresses dsRNA for RNAi of D2R under UAS control	VDRC
PDF-Gal4	Expresses Gal4 in PDF (clock) neurons	Gift from Chris Wegener
UAS-M4D1	Decreases cAMP in response to CNO	Gift from C.D Nichols, LSU
UAS-M5Dbar	Increases cAMP in response to CNO	Gift from C.D Nichols, LSU
UAS-M1D1	Increases Ca2+ in response to CNO	Gift from C.D Nichols, LSU
20XUAS-IVSmCD8::GFP	Expresses mCD8-tagged GFP under the control of 20 UAS-sequences with an intron (IVS) interposed between the UAS and coding sequences	Bloomington Drosophila Stock Center

2.1.8 OLIGONUCLEOTIDES

Table 3: Name of oligonucleotides used for RT-PCR analysis

Name	Sequence (5' to 3')
Capfinder-Sp6-rG1	CAGCGGCCGCAGATTTAGGTGACACTATAGArGrGrG
Adaptor-SP6-PCR	GACGCCTGCAGGCGATGAATTTAGG
Oligo-dT T7 II	GAGAGAGGATCCAAGTACTAATACGACTCACTATAGGG
Oligo-dT-T7 I	GAGAGAGGATCCAAGTACTAATACGACTCACTATAGGG
Droso.DopR1 *	GGCGTCAATTCTGAACCTGT
Droso DopR1 **	GAGATGGGCACAAAGGAGAC
Droso DopR2 *	AACTCCTGCGAGCAGACCTA
Droso DopR2 **	AGGAGTGGTGCTGGTGATG
Droso D2R *	CGATGTATGCGCCTTCTACA
Droso D2R **	GTCTGGGCAATGTTCTCGAT
Droso DDC *	GCCAAGACAATGGTCGACTT
Droso DDC **	GGCATGAAACTTGGGACTGT
DopEcR *	CTTTGCATTCTGGGTGTCCT
DopEcR **	AATATGCCGATCCAGACGAC

* Forward ** Reverse

Table 4: Nucleotides used for qRT-PCR analysis

Name	Sequence (5' to 3')
Rpl32_fwd	TTGGCTTCGGTTTCCGGCAAG
Rpl32_rev	ATCGATCCGACTGGTGGCGGAT
Dad_fwd	CAGATCCACTCGGTGGGTGCC
Dad_rev	CAGATCCACTCGGTGGTGCC
Armadillo_fwd	CTCATTCGCCAGCAGTCGGT
Armadillo_rev	CAAAGAACGCCAGCAGCCAC
Spitz_fwd	AATATTGGGCCTGGGCGTGG
Spitz_rev	CCGCGCCTCTTCGATCTCCTC
l(2)NC136-fwd	TCCTACTGTGGCAGCTATCG
l(2)NC136-rev	ACTGTCCGAGACAGGAAGAC
CaM-fwd	GCTGCAGGACATGATCAACG
CaM-rev	TCTCGGATCTCCTCTTCGCT
Dat-fwd	GGCGCATTAGGCCCACTTAT
Dat-rev	GCTTCCCAGAGACGGTCAAT

2.1.9 MICROSCOPES

Fluorescence microscope Imager. Z1 with Apotome and AxioCam MRm camera and HXP 120 lamp	Zeiss Oberkochen
Laser scanning confocal microscope TCS SP 1	Leica, Heidelberg
Inverted microscope Axiovert S 100	Zeiss, Oberkochen
Stereo microscope SZX12 with U-CMAD3 camera	Olympus GmbH, Hamburg
Stereo light microscope SMZ 745T	Nikon, Tokyo
Stereo light microscope	WILD M3, Heerbrugg

2.1.10 EQUIPMENTS

Agarose Gel ectrophoresis unit;	Biometra, Göttingen
Centrifuge	Thermo electron cooperation
Digital graphic printer UP-D897	Sony, Tokyo
Drosophila Activity Monitor DAM2	Trikenetics, Waltham
Incubator	Thermo electron cooperation
Microarray scanner	GenePix 4000B, Oldendorf
Kontes glass tissue grinder (7 ml) and pestle	Kimble Chase Kontes
Microwave	AFK, Hamburg
MagnaRack	Invitrogen, Karlsruhe
Spectrophotometer	Nanodrop ND-1000, Peqlab,

StepOne Real time PCR system	Applied Biosytems, Life Technologies GmbH
Thermocycler (Labcycler)	SensQuest GmbH, Göttingen
Thermo block HB 130	Unitek
UV-transilluminator	PHASE GmbH
Vortex	Heidolph, Schwabach
Water bath (thermostat 2761)	Eppendorf, Hamburg

2.1.11 OTHERS

Blotting paper	A. Hartenstein GmbH
Cell filters 30 µm	Miltenyi Biotec
Cover slips (24 X 40 mm)	Roth, Karlsruhe
Dynabeads MyOne Streptavidin T1	Invitrogen, Oslo
Plastic vials 22 ml, 68 ml, 178 ml	Greiner Bio-One
Microscope slides	Roth, Karlsruhe
Microarray slide	Canadian Drosophila Microarray Centre
Vial stoppers	Greiner Bio-One

2.2 METHODS

2.2.1 FLY FOOD PREPARATION

Fly food was prepared depending on the amount needed. For a volume of 500 ml medium: 31.25 g beer yeast, 31.25 g maize meal, 5 g agar-agar, 10 g glucose, 15 g melasse and 15 g beet syrup were mixed with H_2O and boiled for 15 min. It was autoclaved for 10 min and let it cool to about 55 °C. Then, 5 ml of 10 % propionic acid and 15 ml Nipagin were added to inhibit the growth of mold and bacteria. Under a clean bench, the medium was dispensed into the sterile vials. The medium was stored at 4 °C until use.

2.2.2 DROSOPHILA CULTURE AND CROSSES

Unless otherwise stated, flies were reared on a standard *Drosophila* medium at room temperature (RT). The RT was approximately 21 °C. Flies were dump-transferred into new vials after every 4 weeks. In case of breeding, flies were maintained in a controlled incubator with 12 hrs on/off light cycle at 25 °C. Virgin females from UAS strains were crossed to GAL4 males. Crosses were transferred to new vials after 2 days. The eclosion was within 10-14 days. After eclosion of first progeny, F1 generation progenies were collected at least once a day for 5 consecutive days. Progenies were maintained at 25 °C for 3 days before subjected to different experiments.

2.2.3 APPLICATION OF ROTENONE

To induce Parkinsonism in flies, rotenone was administered orally. The compound was prepared as follows: 0.02 g of rotenone was dissolved in 1 ml DMSO to get a 50 mM stock solution. Following this, 100 µl of the stock solution was added to 1 ml of 10 % glucose. The final concentration of rotenone was 5 mM. Then, 300 µl out of this solution was used to soak a blotting paper placed on top of normal medium to avoid desiccation (Fig. 6). Flies were shifted to new vials containing fresh contents every 48 hrs.

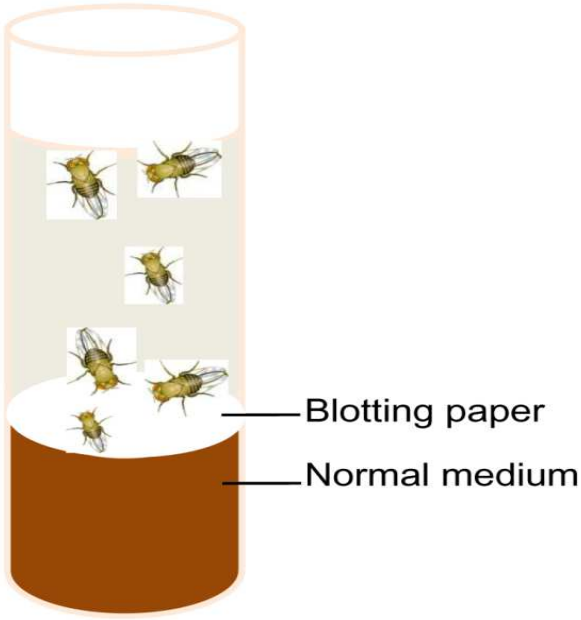

Figure 6: A 22 ml vial for culturing *Drosophila*. The experimental flies feeding on rotenone added onto blotting paper.

2.2.4 APPLICATION OF CLOZAPINE-N-OXIDE (CNO)

To activate DREADD receptors *in vivo*, CNO was also applied to flies through food. A calculated amount of this synthetic ligand was dissolved in 1 x PBS to obtain a 10mM stock solution. This was mixed with a calculated volume of *Drosophila* medium depending on the amount needed. The final concentration of CNO in the medium was 1 mM.

2.2.5 BEHAVIORAL ASSAYS

2.2.5.1 CLIMBING ABILITY (NEGATIVE GEOTAXIS)

Twenty male adult flies were placed into a 17 cm long glass tube at a given time point (see Figure 7). The flies were tapped to the bottom of the tube and let to climb the tube. After 20 secs, a photo was taken in which most of the healthy flies are expected to have crossed the escape line at a height of 6 cm. The height/distance climbed by each fly was analyzed by using Image J software. Three independent experiments were used for the analysis.

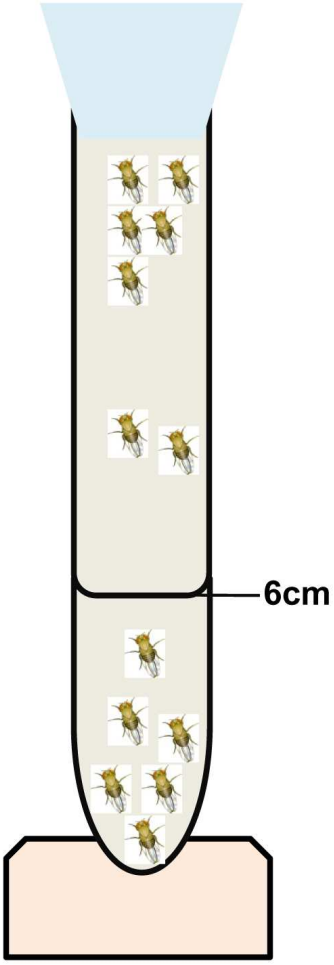

Figure 7: Climbing ability assay. A glass tube of 17 cm long, showing the ability of flies to climb. The normal healthy flies will be able to cross the line at a height of 6 cm after 20sec.

2.2.5.2 LOCOMOTOR ACTIVITY ASSAY

Individual 3-5 days old male flies were placed into glass tubes (5 mm diameter) containing food at one end and capped with a cotton plug at the other end. The tubes were then placed into the *Drosophila* Activity Monitor (DAM) (Fig. 8). The DAM was then placed into the 25 °C incubator and entrained for at least 7 days under light/dark (LD) cycles of 12 hrs light and 12 hrs darkness or constant darkness (DD). The DAM connected to a computer, automatically recorded the number of infrared beam crossings per 5 minutes for each fly. Twenty four hours interval locomotor activity (column graphs) was generated by averaging 5 min activity across the animals, then averaging 5 min activity profiles for 24 hrs over 3 days in LD or DD. For the line graphs, the average of every one hour was taken as a single data point. Zeitgeber

(ZT), ZT0= 8.00 a.m and ZT12= 20.00 p.m. Two to three independent experiments were used for analyses, with 8 flies per group. Difference on the effect of 1 mM CNO between different genotypes was tested by Two-way-ANOVA followed by Bonferroni post test for multiple comparisons using $\alpha < 0.05$.

Figure 8: *Drosophila* activity monitor. It takes 32 individual activity tubes. A single activity tube is shown in place.

2.2.6 LIVE IMAGING

The practice of examining or acquiring the image of the living cells, tissues or whole flies under fluorescent microscope before fixation or staining was considered as a live imaging. Firstly, it was performed to control the UAS-GFP parental lines to make sure that there is not any specific expression of the GFP reporter. Second, to examine whole flies obtained from crossings of specific GAL4 drivers to the UAS-GFP responder lines, to understand the activity of the promoter. Third, to examine the tissues in which the GFP was observed before performing further analyses such as immunohistochemistry.

2.2.7 IMMUNOHISTOCHEMISTRY

2.2.7.1 IMMUNOFLUORESCENT STAINING OF WHOLE-MOUNT LARVAL AND ADULT CENTRAL NERVOUS SYSTEM (CNS)

Larval and adult CNSs were dissected in ice-cold 1 x PBS and immediately fixed in 4 % paraformaldehyde in PBS containing 0.3 % Triton X-100 (PBT) for 20 min at RT. Samples were then washed with PBT three times 10 mins each, blocked for 30 mins with 10 % normal goat serum in PBT at RT, and subsequently incubated with a primary antibody in blocking buffer at 4 °C overnight. After washing the samples five times for 10 mins each in PBT, they were incubated with a secondary antibody in PBT overnight at 4 °C or 4 hrs at RT. Washing was done six times 10 mins each with PBT, and mounted on glass slides and cover slips with Focus clear. Fluorescent z-series images were acquired by Leica TCS SP 1 or Zeiss Axio Imager Z1 with Apotome. Next, images were processed with either AxioVision Rel.4.8 or ImageJ and corrections for brightness, contrast and cropping were done with the Adobe Photoshop 7.0. The following antibodies were used. Primary antibodies: Rabbit α-dopadecarboxylase (1:10), Rat α-GFP (1:200), Rabbit α-GFP (1:400), Mouse α-Nc82 (1:5), Rabbit α-DILP2 (1:100), Mouse α-PDF C7 (1:5). Secondary antibodies: Dylight 488 conjugated Goat α-Rabbit (1:500), Dylight 488 conjugated Donkey α-Rat (1:500), Dylight 549 conjugated Goat α-Mouse (1:200) and Dylight 549 conjugated Goat α-Rabbit (1:500).

2.2.7.2 IMMUNOFLUORESCENT STAINING OF DIGESTIVE SYSTEM

Larval and adult guts were dissected, fixed and stained with specific antibodies as described in section 2.2.7.1 above. Primary antibodies used were: Rabbit α- delta (1:100), Mouse α-prospero (1:10), Mouse α-notch (1:10), Rat α-GFP (1:200) and Rabbit α-GFP (1:500). For the secondary staining the following antibodies were used: Dylight 488 conjugated Goat α-Rabbit (1:500), Dylight 488 conjugated Donkey α-Rat (1:500), Dylight 549 conjugated Goat α-Mouse (1:200), Dylight 549 conjugated Goat α-Rabbit (1:500) and TRITC conjugated Phalloidin (1:1000). Mounting was done in RotiMount containing DAPI for nuclei staining. The images were captured by fluorescent microscope Zeiss Axio Imager Z1 with Apotome.

2.2.8 MAGNETIC BEADS PREPARATION

This protocol was adopted from (Iyer et al., 2009) with some minor modifications. Briefly, Streptavidin T1 coated Dynabeads (100 µl) were washed three times 2 min each in 1 ml HL3- buffer by placing a micro-centrifuge tube on a magnetic block to pellet the beads and discard the supernatant. The washed beads were then resuspended in 100 µl undiluted biotinylated rat anti-mouse CD8a antibody (antibody concentration is 500 µg/ml). Dynabeads T1 can bind 20 µg/ml of biotinylated Ig. The beads-antibody mixture was incubated for 30 min at room temperature (RT) with gentle rotation of the tube. After incubation, the tube was placed on the magnet for 2 min and the supernatant was discarded. The Dynabeads coupled to antibody was again washed three times 2 min each with HL3 buffer using the magnet. Finally, the antibody coupled beads were then resuspended in 100 µl of HL3 buffer and stored at 4 °C and used within 4 weeks.

2.2.9 DISSOCIATING THE TISSUE INTO A SINGLE CELL SUSPENSION

A schematic procedure for dissociation and magnetic bead cell-sorting of dopaminergic neurons is shown in Figure 9. In details, about 70 heads of F1 generation male adult flies from the TH-GAL4 crossed to 20XUAS-mCD8::GFP were dissected in pre-chilled HL3 buffer and transferred to a micro-centrifuge tube. The tube was vortexed for 1 sec. With the use of a fire polished glass pipette the supernatant was discarded and the procedure was repeated 3-4 times until the supernatant became clear. The heads were transferred to a pre-chilled 7 ml Kontes tissue grinder, which was rinsed with 1 % BSA in HL3 buffer in order to avoid the cells from sticking to the glass surface. About 4 ml of HL3 buffer were added to the tissue grinder containing the tissues. Gently, using a pestle, the tissues were given 30-32 douncing strokes. The solution was then triturated 5 times using the fire-polished glass pipette narrowed to approximately 50 % of the standard tip diameter. The level of dissociation was assessed by putting 50 µl of the solution on a microscope slide and observed under the fluorescent microscope with a GFP filter. Then the solution was filtered through a 30 µm cell filter and the filtrate was collected in 4 tubes of 1.5 ml each.

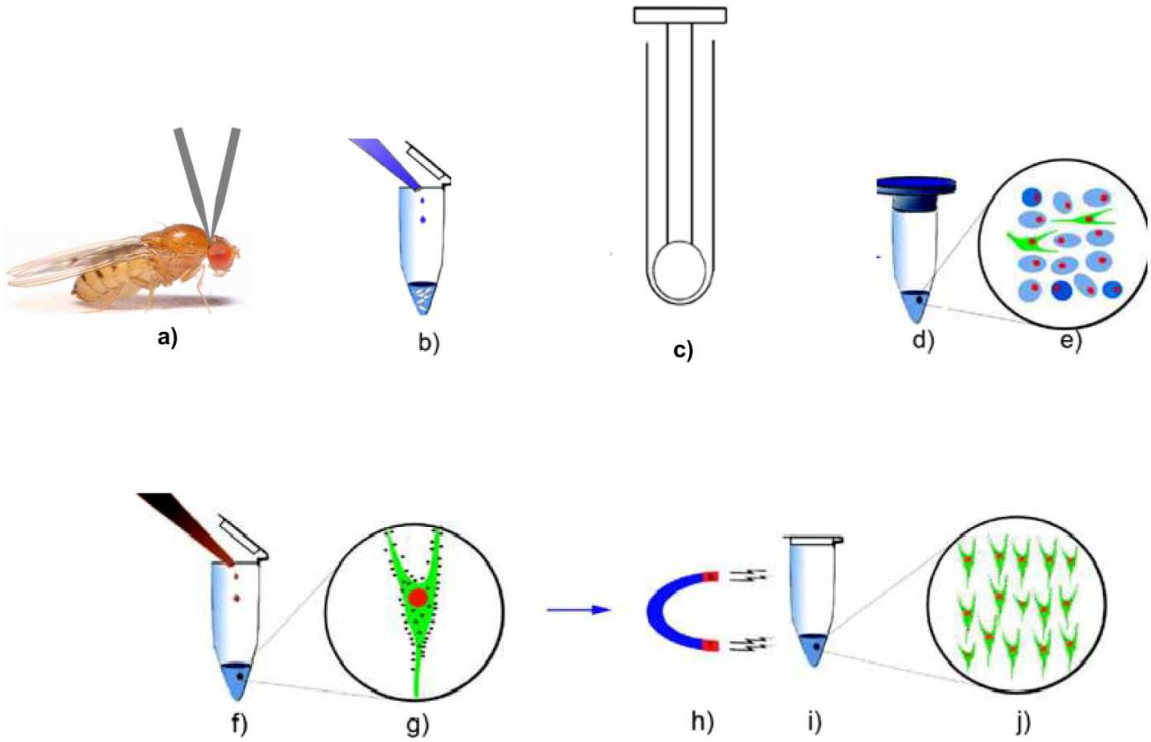

Figure 9: Schematic of the procedure for magnetic bead cell sorting of *Drosophila* dopaminergic neurons. (a) Age matched, intact adult heads carrying the TH-GAL4 and UAS-mCD8::GFP transgenes are dissected. (b) The heads are transferred to a 1.5 ml tube and washed/vortexed to remove any debris. (c) The heads are then transferred into a 7 ml glass tube, dounced to homogenize the brain tissue followed by trituration to further dissociate the tissue into a cell suspension. (d,e) The homogenate is then filtered using a 30 µm cell filter to remove any large cellular debris, including the cuticle from the head and filter out the single cell suspension. The filtrate solute contains a single cell of different cell types including neurons and glia. (f) Biotinylated anti-mouse-CD8a antibody coated magnetic Streptavidin T1 Dynabeads are added to the cell suspension and incubated on ice for 60 min. (g) The magnetic beads specifically bind to the dopaminergic neurons that express a mouse CD8 tagged GFP fusion protein under the control of the TH-GAL4 driver. (h,i) The magnetic bead coated cells are separated by placing the cell solution in a strong magnetic field. The supernatant is discarded and the cells are washed 3 times to remove any non-specific cells, resulting in (j) highly enrichment of specific dopaminergic neurons. Panels (b, d-j) are adopted from (Iyer et al., 2009).

2.2.10 MAGNETIC BEADS CELL SORTING

A volume of 15 µl of antibody-bound beads was added in 1 ml cell suspension and incubated for 1 hour on ice with occasional hand-mixing via inversion of the tube. Following this, the tubes were placed on the magnet for 2 min to pellet the beads along with GFP positive cells. Slowly, the supernatant was pipetted out without disturbing the pellet and was discarded. The cells were washed three times with ice cold HL3 buffer by putting the tubes on the magnet to remove non-specific cell binding. Cells bound to the coupled beads were resuspended in 30 µl of HL3 buffer.

Cell purity and yield were controlled by taking 5 µl and observe it under the fluorescent microscope. Approximately, 8-10 GFP-positive cells were counted at one time point (see Fig. 38 in result section).

2.2.11 RNA ISOLATION FROM MAGNETIC BEAD SORTED CELLS

After assessing yield and purity of the targeted cells, the tubes were again placed on the magnet to pellet the cells and the supernatant was discarded. RNA magic was used as an extraction buffer in which 100 µl of it was added in each of the 4 tubes. The tubes were vortexed shortly, before incubated for 30 mins at 42 °C. To ensure removal of the coupled beads it was necessary to centrifuge for 2 min at 2000 x g and immediately place the tubes on the magnet for 2 mins. The supernatant was transferred to a new tube and total RNA (from approx. 200 DA neurons) was isolated using the RNA magic kit (Bio- Budget Technologies GmbH). The RNA pellet was resolved in 10 µl RNase-free H_2O and stored at -80 °C.

2.2.12 COMPLEMENTARY DNA (cDNA) SYNTHESIS

First strand cDNA was synthesized by using PrimeScript Reverse Transcriptase (Takara) according to the manufacturer's protocol. A volume of 10 µl mixture containing: 2.5 µl CapFinder Sp6rG primer (10 pmol/µl), 2.5 µl anchored Oligo-dT T7 I primer (10 pmol/µl), 1 µl dNTP mixture (10 mM) and 4 µl of template RNA (≤ 5 µg total RNA) was heated at 65 °C for 5 min and immediately cooled on ice. Then, this template-primer mixture was again mixed thoroughly with 4 µl of 5 X PrimeScript buffer, 0.5 µl RNase inhibitor, 1 µl PrimeScript Reverse Transcriptase enzyme and 4 µl RNase free H_2O. The mixture was incubated at 42°C for 50 min. The enzymatic activity was stopped by heating the mixture at 70°C for 10 min and lastly cooled on ice. The cDNA synthesized was used immediately for second strand synthesis or temporarily stored at -20 °C.

2.2.13 cDNA-PCR

Subsequently, the obtained cDNA from above was used for second strand synthesis by PCR. A 50 µl PCR reaction was carried out as shown in (table 5) containing the following: 5 µl 10x LA buffer (Mg^{2+} plus), 8 µl dNTPs (10 mM), 2 µl cDNA template, 2 µl adaptor Sp 6 (10 pmol/µl), 2 µl OdT T 7 II (10 pmol/µl), 0.5 µl Taq/Pwo (20.1) and 30.5 µl distilled H_2O.

Table 5: PCR program

S/No.	Step	Temperature	Time	No. of cycles
1	Initial denaturation	95°C	1 min	1
2	Denaturation	95°C	20 sec	35
3	Annealing	58°C	20 sec	35
4	Extension	72°C	2 min 30 sec	35
5	Final elongation	72°C	5 min	1
6	Final hold	4°C	∞	

2.2.14 CLEANING OF cDNA

The PCR product from section 2.2.13 was cleaned with Sureclean reagent. Shortly, the PCR products were pooled in one micro-tube and an equal volume of Sureclean was added and mixed thoroughly before incubated at RT for 10 min. The mixture was then centrifuged at 17,000 X g for 10 min and the supernatant was discarded. The obtained pellet was washed twice with 70 % alcohol by centrifugation as previous. The pellet was air-dried for at least 5 min and resolved in 10 µl distilled H_2O. The concentration and purity of DNA was measured twice by Nanodrop spectrophotomer.

2.2.15 AMINO ALLYL-CRNA (AA-CRNA) SYNTHESIS

Amino allyl-cRNA was synthesized by using T7- MegaScript (Ambion kit). The following reagents were mixed at RT: 2 µl ATP (75 mM), 2 µl GTP (75 mM), 2 µl CTP (75mM), 1 µl UTP (75 mM), 1.5 µl aa-UTP (50 mM) and 2 µl buffer (10x). Then, 3 µl

template cDNA (approx. 400-800 ng), 2 µl T7 enzyme and 4 µl of H_2O water was added to the mixture and incubated at 37 °C for 16 hours.

2.2.16 CLEANING OF aa-cRNA

The aa-cRNA was purified using Nucleospin RNA II kit.

- The volume of RNA above was filled up to 100 µl with RNase-free H_2O.
- 350 µl of RA1 lysis buffer were added and vortexed shortly.
- Followed by 350 µl of 70 % ethanol and vortexed again.
- About 400 µl of the mixture was loaded to the purification column and centrifuged at 11,000 x g at 4 °C for 30 sec.
- Then, the collected flow was loaded to the column again and centrifuged as before and the same procedure was done for the rest of the mixture.
- The column was then washed twice with 600 µl RA3 washing buffer and centrifuged like before.
- Using a new collection tube, 250 µl of RA3 was added and centrifuged at 11,000 x g at 4 °C for 2 min.
- The column was then transferred into the new tube and RNA was eluted twice with 50 µl RNase-free H_2O (65 °C) and incubated at 65 °C for 1 min before centrifuged at 11,000 x g at 4 °C for 1 min each.
- Next, 10 µl of 3 M Sodium acetate and 250 µl of 96 % ethanol were added and vortexed.
- Precipitation was performed at -20 °C for at least 30 min and centrifuged at 17,000 x g for 60 min.
- The supernatant was discarded and the pellet was washed twice with 70 % ethanol by centrifugation at 17,000 x g for 10 min each.
- Lastly, the pellet was air-dried and resuspended in 6 µl of RNase-free H_2O. Samples were diluted 1:20 in H_2O. The amount and purity of aa-cRNA was measured twice by spectrophotometer. The yield should be at least 5 µg RNA per sample.

2.2.17 LABELING OF cRNA AND CLEANING OF LABELED cRNA

The cRNA was labeled by Alexa fluor dyes. The dyes were dissolved with 40 µl DMSO and used within one week. Alexa fluor 555 was used to label a control sample and Alexa fluor 647 to label a treated sample. Approximately, 20 µg of aa-cRNA was used for each sample. Basically, a reaction mixture composed of 1 volume template aa-cRNA, 2 volumes $NaHCo_3$ buffer (0.3 M, pH 9) and 3 volumes dye. The mixture was then incubated at RT for 2 hrs in darkness conditions and the labeled cRNA was cleaned as described in section 2.2.16. The concentration of the dyes was measured by spectrophotometer.

2.2.18 HYBRIDIZATION OF THE ARRAY

The labeled samples were mixed and hybridized to one single microarray glass slide. In brief, the hybridization buffer composed of 400 µl DIG Easy hybridization buffer, 2.2 µl salmon sperm DNA and 2.2 µl yeast tRNA. The dye mixture consisted of 200 pmol/µl Alexa fluor 647 and 400 pmol/µl Alexa fluor 555. The hybridization buffer was added to the dye mixture and incubated at 65 °C for 10 mins. Slowly, the whole solution was pipetted onto the array. The array was then placed on the hybridization chamber and incubated on the thermoshacker at 42 °C with mild shaking for 18 hrs.

2.2.19 WASHING OF THE ARRAY

To avoid photo-oxidation the washing steps was performed in the darkness conditions. The array was placed into 50 µl falcon tube wrapped with aluminium foil containing the washing buffer at different series with gently rotation.

a. The array was washed with 1 X SSC buffer at RT for 1 hour.
b. Washed twice with 1 X SSC + 0.1% Triton-X-100 at 60°C for 30 min each
c. Washed twice with 0.1 X SSC + 0.1% Triton X-100 at 37 °C for 30 min each
d. Washed with 0.1 X SSC at RT for 30 sec
e. Washed with ddH_2O at RT for 30 sec
f. Quickly rinsed with ddH_2O at RT and immediately dried with N_2 gas.

2.2.20 SCANNING AND ANALYSIS OF THE MICROARRAYS

The microarray slides were scanned by Gene Pix 4000B scanner with Gene Pix Pro 6.0 software. The analysis was performed first by aligning the features (spots) in all the blocks by the help of Gene Pix Pro software. Second, the normalization of the probe signal intensity levels across the arrays was performed by Acuity 4.1 program. Lastly, the enrichment of Gene Ontology terms, and visualization of genes on KEGG (Kyoto Encyclopedia of Genes and Genomes) pathway maps were done with the help of the online s FlyBase (http://flybase.org/) and DAVID (Database for Annotation, Visualization and Intergrated Discovery) (Huang da et al., 2009) (http://david.abcc.ncifcrf.gov) databases.

2.2.21 REVERSE TRANSCRIPTASE PCR (RT-PCR)

A 25 µl PCR reaction consisted of 2.5 µl 10x PCR buffer, 0.5 µl dNTPs (10mM), 0.5 µl forward primer (5 pmol/ul), 0.5 µl reverse primer (5 pmol/ul), 0.25 µl Taq polymerase, 0.5 µl cDNA template (100 ng), and 20.75 H_2O.

The PCR amplification program was as shown below.

95°C	1 min	
95°C	30 sec	28 cycles
55°C	30 sec	
72°C	1 min	
72°C	5 min	
4°C	∞	

2.2.22 QUANTITATIVE REAL TIME PCR (qRT-PCR)

In a 10 µl qRT-PCR reaction mixture, a 10 ng of the 28 cycle's pre-amplified cDNA was used. cDNA synthesis was performed as described in 2.2.12. The reaction mixture contained the following: 0.5 µl forward primer, 0.5 µl reverse primer, 0.25 µl ROX, 5 µl Sybr Green, x µl cDNA, which was brought to final volume of 10 µl by HPLC grade H_2O. The program used in this analysis is shown in table 6.

Table 6: qRT-PCR program

S/No.	Step	Temperature	Time	No. of cycles
1	Initial denaturation	95°C	10 min	1
2	Denaturation	95°C	10 sec	40
3	Annealing	60°C	20 sec	40
4	Extension	72°C	35 sec	40
5	Melting curve	95°C	15 sec	
6	Melting curve	60°C + 0.3°C until 95°C		

A fold change of expression of a gene was calculated according to (Pfaffl, 2001) that put into consideration the primer efficiencies of both target and reference genes. The primer efficiencies were obtained by (1:2) serial dilutions of cDNA from 50 ng to 3.125 ng. After runs of primer efficiency the program in the amplification machine (StepOne) automatically gives the standard curve and the slope. Then the slope was used to calculate the efficiency with the following formula:

$$E=10^{-1/slope}$$

From this the relative expression ratio of target gene to reference gene (Rpl32) was calculated as follows

$$Ratio = \frac{(E\ target)^{\Delta ct\ target\ (control-treated)}}{E\ (ref)^{\Delta ct\ ref\ (control-treated)}}$$

Where ∆ct is change of cycle threshold (ct) calculated by the StepOne program during amplification.

2.2.23 GEL ELECTROPHORESIS

Agarose gel electrophoresis was used to separate the sizes of the nucleic acids. The 1.5 % agarose gel in TBE buffer was made by boiling the mixture. The gel was left to cool to about 55 °C before adding 2.5 µl ofethidium bromide (10 mg/ml). Samples were mixed with 6 X DNA loading dye and loaded onto the gel. A volume of 2 µl of 50 bp or 1 kb Gener ruler marker was loaded depending on the expected size of the nucleic acid. The electromotive force of 100 V was applied for 30 to 40 min. The gels were visualized and captured with an UV transilluminator equipped with a camera.

3 RESULTS

3.1 EXPRESSION PATTERN OF DOPAMINE RECEPTORS IN THE CNS AND DIGESTIVE SYSTEM

To analyse the expression pattern of the four dopamine receptors; DopR (CG9652), DopR2 (CG18741), DopEcR (CG18318) and D2R (CG33517), the GAL4/UAS system was employed (Brand and Perrimon, 1993) to express a marker green fluorescent protein (GFP) under transcriptional control of gene specific promoters. The GAL4 driver lines were crossed to the responder strains carrying either a 20xUAS-IVS-mCD8::GFP (Pfeiffer et al., 2010) or a UAS-Cameleon 2.1 (Diegelmann et al., 2002) and their progenies were used for analyses. All nomenclatures of the larval brain regions are according to Selcho and colleagues (Selcho et al., 2009), the nomenclature of the cell clusters and adult ventral brain is according to Busch et al. (Busch et al., 2009) and the nomenclature of the adult brain hemispheres is after Chiang et al. (Chiang et al., 2011).

3.1.1 DOPR EXPRESSION IN LARVAL AND ADULT CENTRAL NERVOUS AND DIGESTIVE SYSTEMS

A previous immunohistochemical analysis of the expression pattern of *Drosophila* dopamine receptor 1, DopR, in the larval and adult brain revealed prominent immunoreactivity in the mb, the cc and some neurosecretory cells (Kim et al., 2003). This study was based on an antibody raised against the putative third cytoplamic loop of the DopR. To further investigate the localization of this receptor, I analysed the expression of the DopR using the Gal4/UAS system. The DopR-GAL4 was used to drive the Green fluorescent protein (GFP) transgene (20xUAS-IVS-mCD8-GFP (Pfeiffer et al., 2010)) under transcriptional control of UAS promoter. Using double-labeling immunohistochemical analysis, anti GFP immunohistochemistry (green) was used to visualize the neurons and their processes, and a neuropil-specific antibody nc82 to visualize overall brain structures (red).

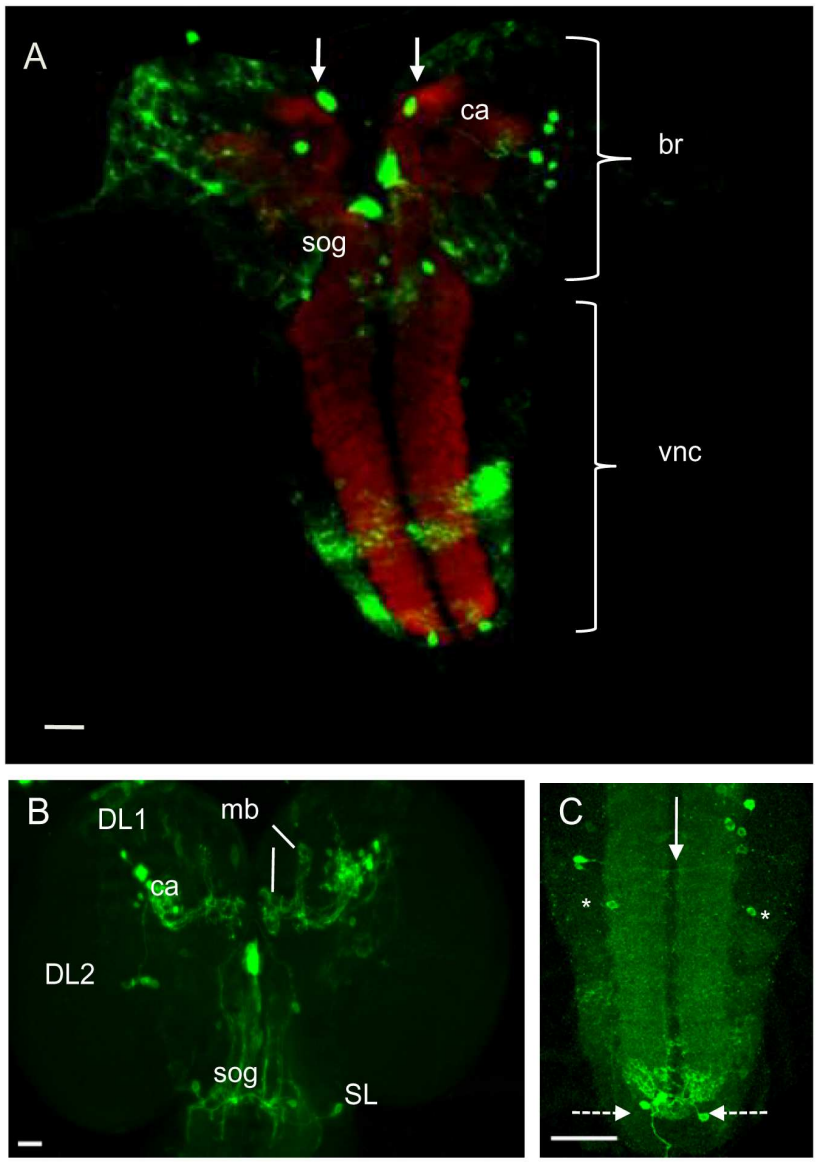

Figure 10: DopR-GAL4 expression in the whole-mount third instar larval CNS. Figures (A-C) show immunofluorescence by GFP staining (green) in the cell bodies and the processes of DopR-expressing neurons. The brain was counterstained with an anti-nc82 antibody (red) for neuropils. Each panel shows a projection of optical sections, illustrating the brain hemispheres (br); and ventral nerve cord (vnc). Throughout the figures, cell clusters and brain regions are labeled with upper and lower cases, respectively. (A) Two large neurosecretory cells located on the pars intercerebrallis regions (arrows) and a group of 5-6 cell bodies are seen innervating the dendritic calyx (ca). (B) Shows the br with the strong GFP signal on the axonal terminal of the mushroom body lobes (mb) and the dendritic ca. Anterior and posterior to ca are two clusters; the dorsal lateral 1-2 (DL1,DL2), respectively. GFP is also seen in the subesophageal ganglia (sog) and the cluster lateral to it (SL). (C) Close-up-view of the vnc. Asterisks mark the cell bodies located on the cellular area and to the edge of the neuropil, sending their processes horizontally across the midline (arrow). At the tip of vnc, two large cells with multiple neurites are seen (dotted arrows). Scale bars: A-B = 20µm, C = 100 µm

In the larval CNS the GFP-expressing neurons innervated the entire protocerebrum (br), the subosephageal ganglion (sog), as well as the ventral nerve cord (vnc) (Fig. 10A). In the brain lobes, DopR-GAL4 was strongly expressed in the mb lobes (Fig 10B) and the calyx (ca) (Fig. 10A, B). The latter was innervated by two intensely GFP labeled clusters; DL1 and DL2 (Fig. 10B). Two large neurosecretory cells, one on each side of the brain hemisphere at the *pars intercerebralis* region, were also

strongly labeled (Fig.10A, arrows). In the sog, one cluster (SL) was also intensely labeled by GFP (Fig.10B). The vnc of the larval CNS also contained DopR-GAL4 expressing neurons. The cell bodies of some of these cells are located on the cellular area while others are located in the neuropil region. These neurons send their processes medially across the midline to join other processes from the adjacent neurons (Fig. 10C, asterisks and arrow). Characteristically, in each larval CNS examined, two strongly GFP labeled neurons laterally located at the tip of last abdominal neuromere sent their primary neurites dorsally (Fig. 10C, dotted arrows).

In contrast to what was observed in the larval CNS, the DopR-GAL4 was highly expressed in the adult brain neurons (Fig. 11A). GFP decorated several neuronal cell bodies, some of which form characteristic clusters. About six to eight larger neurons along the midline in the ventral part of the sog form the ventral medial cluster (VM) (11 B). Two joined intensely labeled cell bodies were visible on each side of the brain hemisphere sending their projections to the sog (11B white arrows). The Insulin producing cell cluster (IPCs) was strongly decorated by GFP (Fig. 11B). This cluster sends its bulky axonal projections to the sog/ tritocerebrum (Fig. 11B, yellow arrow). The anterior superior medial cluster (ASM) comprises several discrete cell bodies on the supra-dorsal-frontal-protocerebrum (sdfp). Two clusters were visible around the antennal lobes (al); AL1 and AL2. Cluster AL1 is located at the anterior margin of the al whereas cluster AL2 is located ventromedial to the al. Another cluster that was highly labeled by GFP comprises of the large lateral ventral neurons (l-LNvs), which are located between the optic lobes (ol) and the brain hemispheres (Fig. 11B). In addition, DopR-GAL4 was expressed in cell bodies located between the ca and the protocerebral bridge (PB1; Fig. 11E), and ventral to the protocerebral bridge (PB2; Fig. 11E). A robust GFP signal was observed in the area surrounding the subesophageal opening (oes) in the posterior slope and to the tracts between the brain hemispheres and the ol (Fig. 11A).

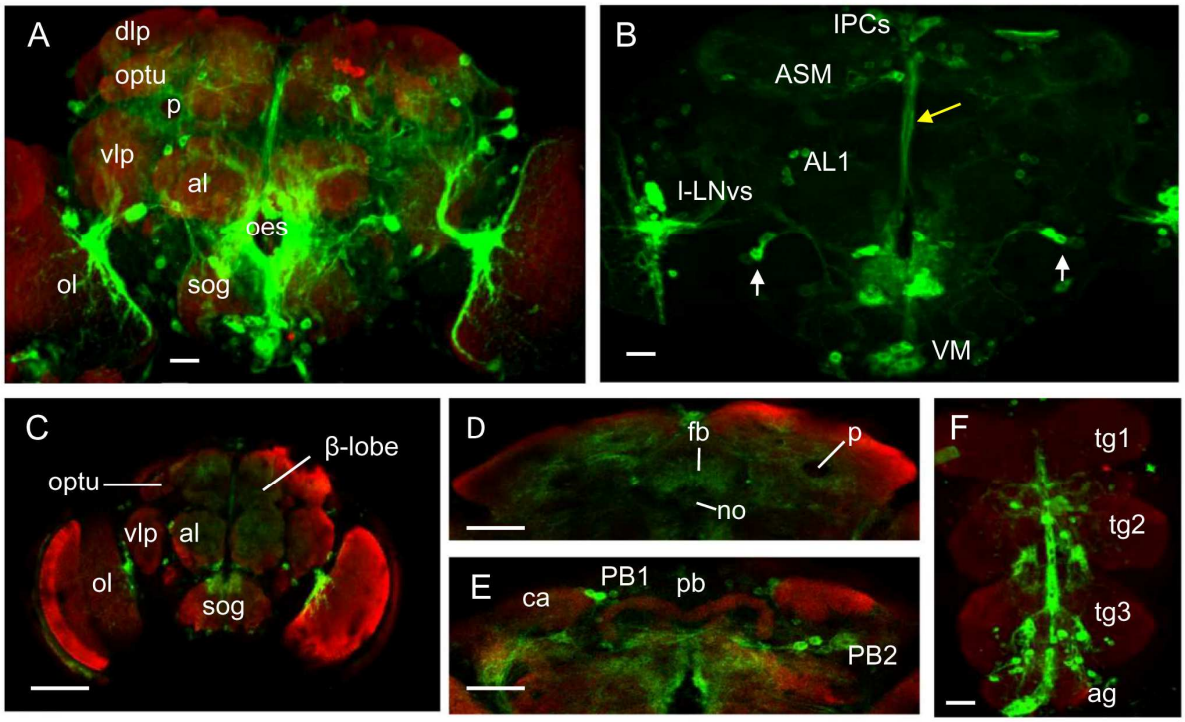

Figure 11: DopR-GAL4 expression in the adult CNS. Figures (A-F) show immunofluorescence by GFP staining (green) in the cell bodies and the processes of DopR-expressing neurons. The brain was counterstained with an anti-nc82 antibody (red) for neuropils. Each panel shows a projection of optical sections except (C-E), which are single optical sections. (A-B) Show the major regions and cell clusters that express DopR-GAL4. To avoid overcrowding of words, the brain regions are named in (A) and the cell clusters in (B). (A) The major regions shown are the dorsal lateral protocerebrum (dlp), optic tubercle (optu), super-dorsofrontal protocerebrum (sdfp) and the pedunculus (p). Others are the ventrolateral protocerebrum (vlp), the antennal lobe (al), the optic lobe (ol) and the subesophageal ganglion (sog) below the esophageal opening (oes). (B) Shows the cell clusters that express DopR-GAL4. The yellow arrow shows the midline projections from the Insulin producing cell cluster (IPCs) and the white arrows show the two joined cell bodies projecting to the sog. Ventral to the sog is a ventral medium cluster (VM). Clusters AL1 and AL2 are located anterior and ventromedial to the al, respectively. The ASM cluster is located on the sdfp and the l-LNvs cluster is seen at the margin of the ol and the brain hemispheres. (C) Shows the major neuropils named in (A) and the β-lobe of the mushroom bodies. (D-E) Posterior view of the adult brain showing DopR-Gal4 expression in the fan shaped body (fb) and noduli (no; D). (E) Shows the two clusters expressing DopR-GAL4; the PB1 and PB2 located dorsal and ventral to protocerebral bridge (pb) which itself lack the GFP signal. The calyx (ca) is faintly labeled by GFP. (F) DopR-GAL4 is expressed in all the thoracic ganglia 1-3 (tg1-3) and the abdominal ganglion (ag). Scale bars: A, B, F: 20 µm, C-E: 96 µm.

With respect to the neuropil regions, DopR-GAL4 was highly expressed in the outer layer surrounding the pedunculus (p) (Fig. 11A, D). As in the larval CNS, only the outer margin of the entire mb lobes was labeled by GFP with a weak signal, but the moderate signal was evident on the β-lobe (Fig. 11C). The calyx was also faintly marked by GFP (Fig. 11E). In the cc, GFP labeled the fan-shaped body (fb), and the

paired noduli (no; Fig. 11D). The protocerebral bridge (pb) was devoid of GFP signal (Fig. 11E), while the ellipsoid body (eb) was moderately labeled only on its outer margin (data not shown). Furthermore, GFP marked the superior dorsofrontal protocerebrum, the dorsal and ventral lateral protocerebrum, the optic tubercle, the al and the sog (Fig. 11A, C). In the adult ventral CNS (thoracicoabdominal ganglia), DopR-GAL4 was strongly expressed along the midline and the cell bodies located lateral to this midline in each segment (Fig. 11F).

A previous transcriptomic study (Shang et al., 2011) showed that dopamine receptor mRNAs are present in purified l-LNvs, a subset of clock neurons. Moreover, Renn and co-author (Renn et al., 1999) reported earlier that there are ten l-LNvs (five on each side of the brain) that have related neurons nearby, the eight small LNvs (s-LNvs). Both l-LNvs and s-LNvs express a neuropeptide pigment dispersing factor (PDF). To test this immunohistochemically, I stained several brains with an anti-PDF antibody. A high degree of colocalization of signals was observed between the GFP and the anti-PDF on the l-LNvs. There was no specific signal for anti PDF on the s-LNV (Fig. 12A-D).

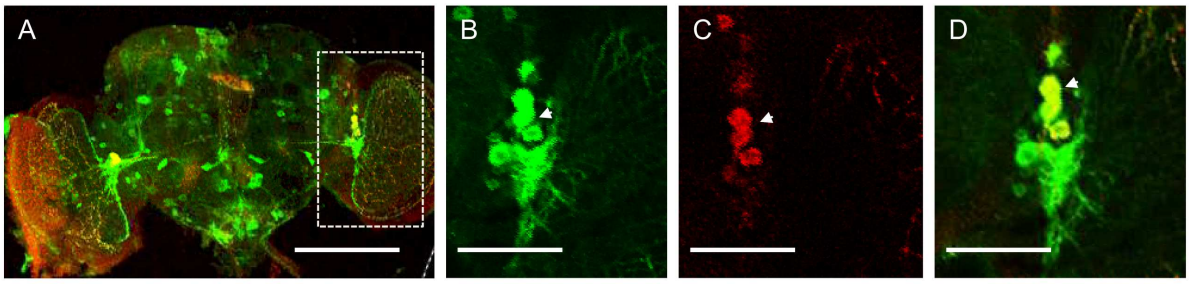

Figure 12: Colocalization of DopR expressing cells with clock neurons expressing pigment dispersing factor (PDF). (A-D) show immunofluorescence by GFP staining and co-staining with anti PDF. (A) Large and small ventral lateral clock neurons (dotted box). (B-C) Enlargement of A, anti GFP (green, arrow) and anti PDF in (red, arrow). (D) The l-LNvs show a high degree of colocalization with DopR-expressing cells (merge, yellow, arrow). Scale bars: 200 µm

In mammals it is known that D2 receptors have a presynaptic location (Civelli et al., 1991). To test this in *Drosophila,* several brains from DopR were stained with anti dopa-decarboxylase (DDC) antibody. Since DDC encodes an enzyme catalyzing the biosynthesis of dopamine from its precursor L-3,4-dihydroxyphenylalanine (L-DOPA),

the dopaminergic neurons will express DDC. Some of the DopR-GAL4 expressing neurons were strongly positive for DDC (Fig. 13A-D), suggesting an auto-receptor function of this receptor at least in these cells. This was further confirmed by a semi-quantitative reverse transcriptase (RT-PCR) analysis (Fig. 13E). The cDNA used for this analysis was isolated from specific dopaminergic cells and tested against specific primers for all four dopamine receptors. A single band of approximately 160 bp was detected for DopR. DDC was used as a positive control. No single band was detected in DopR2 and D2R with exception of DopEcR. The expression patterns of these three receptors are discussed in later sections.

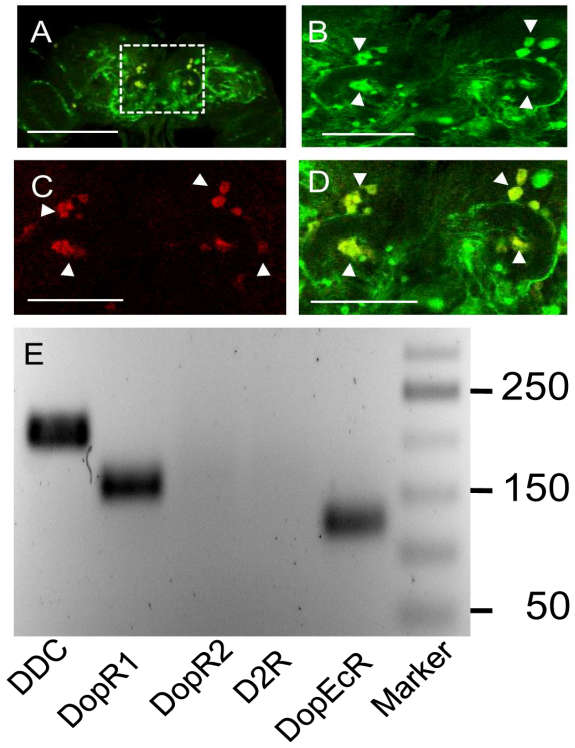

Figure 13: Expression and detection of DopR in dopamine producing cells indicate DopR as an autoreceptor. (A-D) Single optical section stained with anti GFP (green) and co-stained with anti DDC (red) in the adult brain of DopR-Gal4>UAS-GFP. (A) Shows colocalization of anti-GFP and anti-DDC signals (dotted box). (B-D) Enlargement of A showing DopR expressing neurons, (green, arrows); DDC expressing neurons, (red, arrows); and a composite image (yellow, arrows). Scale bars: 200 µm. (E) RT-PCR analysis of the RNA isolated from dopamine producing cells. Specific single bands were detected in DopR1 and DopEcR with DDC as a positive control. No single bands were detected in DopR2 and D2R. Marker is a 50 bp GeneRuler.

In the fly there are seven insulin like peptides (DILP1-7) with striking homology with mammalian and human insulin and insulin like growth factor (Rulifson et al., 2002). The IPC cluster observed in the *Pars Intercerebralis* region (Fig. 11B) has been shown to express DILP2, 3, and 5 (Rulifson et al., 2002). To test this in flies bearing the transgenes DopR-Gal4;UAS-mCD8-GFP several larval CNS and adult brains

were stained with anti GFP and co-stained with anti-DILP2 antibodies. The result showed no colocalization of fluorescent signals between the two antibodies (Fig.14).

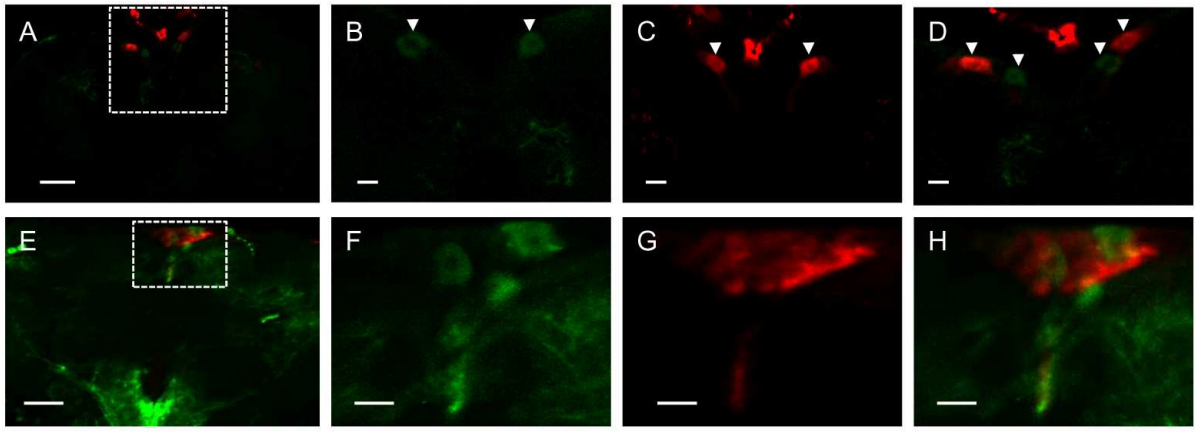

Figure 14: Expression of DopR in Insulin-Producing Cells (IPCs). (A-H) DopR-Gal4 driven GFP in IPCs immunostained with anti GFP (green) and anti DILP2 (red). (A) Larval brain median neurosecretory IPCs (dotted box). (B-D) Enlargement of A; Two cell bodies located on pars intercerebralis region (green, arrows) are not superimposed with DILP2 expressing cell bodies (red, arrows). E. Adult brain IPCs cluster (dotted box). (F-H) Closer view shows no colocalization between DopR expressing neurons with DILP2 expressing neurons. Scale bars: 20 µm

With respect to peripheral nervous system, DopR was found to be expressed in the mid-gut secretory enteroendocrine cells (EEs). This was confirmed by staining the DopR-Gal4>UAS-mCD8-GFP midguts with anti-prospero antibody. Prospero is a transcription factor expressed in EEs (Ohlstein and Spradling, 2006). All the GFP positive cells were positive for prospero expressing cells, suggesting the expression of DopR in a subset of EEs (Fig. 15B-F). Similar results were obtained when the gut tissues were stained with anti NC82 (Appendix 1, Fig. A1).

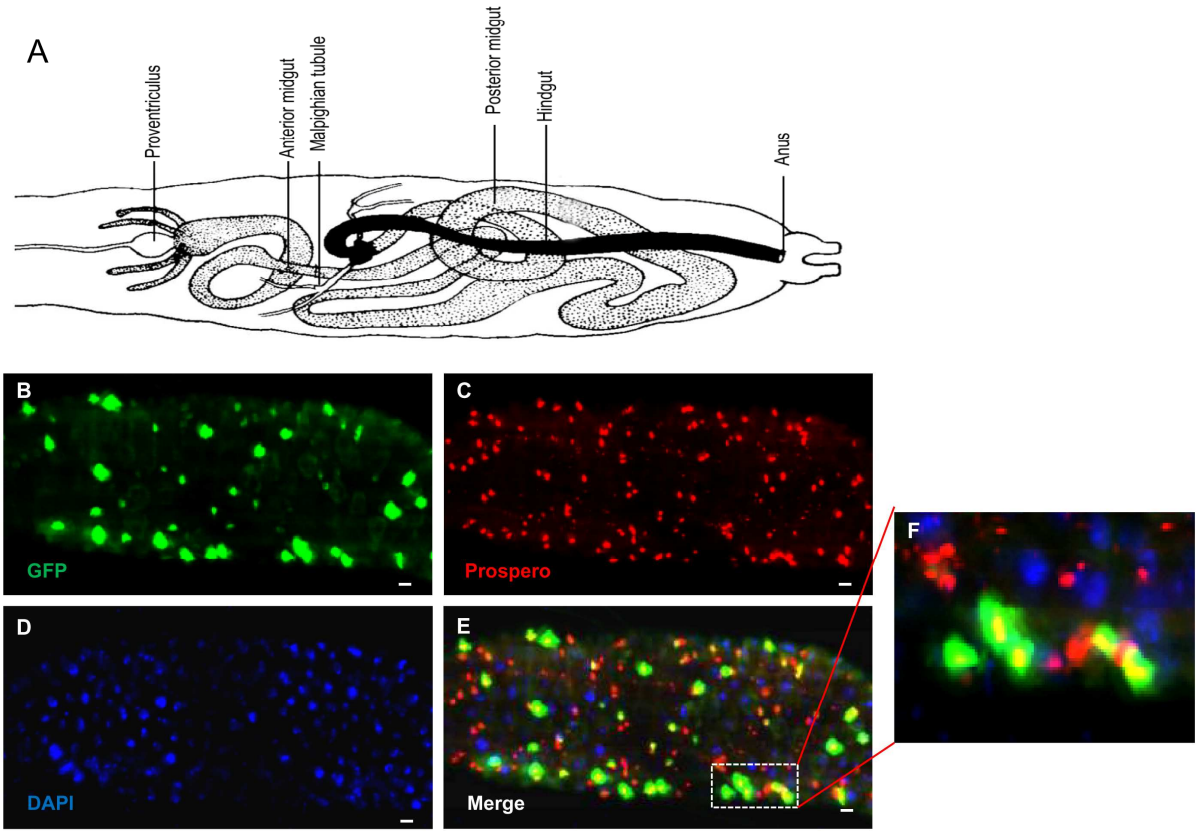

Figure 15: DopR is expressed in the Enteroendocrine cells (EEs). (A) Schematic diagram showing the structure of the third instar larval gut system modified from http://www.docstoc.com/docs/89461663/ANATOMY-AND-DEVELOPMENT-OF-DROSOPHILA-LARVA. Throughout the gut system figures, the posterior midgut is the part that was analyzed unless otherwise noted. (B) Enhancement of GFP reporter for DopR-Gal4 expression in EEs by anti-GFP antibody. (C) Prospero positive cells stained by anti prospero antibody. (D) DNA/nuclei marker, DAPI. (E) A composite image, all the GFP positive cells overlap with a subset of prospero positive cells. Prospero is a transcription factor hence localizes nuclearly, yellow. (F) Enlargement of dotted box in E. Scale bars: 20 µm

3.1.2 DOPR2 EXPRESSION IN LARVAL AND ADULT CENTRAL NERVOUS AND DIGESTIVE SYSTEMS

Immunohistochemical analysis from a previous study (Kim et al., 2003) showed that DopR2 receptor is localized specifically in the mb lobes. However, when I analysed the expression of DopR2 in the larval CNS using GFP as reporter under transcriptional control of the DopR2 promoter, I detected no GFP signal in this region; instead it was possible to see a large number of neurites spreading all over the entire neuropil. These neurites formed a mesh- like structure, (Fig 16A, B) in which some of them project to the ol. For every specimen examined, the terminal tracheal branches were strongly labeled with GFP (see arrow, Fig.16B). As shown in Fig 16A, GFP was

strongly detected in the two clusters; DM and DL (dorsomedial and lateral protocerebrum), respectively.

In the ventral nerve cord, I observed pairs of well labeled neurons (Fig 16B dotted arrows). Each neuron projects to the midline. They form a “fishbone”-like structure like it was described by Draper et al. (Draper et al., 2007) for another dopamine receptor (D2R).

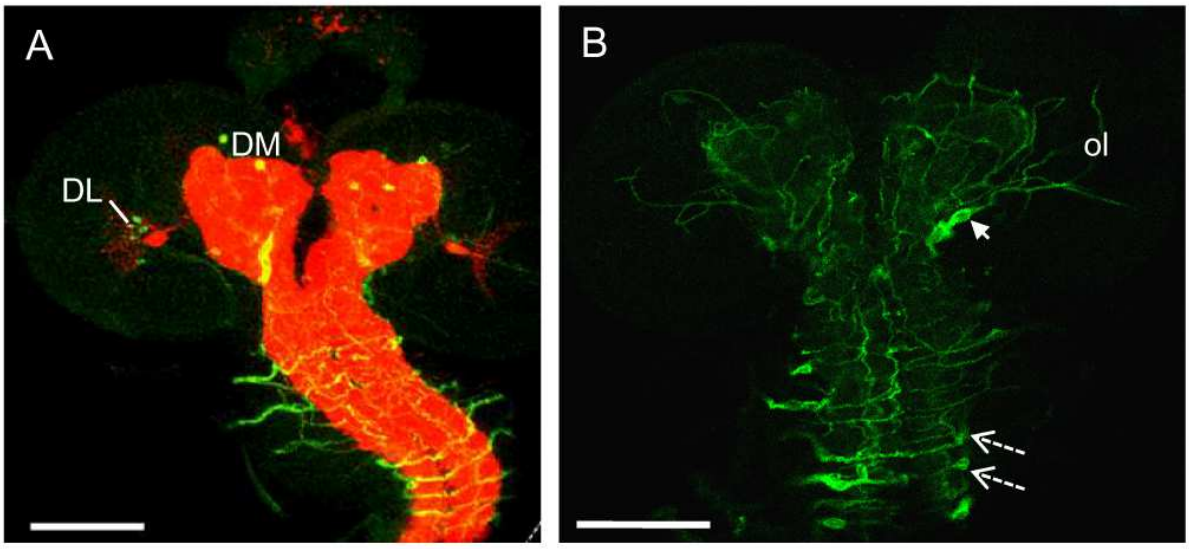

Figure 16: DopR2-GAL4 expression in the whole mount third instar larval CNS. (A) Shown is the maximum projection of optical stacks of the larval CNS. Neuropils and cell bodies and their processes are visualized by anti-nc82 (red) and anti-GFP (green), respectively. GFP labels cells of the dorso-medial and lateral (DM, DL,) respectively. (B) Higher magnification of a single optical section of the larval brain hemispheres and part of ventral nerve cord. Networks of neurites, some projecting to the optic lobe (ol) are seen. The arrow shows the terminal branches of the tracheal system running close to the neurites. Laterally located cell bodies (dotted arrows) projecting to the midline (a “fishbone-like” structure) are also seen. Scale bars: 200 µm.

In the adult brain, DopR2 is reported to be localized in mb and cc (Han et al., 1996, Kim et al., 2003). As for the DopR, the enhancement of GFP expression by an anti-GFP antibody revealed an additional distribution pattern for this receptor in all brains examined. Both, the lower and the upper layers of the fb were strongly positive for GFP. The latter was found to be connected with a highly DopR2 enriched area, the frontal super peduncular protocerebrum (fspp; Fig. 17A). Moreover, it was observed that some of the cell bodies located on the fspp as well as those located at the dorsal midline send their putative axonal projections to the lower layer of the fb. However, GFP expression on the mb was weakly detected only on the β lobe (Fig. 17B). A

remarkable signal was evident in the fibers that innervate the sog, as well as the cell bodies located lateral to it. The signal was also present in the al, the entire protocerebra including dorsal and ventral protocerebrum. In addition, GFP decorated the lamina monopolar cells in the ol (Fig 17A).

As for the DopR, DopR2 was found to be well expressed in the thoracicoabdominal ganglion. A group of four cell bodies, arranged in a row, was seen between the junction of the brain and the thoracicoabdominal ganglia. They send their projections towards the midline. Most of the cell bodies were located along the midline and send their fine ramification to either ipsilaterally or contralaterally nearby ganglia (Fig 17C).

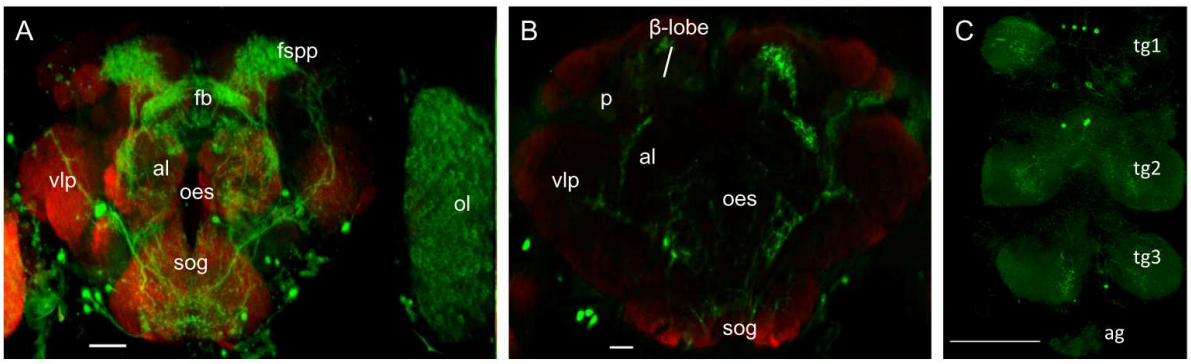

Figure 17: DopR2-GAL4 expression in the adult CNS. Figures (A-C) show immunofluorescence by GFP staining (green) in the cell bodies and the processes of DopR-expressing neurons. The brain was counterstained with an anti-nc82 antibody (red) specific for neuropile regions. (A) Dorsal view of the adult brain showing DopR2-GAL4 expression in neuropils and cell bodies. The frontal-super-peduncular-protocerebrum (fssp), fan-shaped body (fb) antennal lobes (al) and the ventral lateral protocerebrum (vlp) are the most stained neuropils above the esophageal opening (oes) i.e. in the Supraesophageal ganglion. The subesophageal ganglion (sog) is innervated by strongly GFP labeled fibers. GFP decorates the lamina monopolar cells in the optic lobe (ol). Other cell bodies are seen around the vlp, between vlp and ol, around the al and lateral to the sog. (B) Single optical section showing the major neuropil named in (A) and the ß-lobe and pedunculus (p) of the mushroom bodies. (C). DopR2-GAL4 is expressed in the thoracic ganglia 1-3 (tg1-3) and the abdominal ganglion (ag). Scale bars: A-B: 20 µm, C: 200 µm.

Regarding the PDF expressing cells, as for DopR, DopR2 was also expressed in these cells. DopR2-GAL4 driver labeled the clock neurons that colocalized with PDF positive cells, indicating the expression in l-LNvs (Figure 18A-D) and a relatively weak GFP signal was seen in s-LNvs clock neurons (data not shown).

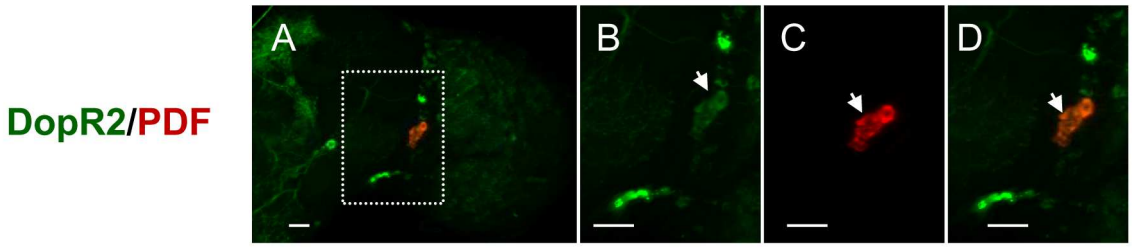

Figure 18: Colocalization of DopR2 expressing cells with clock neurons expressing pigment dispersing factor (PDF). (A-D) Single optical sections; DopR2-GAL4 expressing cells stained with anti GFP (green), in the ventral lateral clock neurons and anti PDF in red. Both labels, specific for DopR2 neurons and for PDF show an unequivocal colocalization (merge, yellow). Scale bars: 20 µm.

In contrast to DopR, DopR2 is not expressed in the dopaminergic neurons as evidenced by immunostaining with anti DDC antibody. There was no colocalization of signals between anti GFP and anti DDC (Fig. 19) and also DopR2 transcript was not detected by RT-PCR (Fig. 13E).

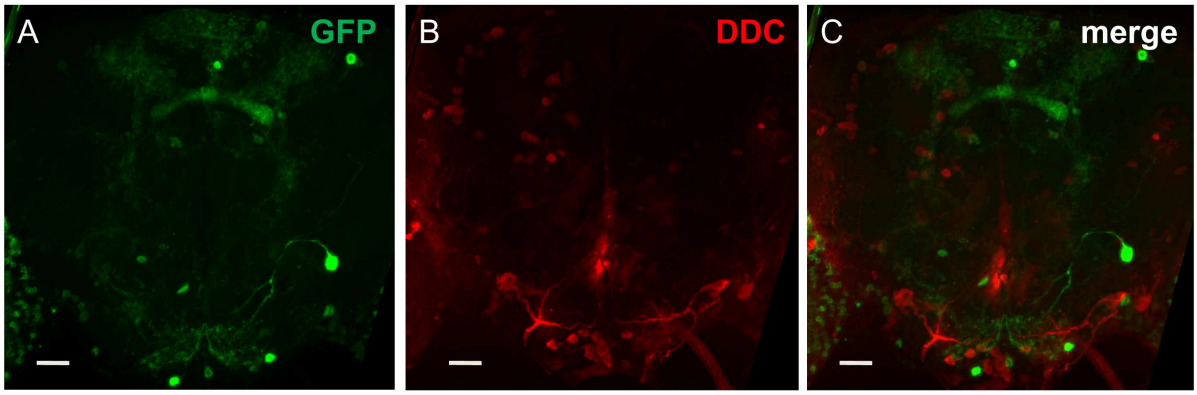

Figure 19: DopR2 is not expressed in the dopaminergic neurons. (A) A projection of optical sections from adult central brains immune-stained by anti-GFP antibody (green) and (B) co-stained by anti DDC (red). (C) No overlaps between the two fluorescent signals. Scale bar: 20 µm.

In the third instar larval guts, DopR2 was found to be expressed in the absorptive Enterocytes (ECs) of the mid and hind guts. In the midgut the GFP positive ECs were identified by their large nuclei size stained by DAPI (Fig. 20A).

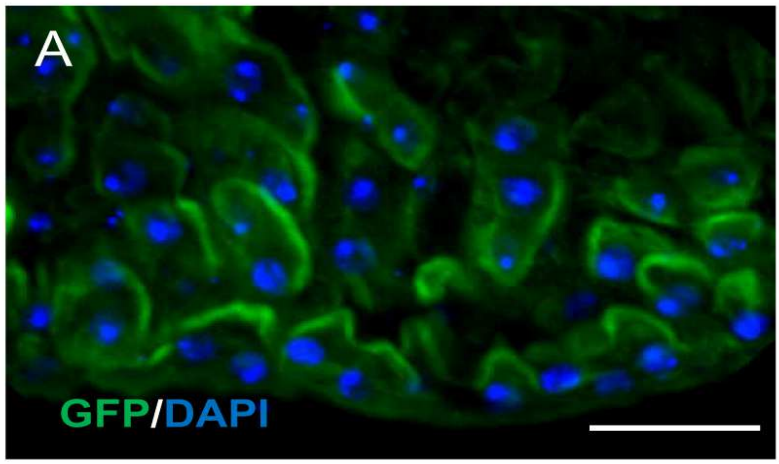

Figure 20: DopR2 is expressed in the Enterocytes of the midgut. Section of the larval midgut stained by anti GFP (green) and co-stained with nuclear marker, DAPI (blue). Due to fusion of mCD8 protein to GFP (mCD8-GFP) the localization is seen in the cell membrane. Scale bar: 50 µm.

In the hindgut it was important to counter stain with fluorescent phalloidin to rule out the expression of DopR2 in the gut muscles. Phalloidin binds to F-actin filaments in the cells. There was no overlap between phalloidin stain and GFP that was observed in stained hindguts (Fig. 21A-C).

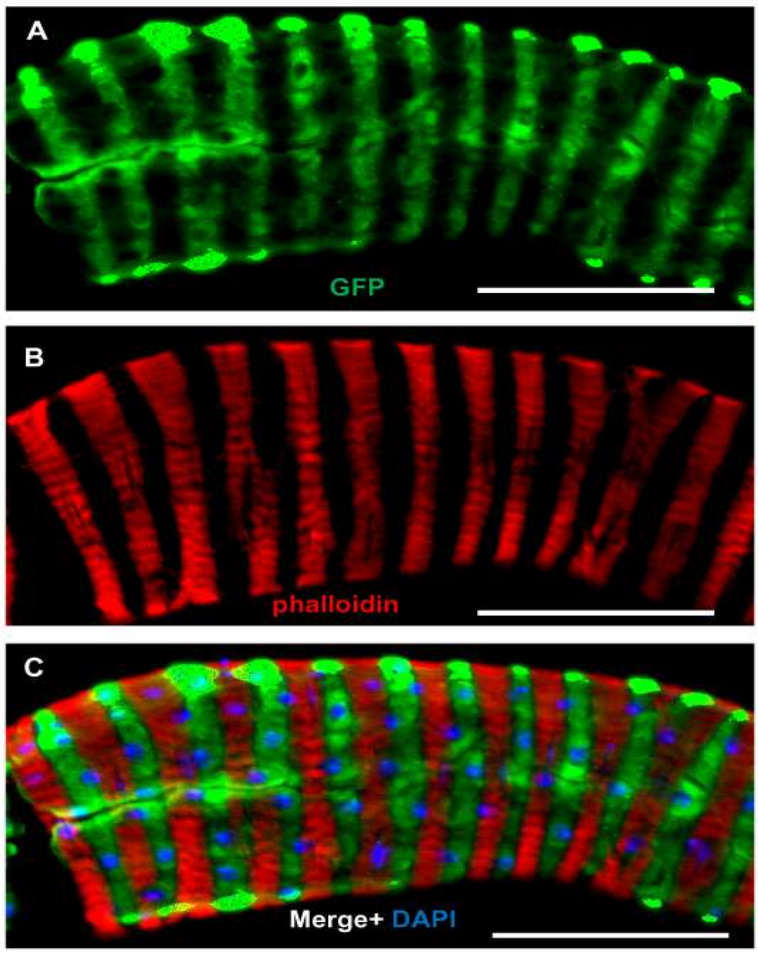

Figure 21: DopR2 is expressed in enterocytes of the larval hindgut. Immunofluorescence staining by anti-GFP (A), phalloidin marking actin filaments in muscle cells (B) and a composite image of A and B, plus nuclei marker, DAPI (C). Scale bars: 50 µm.

3.1.3 DopEcR EXPRESSION IN LARVAL AND ADULT CENTRAL NERVOUS AND DIGESTIVE SYSTEMS

A previous *in situ* hybridization study (Srivastava et al., 2005) showed that the DopEcR expression level was downregulated in third instar larval CNS. The expression was restricted to a narrow band of cells extending from the anterior dorsal to the posterior ventral regions of the brain lobes. Noteworthy, this study sought to determine the expression pattern using the GAL4/UAS system. In general, the expression pattern of DopEcR in larval CNS is similar to what was described for DopR. In the brain lobes, the GFP signal was strong in the mb lobes and the ca. Both, the mb lobes and the ca were innervated by strongly GFP labeled clusters: the DM, DL1, and DL2 (Fig.22B). Concerning the sog, I was able to distinguish one anteriomedial cluster, SM1 (Fig 22A) and a lateral cluster SL (Fig 22B). The GFP

signal was barely seen in the larval vnc, except in the few cell bodies located within or lateral to the neuropil (Fig 22A, asterisks).

In contrast to what was observed in the larval CNS, the DopEcR-GAL4 was weakly expressed in the adult brain. There was no single cell or cluster of cells which was labeled by GFP. A faint GFP signal was detected in the mb lobes (Fig 22C). The antennal mechanosensory and motor center (ammc), the ca and the laminal layer (lm) were the only regions with the moderate GFP signal (Fig 22C, D). GFP was also seen in the few nerve fibers within the sog (Fig 22D). There was no specific GFP signal detected in the thoracicoabdominal ganglia (data not shown).

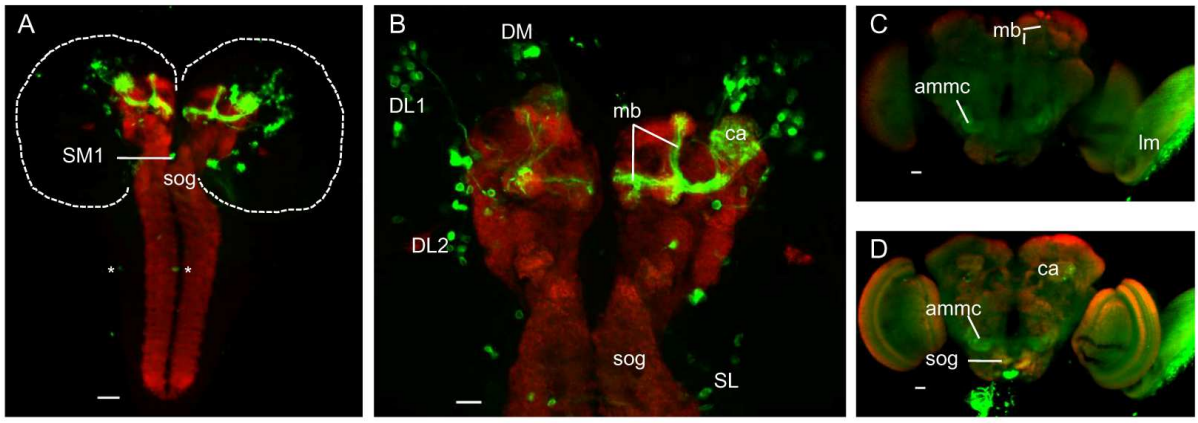

Figure 22: DopEcR-GAL4 expressions in whole-mount third instar larval and adult CNS. (A-D) Shown is the immunofluorescence obtained with anti- GFP staining (green) in the cell bodies and the processes of DopEcR-expressing neurons. The brain was counterstained with an anti-nc82 antibody (red) for neuropils. (A) Shows the DopEcR expression in the brain hemispheres (circled area) and the vnc below the sog. Antero-medial to sog is the cluster SM1. In the vnc, few cell bodies are positive for GFP (see asterisks). (B) Higher magnification of the brain hemispheres showing the strong GFP signal on the axonal terminal of the mushroom body lobes (mb) and the dendritic ca. Three clusters the DM, DL1 and DL2 with their processes projecting to the mb lobes and the ca are also positive for GFP. GFP is also seen in the sog and in another cluster located lateral to it, the SL. (C-D) Show a subset of optical sections of the adult brains, anterior and posterior views, respectively. The GFP signal is seen in the antennal mechanosensory and motor centers (ammc), laminal layer (lm), ca and the sog. A faint signal is also detected in the mb lobes. Scale bars: 20 µm.

The intestinal system was not subjected to a detailed analysis using DopEcR>UAS-mcD8-GFP progenies, as no expression was detected via live imaging by fluorescent microscope.

3.1.4 D2R EXPRESSION IN LARVAL AND ADULT CENTRAL NERVOUS AND DIGESTIVE SYSTEMS

Hearn and colleagues (2002) reported the existence of eight isoforms of the D2R transcript. In connection with the spatial expression pattern of the D2R, (Draper et al., 2007) showed that the D2R is expressed in the larval and adult CNS. Their results were based on the anti-D2R antibody, which was produced from a sequence that corresponds to the third extracellular loop of D2R, a segment conserved among all known D2R variants (Hearn et al., 2002).

Unlike for D1-like receptors, D2R-GAL4 was used to drive either the expression of the responder strains UAS-Cameleon 2.1 (Diegelmann et al., 2002) or 20xUAS-IVS-mCD8-GFP) (Pfeiffer et al., 2010) (data not shown). As reported before by Selcho and colleagues (Selcho et al., 2009) regarding the anatomy of the dopaminergic system, a significantly stronger signal was obtained with UAS-Cameleon 2.1 compared to UAS-mCD8-GFP. By double labeling with anti-GFP (Fig. 23B) and anti-nc 82 (Fig. 23C) antibodies, it was possible to visualize a comprehensive network of neurons spreading all over the larval CNS. Interestingly, their cell bodies were located on the lateral side of the neuropils including the mb regions, ca, the dorso- and baso-medial protocerebra and the sog (Fig 23A).

With respect to the ventral nerve cord, the pattern of expression for D2R-GAL4 neurons was similar to that of DopR. Some of the neurons had their cell bodies located on the cellular area while others were located either to the lateral edge or within the neuropil region (Fig.23A asterisk, arrow head and arrow respectively). In general, this receptor was highly expressed in the larval CNS.

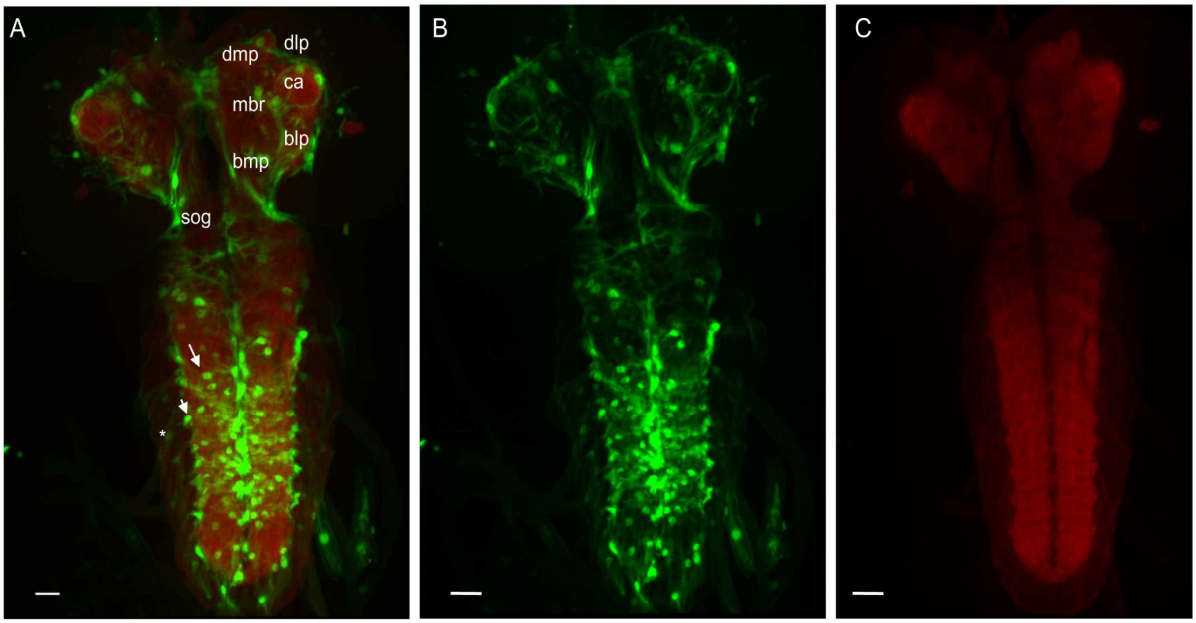

Figure 23: D2R-GAL4 expression in the third instar larval CNS. (A-C) Shown is the immunofluorescence by anti-GFP staining (green) in the cell bodies and the processes of D2R-expressing neurons. The brain was counterstained with an anti-nc82 antibody (red) for neuropils. Each panel shows the projections of optical stacks. (A) A composite image of B and C larval CNS showing the GFP labeled cells located around the dmp and dlp (dorsomedial and lateral protocerebrum, respectively), and the basalmedial and lateral protocerebrum (bmp and blp, respectively). Other areas include the dendritic ca and the sog. In the vnc, some of the neurons have their cell bodies located on the cellular area while others are located either on the lateral edge or within the neuropil region (asterisk, arrow head and arrow, respectively. Scale bars: 20µm.

Similar to what was observed in the larval CNS, the D2R was expressed in the outer margin of the major neuropils, such as the mb lobes, ca, pedunculi and the cc in the adult brain. Because of the weak signal in the mb lobes, they were not visible when the maximum projection of z-optical stacks was made (Fig 24A, B). The GFP signal was also detected in all the cc substructures. The strongest signal was displayed in the pb (Fig 24B, white arrow). D2R was weakly expressed in the ol, al and the midline toward the sog (Fig 24A).

In contrast to what was observed in the larval ventral nerve cord, the thoracicoabdominal ganglion was only weakly expressing D2R. The GFP signal was detected in few neurons, which were found along the midline between the third thoracic ganglion and the abdominal ganglion (Fig 24C).

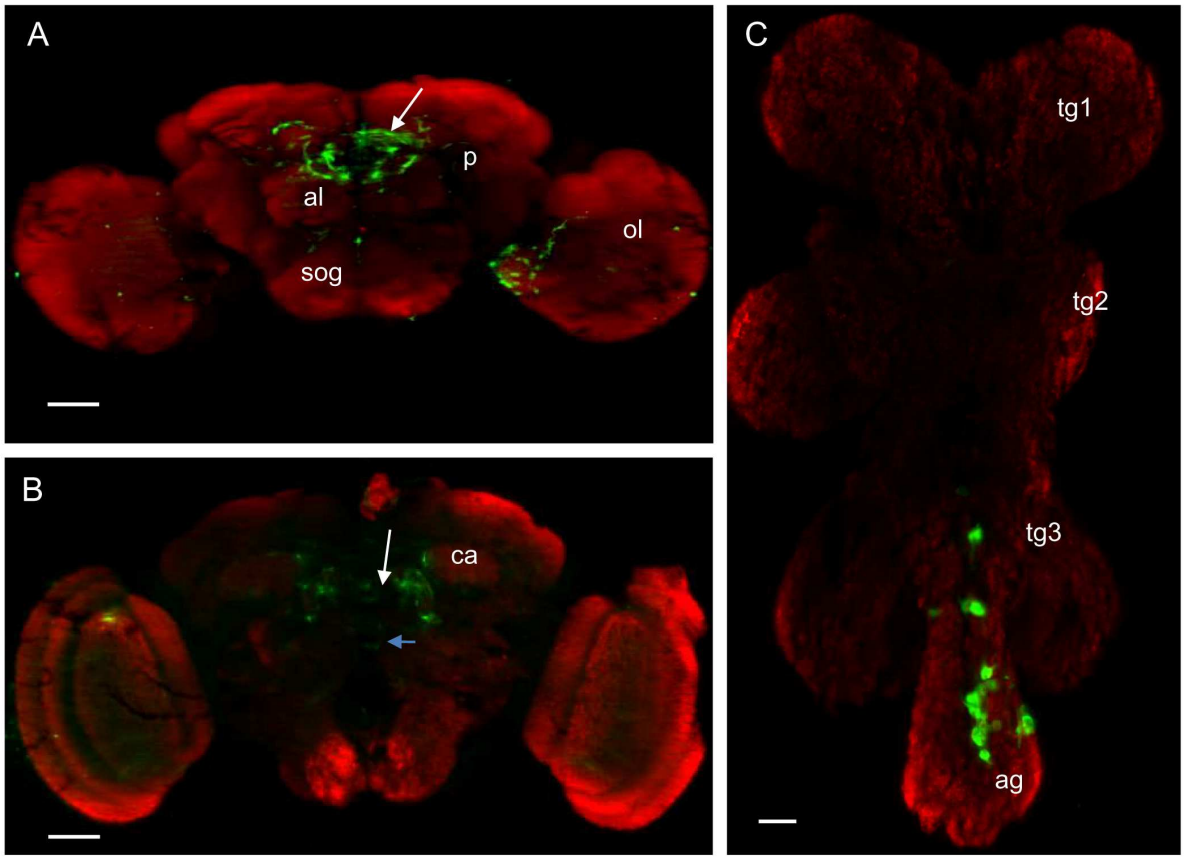

Figure 24: D2R-GAL4 expression in the adult CNS. (A-C) Shown is the immunofluorescence obtained by anti-GFP staining (green) in the cell bodies and the processes of D2R-expressing neurons. The brain was counterstained with an anti-nc82 antibody (red) for neuropils. Each panel shows the projections of optical stacks. (A) Anterior view showing the neuropils, which are GFP positive; the central complex (arrow), around the pedunculus (p), weakly around the al, and few cells in the ol. (B) Posterior view showing GFP signal in the protocerebral bridge (white arrow), around the ca and the nodulus (blue arrow). (C) D2R-GAL4 expression in the adult ventral nervous system. The GFP signal is seen in the few cells located along the midline between the third thoracic ganglion, tg3 and the abdominal ganglion, ag. Scale bars: 20 µm.

In conjunction with what was observed in the CNS, D2R was expressed in intestinal stem cells (ISC) and enteroblasts (EB). Earlier studies reported the expression of D2R in the cell bodies located in the posterior midgut (Draper et al., 2007; El-Kholy PhD thesis, 2010). To unequivocally specify the type of cells, several midgut tissues were first immunostained with anti GFP and anti prospero and anti Nc82 antibodies. These preparations show no colocalization of signals between GFP positive cells and either prospero positive cells or Nc82 positive cells (Appendix 1, Fig. A2 & A3). These findings suggested that D2R is not expressed in the EE cells. Based on their shapes and size of their nuclei they were definitely not EC cells. The only remaining possibility was them been either ISC or EB or both. To confirm this, several tissues

were first immunostained with anti delta antibody. Delta is used as a specific marker for ISC in the *Drosophila* midgut. It acts as an ISC membrane bound ligand to stimulate the receptor Notch in the neighboring EB. It was observed that a subset of GFP positive cells were also positive for anti delta antibody (Fig. 25A-D). This brought a speculation that the GFP positive cells, which were not delta positive, could be EB cells.

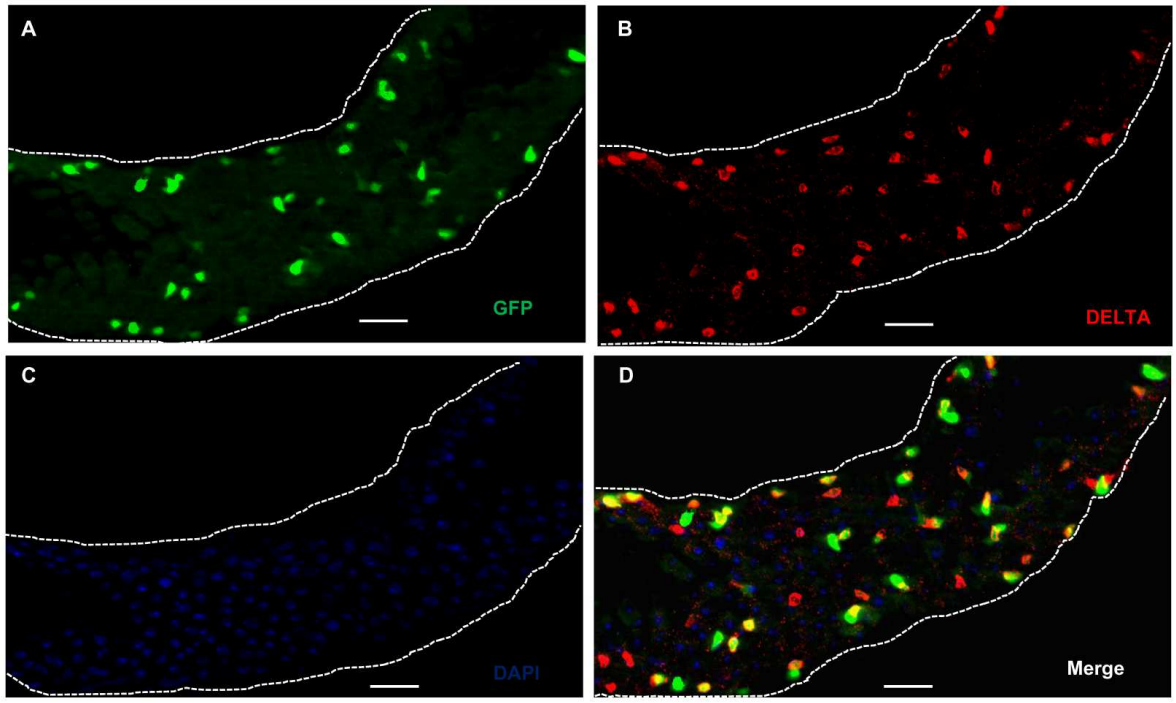

Figure 25: D2R is expressed in the intestinal stem cells (ISC). (A-D) Shown is a projection of optical sections of the third instar larval midguts of D2R-Gal4>UAS-GFP. (A) Enhancement of GFP reporter for D2R-Gal4 expression in ISC by anti GFP antibody. (B) Delta positive cells stained by anti delta antibody. (C) DNA/nuclei marker, DAPI. (D) A merged image showing overlaps of fluorescent signals, yellow and some GFP positive cells (green) which were not marked by delta. Dotted lines demarcate the tubular structure of the gut. Scale bars: 20 µm.

To confirm this, again several midgut tissues were immunostained with anti Notch antibody. It was clearly shown that the remaining GFP positive cells were also labeled by an anti Notch antibody, suggesting expression of D2R also in the EB cells (Fig. 26A-D).

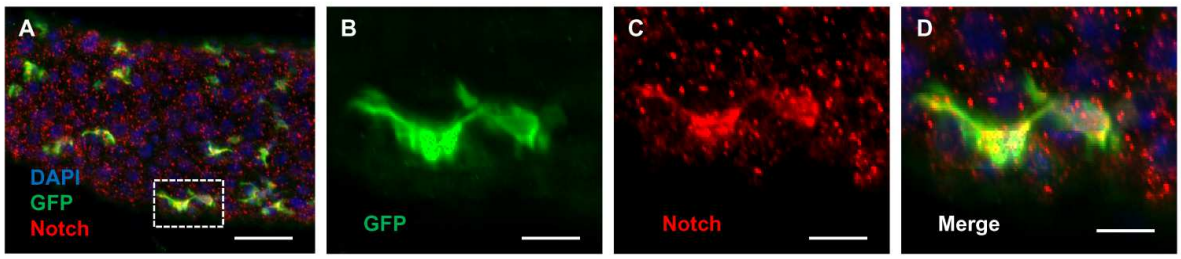

Figure 26: D2R is expressed in the Enteroblast cells (EB). (A-D) D2R-Gal4 driven GFP in the larval midgut; immunofluorescence staining with anti GFP (green), anti Notch (red) and with DAPI (blue). (A) Dotted box shows a single EB with its enlargement shown in B-D. Scale bars: 20 µm.

3.2 DOPAMINERGIC CELLS DISTRIBUTION IN THE LARVAL MIDGUT

Having analyzed the expression patterns of dopamine receptors in the midgut system, it was interesting to show where dopamine is secreted within the system. The dopaminergic cells (DA) were identified by use of the TH-GAL4 driver. TH-GAL4 is a driver that expresses GAL4 under the control of promoter sequences of the tyrosine hydroxylase gene (Friggi-Grelin et al., 2003). Tyrosine hydroxylase (ple) catalyzes the rate limiting step in DA biosynthesis, thus all DA cells express TH. Tissues from TH-GAL4>20xUAS-mcD8::GFP progenies were immunostained by anti GFP and anti prospero antibodies. Six GFP positive cells found at the anterior part of the midgut were also positive for prospero, suggesting their secretory role in the gut (Fig. 27A-C).

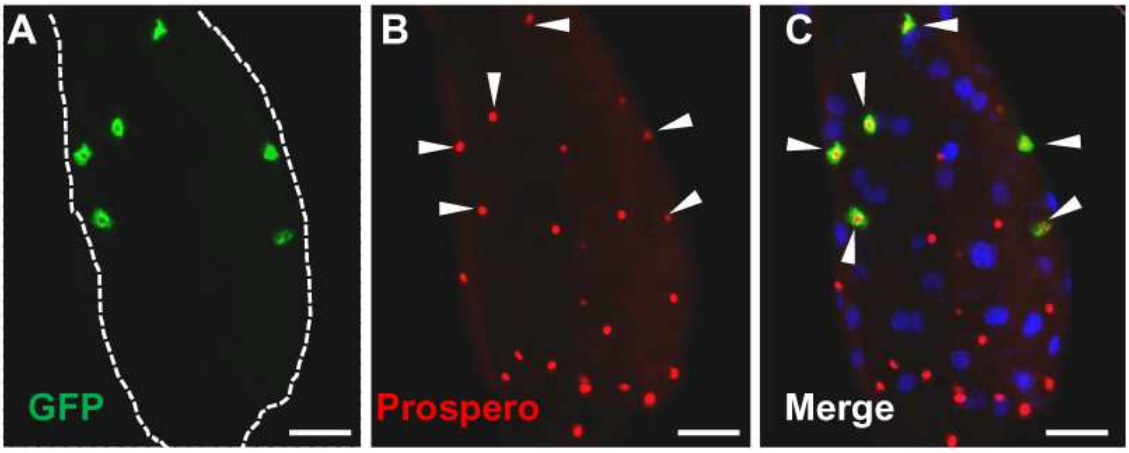

Figure 27: Distribution of Dopaminergic cells in the larval midgut. (A-C) Shown is a projection of optical sections of the third instar larval anterior midgut of TH-GAL4>20xUAS-mCD8::GFP. (A) Six GFP positive cells (green). (B) Prospero positive cells stained by anti prospero antibody (red, arrow heads). (C) A composite image showing overlaps of fluorescent signals (arrow heads) and a DNA marker, DAPI (blue). Scale bars: 20 µm.

3.3 FUNCTIONAL ANALYSIS OF DOPAMINE RECEPTORS

3.3.1 MODULATION OF INTRACELLULAR SIGNALING IN DOPAMINE RECEPTOR EXPRESSING NEURONS

Designer Receptors Exclusively Activated by a Designer Drug (DREADDs) are modified G-protein coupled receptors that are activated only by a synthetic ligand, namely by Clozapine-N-Oxide (CNO) (Armbruster et al., 2007). In mammals, DREADD technology has been used to manipulate cellular signaling and control of behaviors (Nichols and Roth, 2009). Recently, the Nichols laboratory demonstrated the utility of this technology in *Drosophila* (pers. comm. CD Nichols, USA). They created three important UAS-DREADD transgenes, the UAS-M1D1 that allows to induce the increase of Ca^{2+} levels, UAS-M4D1 that decreases cAMP levels and UAS-M5Dbar that increases the levels of cAMP. Dopamine receptors being GPCRs control many physiological and behavioral processes through either activity of adenylate cyclase, which increases or decreases the levels of cAMP or phospholipase C beta (PLC-β) that modulates the release of Ca^{2+} in the cytosol. To test whether DREADD expression *in vivo* modifies the locomotor behavior of adult flies, all four dopamine receptor Gal4 strains were used to drive the expression of matching UAS-DREADD transgenes. DopR-Gal4, DopR2-Gal4 and DopEcR-Gal4 are known or are believed to induce activation of the adenylate cyclase, thus leading

to cAMP production. Thus, I used the corresponding Gal4 lines to drive expression of UAS-M5Dbar that allows to induce an increase in cAMP in these cells. The corresponding F1 flies were fed 1 mM CNO and compared with non-induced animals of the same genotype. CNO itself had no effects on the mean locomotor activity. Activation of the DopR and DopR2 led to decreased locomotor activity levels per 24 hours. This was quantified using the DAM system (Fig. 28A). Monitored hourly (circadian activity), the same flies showed the bimodal pattern of activity with a prominent burst of activity around the light-off-to light-on transition (ZT0-ZT2, morning peak). The evening peak was observed around lights-on-to-light-off transition (Fig. 28B-C). The DopEcR-Gal4 x UAS-M5Dbar F1 flies fed with 1 mM CNO showed a slightly decreased locomotor activity compared to control flies but the difference was not significant. Similar results were obtained when M1D1 was overexpressed in DopR2 cells with the DopR2-Gal4 driver (DopR2>M1D1). The overexpression of M4D1 in relation to D2R-Gal4 showed the same performance in activity between CNO fed and not fed flies. As already mentioned, the activity of wild type flies (Canton-S), which were used as an overall control was not affected (Fig. 28).

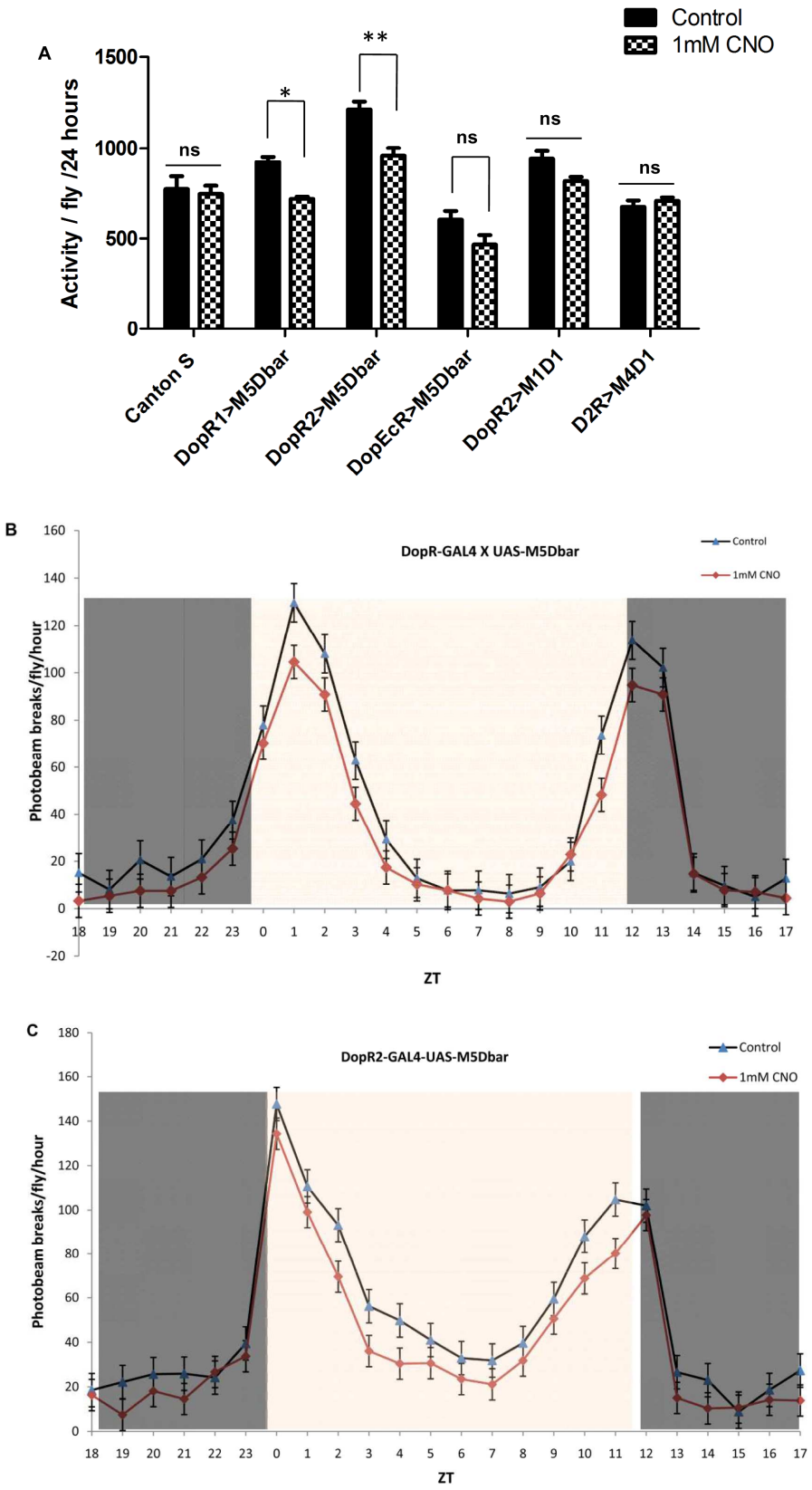

Figure 28: Locomotor activity of flies overexpressing DREADDs in the pattern of different dopamine receptors. (A) F1 flies obtained from DopRs-Gal4 drivers crossed to UAS-M5Dbar, UAS-M1D1 and UAS-M4D1, respectively. The patterned bars show activity levels of flies treated with 1 mM CNO compared to matching control flies (black bars), monitored using the DAM system for 3 days. Activation of M5Dbar in relation to DopR and DopR2 reveals

a significant decrease in total activity counts per 24 hours. No significant changes in activity observed in other groups including wild type strain, Canton S. *p<0.05, **p<0.01, two way ANOVA with Bonferroni post hoc test for multiple comparison; n = 16 flies per genotype and error bars represent SEM. (B-C) Line graphs showing the circadian activity per fly per every hour of F1 flies overexpressing M5Dbar in to the pattern of DopR and DopR2, respectively. Gray shaded area illustrates dark condition, ZT0= light on, ZT12= light off.

3.3.2 EXPRESSION OF INTERFERENCE TRANSGENES IN VIVO IN THE PATTERN OF DOPAMINE RECEPTORS

Expression of endogenous DopRs mRNA was silenced by an RNAi approach. Flies carrying either the UAS-ds-DopR, UAS-ds-DopR2 or UAS-ds-D2R transgene were crossed to the n-syb-Gal4 driver which drives expression in all neurons. These flies will be referred hereafter as DopR-RNAi, DopR2-RNAi and D2R-RNAi, respectively. To monitor their locotomor activity the DAM system was used again under the identical setting as described above. These analyses demonstrated that only D2R-RNAi flies showed a significant decrease in total activity counts. DopR-RNAi and Dop2RNAi flies showed no significant change in their performances relative to negative control flies Nos-RNAi (Fig. 29). Nos stands for nitric oxide synthase, an enzyme that catalyzes the production of nitric oxide from L-arginine. Among other tissues, it is highly expressed in the nervous system. Importantly, there was a significantly different level of activity between DopR-RNAi and DopR2-RNAi and D2R-RNAi flies. Nevertheless, there was no significant difference in total activity between DopR2-RNAi and D2R-RNAi flies (Fig. 29).

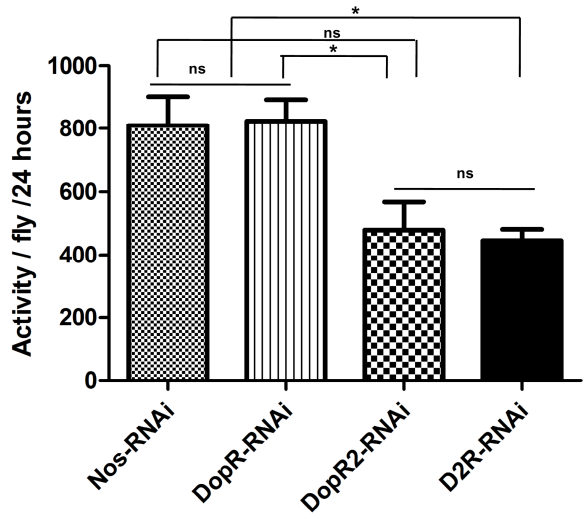

Figure 29: Locomotor activity of DopRs-RNAi flies. Locomotor activity counts of four RNAi-interference fly lines (UAS-ds-DopR, UAS-ds-DopR2, UAS-ds-D2R and UAS-ds-Nos) driven by n-syb-Gal4 driver and analyzed by the DAM system. D2R-RNAi flies showed substantially reduced locomotor activity counts per 24 hrs in comparison to control flies (Nos-RNAi) and DopR-RNAi flies. DopR-RNAi and DopR2-RNAi flies have no significant difference in activity with respect to control. However, there is a significant difference between DopR-RNAi and DopR2-RNAi flies. The levels of activity counts of DopR2-RNAi and D2R-RNAi flies seemed to be similar. *p<0.05, one way ANOVA with Tukey's post hoc test for multiple comparison; n = 8 flies per genotype and error bars represent SEM.

3.3.3 EFFECT OF LOSS-OF-FUNCTION MUTATIONS OF THE DOPR

As explained in the section 3.3.2 above, the knockdown of DopR did not affect the basal locomotor activity of the tested flies. Locomotor activity in flies reflects sleep-wake transitions. It has been shown that, dopamine controls this endogenous generated form of arousal through DopR (van Swinderen and Andretic, 2003)

It was then interesting to test this behavior in flies with a hypomorphic mutation in DopR. These flies will be referred hereafter as $DopR^{f02676}$ and the wild type strain Canton-S (CS) was used as a control. As it was the case for DopR-RNAi flies, the locomotor activity was monitored using the DAM system. In contrast to what was observed in DopR-RNAi flies, $DopR^{f02676}$ mutant flies showed a decreased activity pattern over a 24 hours period in comparison to control flies in LD cycle (Fig.30A). The phenotype was stronger in constant darkness (DD) conditions (Fig. 30B). Monitoring at one hour intervals, $DopR^{f02676}$ flies showed considerably decreased activity in comparison to control flies during the night phase (Fig. 31A). In constant DD conditions $DopR^{f02676}$ maintained the morning and evening peaks but with highly reduced activity in comparison to control flies (Fig. 31B).

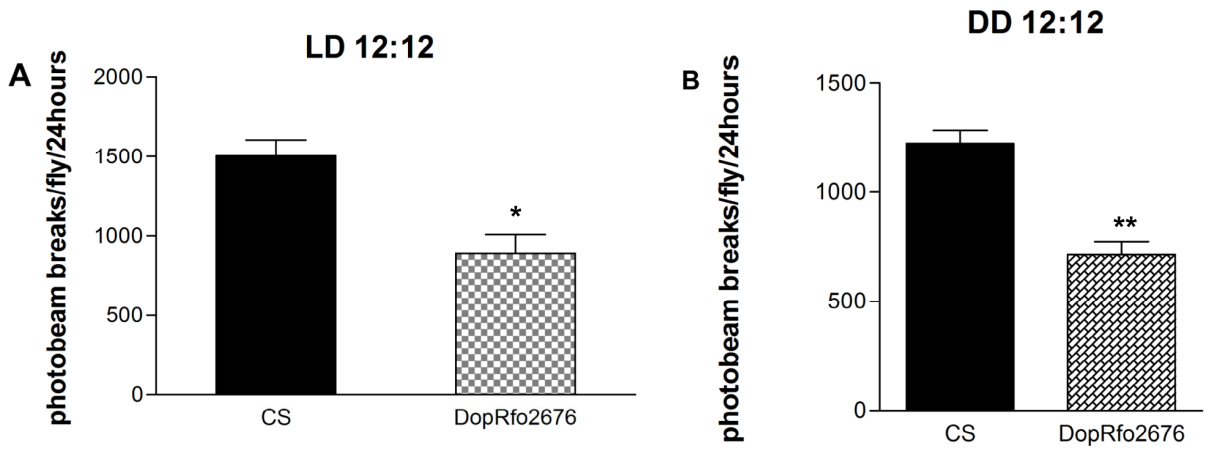

Figure 30: DopR mutant flies show reduced locomotor activity. (A-C) Total activity counts per 24 hrs in both light/dark (LD) and dark/dark (DD) conditions. (A) DopR mutant flies (DopRf02676) showed decreased locomotor activity in comparison to control, Canton-S (CS) flies in LD cycle. (B) The stronger effect of reduction is seen in DD cycle. *p<0.05, **p<0.01, Unpaired t-test with Welch's correction; n = 16 flies per genotype and error bars represent SEM.

To further confirm the observation that DopR deficiency leads to night hypoactivity during LD cycle, a DopR rescue experiment was performed. The $DopR^{f02676}$ mutation was caused by a piggyback transposon insertion on the first intron of the DopR allele. Taking advantage of Gal4 UAS element in the first intron of the $DopR^{f02676}$ allele (Fig. 32A) (Lebestky et al., 2009), a Pdf-Gal4 driver was employed. This strategy has been used successfully to rescue the learning and memory deficit observed in DopR mutant flies (Kim et al., 2007). Interestingly, Pdf-Gal4x $DopR^{f02676}$ F1 flies showed a partial rescue of this phenotype especially at and post evening peak hours relative to w^{1118}x $DopR^{f02676}$ F1 flies (Fig. 32B).

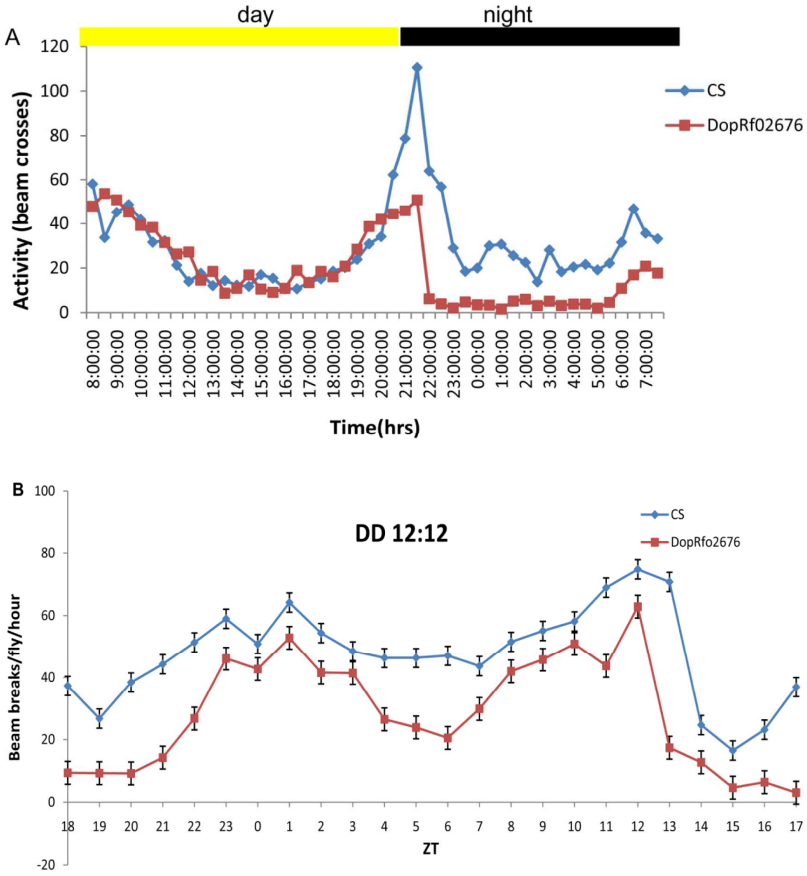

Figure 31: DopR mutant flies have reduced night phase activity. (A-B) Circadian activity of DopR mutants (DopRf02676) and matching controls, CS flies. (A) Note lessened activity of DopR mutants (red) relative to CS (blue) during the night phase. (B) Circadian activity of the DopR mutants and control flies in constant darkness conditions.

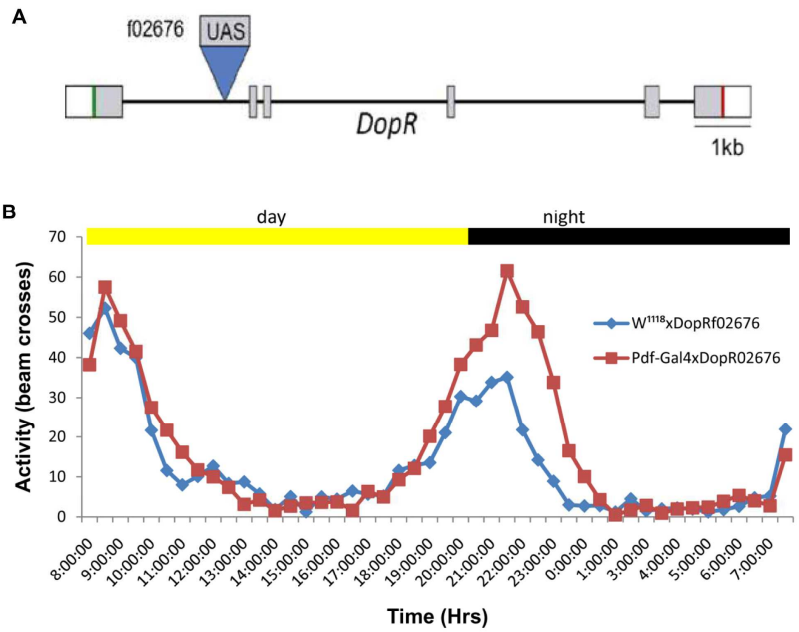

Figure 32: Rescue of the night hypoactivity phenotype of DopR mutant flies. (A) Structure of the DopRf02676 insertional allele, the UAS is in the first intron (Lebestky et al., 2009). (B) Circadian activity of control flies, w^{1118}x DopRf02676 (blue) and rescue flies, Pdf-Gal4x DopRf02676 (red). Note the partial rescue of night hypoactivity at and post evening peak (20-1 hrs).

3.3.4 ACTIVATION OF PHOSPHOLIPASE C-BETA (PLC-β) WITH REGARD TO DOPR2

Stimulation of PLC-β activity leads to mobilization of intracellular Ca^{2+} within the cell. As shown earlier in Fig. 20, DopR2 was expressed in enterocyte cells of the midgut. This study then sought of testing whether activation of this receptor *in vivo* would trigger the action of PLC-β within the enterocytes. To achive this, NP1-Gal4 x UAS-PLC-β::mRFP F1 fly midguts were used for the experiment. Immediately upon dissection, the endogenous agonist for DopR2, 3-Hydroxytyramine (dopamine) was applied on top of the tissue. The concentration of agonist was ranging from 10^{-1}M to 10^{-9}M and HL3 buffer was used as a vehicle control. As seen in Fig. 33 all the concentrations used trigger the translocation of PLC-β from the cytoplasm to the plasma membrane in comparison to the control.

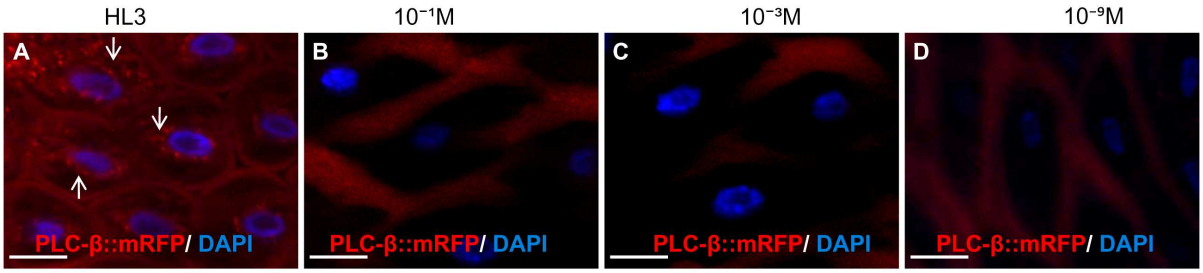

Figure 33: DopR2 mobilizes intracellular Ca^{2+} via PLC-β in enterocytes. (A-D) Optical sections of midgut enterocyte cells with native PLC-ß fused to monomeric Red Fluorescent Protein (PLC-ß::mRFP, red) and DAPI staining, blue. (A) Signal for PLC-ß::mRFP is seen in cytoplasm surrounding the nuclei (arrows) in a vehicle control (HL3 buffer). (B-D) Cytoplasm is devoid of signals after PLC-ß::mRFP has been recruited to the plasma membrane upon dopamine application (10^{-1} M, 10^{-3} M, 10^{-9} M). Scale bars: 20 µm

3.4 INDUCTION OF PARKINSONIAN SYMPTOMS IN DROSOPHILA

To model PD in a fly, the TH-GAL4 transgenic line was crossed to the 20xUAS-mCD8::GFP reporter line and the progenies were used for the subsequent experiments. As described before in section 3.2, TH-GAL4 is a driver that expresses GAL4 under the control of promoter sequences of the tyrosine hydroxylase gene. Tyrosine hydroxylase codes for the enzyme catalyzing the rate-limiting step in DA biosynthesis. Thus, DA neurons express TH.

3.4.1 EFFECT OF ROTENONE TO FLIES IS DOSE DEPENDENT

To determine the effect of rotenone in flies, a series of concentration was added to the food. After 9 days of exposure, the effect of rotenone was determined by using the climbing ability test. Normally, flies climb up the sides of the vial after mechanical stimulation (Le Bourg and Lints, 1992). This behavior was impaired in flies treated with higher doses of rotenone. Rotenone was applied at sublethal doses (<10 mM) i.e. concentration above this was lethal to flies. It was observed that in absence of rotenone most flies cross the escape line (see section 2.2.5.1) after 20 sec. On the contrary, flies, which were exposed to rotenone showed difficulties crossing this line and the effect was stronger with higher doses (Fig. 34). The 5 mM concentration was chosen for the subsequent experiments.

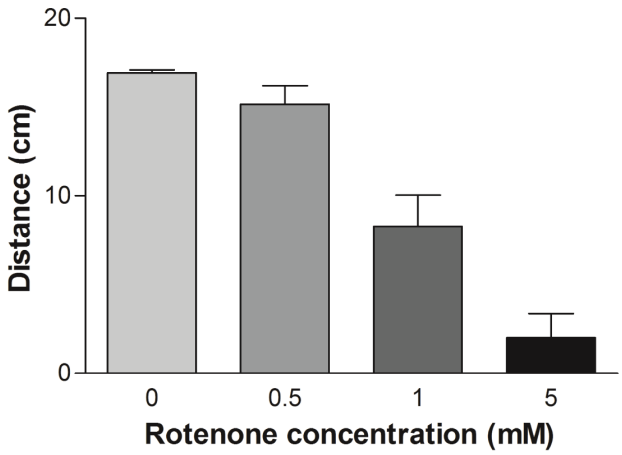

Figure 34: Effect of rotenone to *Drosophila* is dose dependent. Climbing ability test of 12 days old male flies exposed to various concentration of rotenone for 9 days. The median distance/height climbed ± SEM (n=20) is shown.

3.4.2 ROTENONE EXPOSURE AFFECTS LOCOMOTOR BEHAVIOR IN FLIES

Locomotor behavior of flies treated with 5 mM rotenone for 9 days was quantified by negative geotaxis assay and the DAM system. In both assays, the treated flies showed reduced locomotor ability in comparison to untreated flies (Fig. 35 A&B).

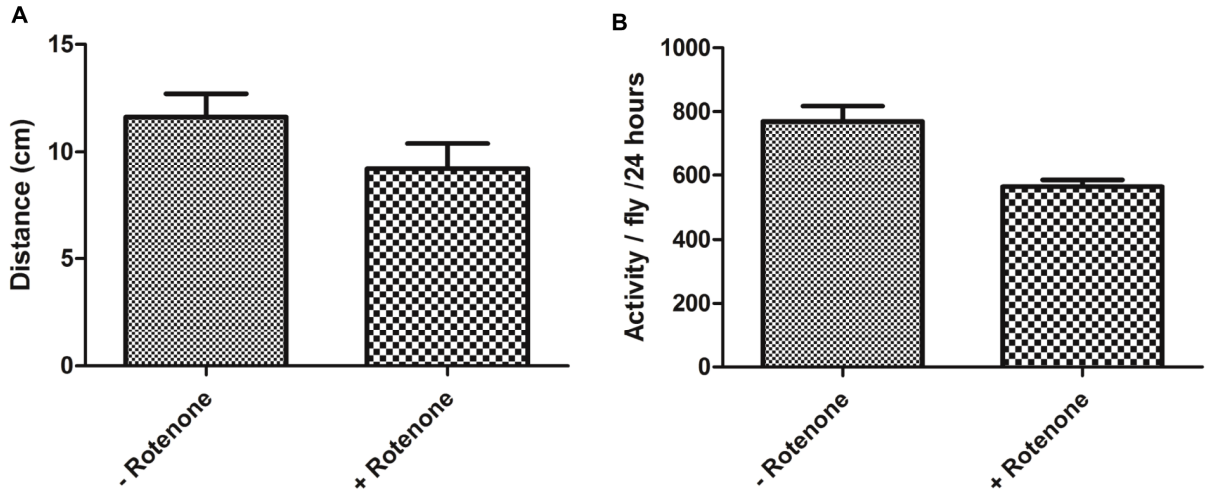

Figure 35: Rotenone induced locomotor deficits in *Drosophila*. A. Negative geotaxis assay of flies treated with 5 mM rotenone (+Rotenone) and control flies (-Rotenone) for 9 days, n = 20 flies per group. (B) Locomotor activity assay measured using the DAM system, n = 16 flies per group.

3.4.3 EFFECT OF ROTENONE ON FLIES DEPENDS ON EXPOSURE TIME

Chronic exposure of *Drosophila* to rotenone induced locomotor deficits and dopaminergic neurodegeneration (Coulom and Birman, 2004). In this study the symptoms of locomotor impairment induced by rotenone were observed after 9 days of exposure as shown in (Fig. 35). There was no obvious locomotor deficit observed in flies treated with 5 mM rotenone for 3 days. The phenotype was quantified by climbing ability (Fig. 36) and physical observation.

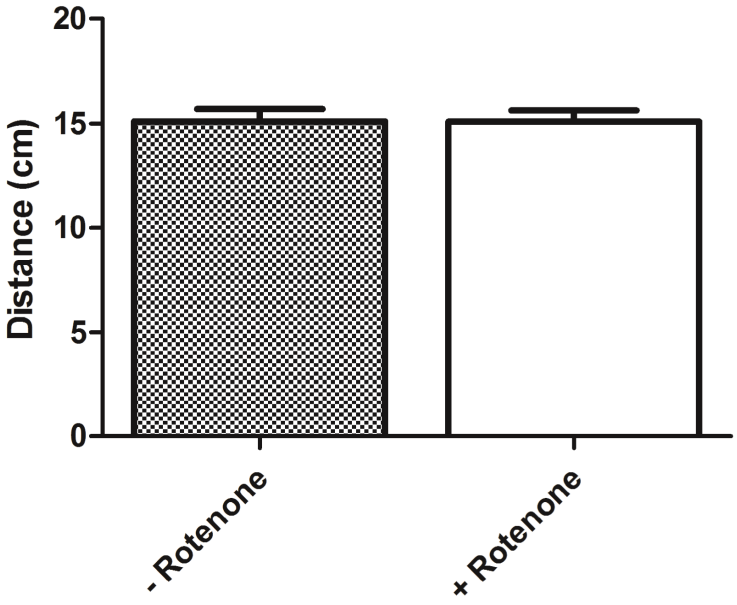

Figure 36: Rotenone effects depend on exposure time. Negative geotaxis assay of 3 days old male flies treated with rotenone (+Rotenone) and control flies (-Rotenone) for 3 days. Note: all flies showed the normal climbing ability, n = 20 flies per group.

3.4.4 GENE PROFILING ANALYSIS AT PRESYMPTOMATIC STAGES OF INDUCED PARKINSON-LIKE PHENOTYPES

This study was chosen to elucidate the molecular changes taking place in DA neurons, the most affected cells in PD patients, of presymptomatic flies (after 3 days of rotenone treatment). I chose this time-point because it has been shown in previous studies that the motor impairment and DA neuron loss begins after chronic exposure with rotenone for few days and that the symptomatic phase starts after the majority of DA cells already died (Coulom and Birman, 2004, Bayersdorfer et al., 2010). Thus, the time chosen ensures that the initial manifestation of PD, when neuronal dysfunction due to rotenone pathology starts or develops, while DA neurons are not yet lost. Consequently, I performed the whole transcriptome analysis with RNA isolated specifically from DA neurons at this stage.

There are numerous DA neurons scattered throughout the adult fly brain but some form specific clusters. Six major DA clusters have been identified (Fig. 37A-B) that project to the specific regions such as mb and cc (Nassel and Elekes, 1992, Tanaka et al., 2008, Mao and Davis, 2009).

Figures 37A'&B' show the anterior and posterior views of adult brains, from which the DA neurons were dissociated. The DA neurons were sorted by biotinylated anti-mouse-CD8 antibody coated magnetic Streptavidin T1 Dynabeads. As a result, the

magnetic beads bound to the mCD8::GFP expressing cells only i.e. DA neurons (Fig. 38A-D).

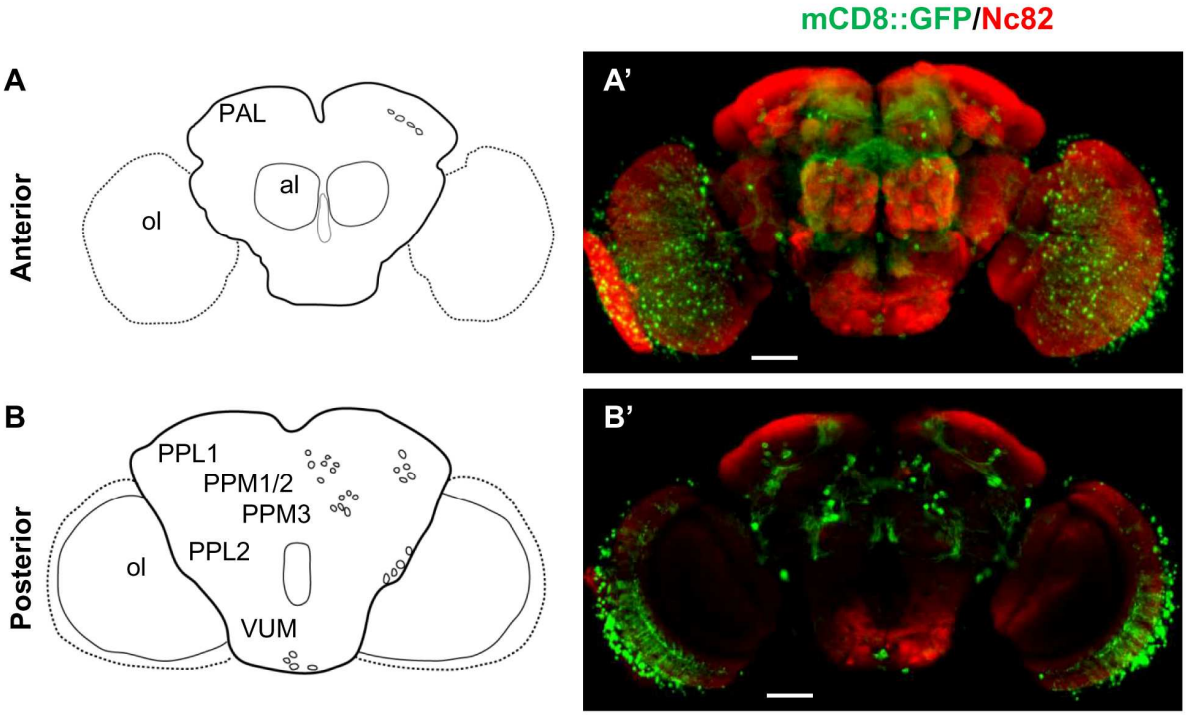

Figure 37: DA neurons in the adult brain of *Drosophila* as visualized with TH-GAL4>20xUAS-mCD8::GFP. (A, A') Anterior view. (B, B') Posterior view. (A, B) Schematic diagram of (A', B') designating the name and location of TH-GAL4 expressing cell clusters in the brain. Circles symbolize cell bodies. PAL: Protocerebral anterior lateral, PPL1: Protocerebral posterior lateral 1 (inferior), PPL2: Protocerebral posterior lateral 2 (superior), PPM (1/2, 3): Protocerebral posterior medial 1/2 and 3, respectively. Cell cluster nomenclature after (Nassel and Elekes, 1992, Mao and Davis, 2009). (A', B') Anti-GFP staining (green) showing cell bodies and processes of TH-GAL4 expressing cells. The brain was counterstained with an anti-nc82 antibody (red) for neuropils. Scale bars: 20 µm.

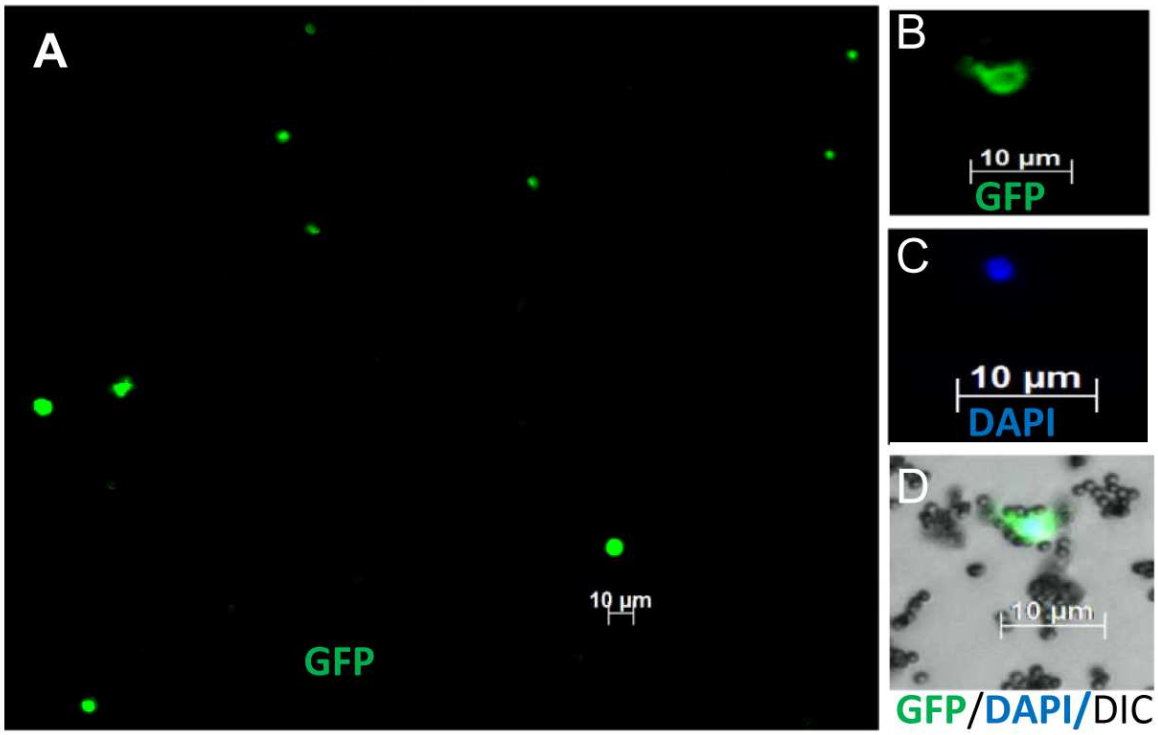

Figure 38: Magnetic beads sorted DA neurons. (A) The purified GFP positive DA neurons sorted with magnetic beads from adult TH-GAL4>UAS-mCD8::GFP brains. (B) Single GFP positive neuron (green), (C) its nucleus stained with DAPI (blue). (D) A composite image of B and C plus differential interference contrast (DIC), note: the cell captured with the beads.

3.4.4.1 ROTENONE INDUCES GENE EXPRESSION CHANGES

While flies treated with 5 mM rotenone for three days appear to move normally (see Fig.36), 765 genes were up-regulated and 357 genes were down-regulated relative to DA neurons isolated from untreated animals. Analysis of differentially expressed genes was performed using the Acuity 4.0 program whereby fold change of >1.5 of the mean signal intensity of a specific gene in at least 2 arrays out of three was considered as upregulated and fold change < 0.67 as downregulated. A complete list of the differentially expressed genes is available in appendix 2, Table A2 & A3. To further filter and identify relevant regulated genes in the two lists, I used the online database DAVID (http://david.abcc.ncifcrf.gov/), which implements the Gene Ontology (GO) terms that associate gene products with biological processes, molecular functions and cellular components. Normally, the program gives several clusters of the overrepresented GO terms containing redundant genes. After removal

of redundant genes, a list of 381 upregulated genes was generated and further clustered into 12 relevant GO terms (referred to as functional categories hereafter). Among those transcripts whose levels were increased in rotenone treated flies were many synapse and protein synthesis related genes. A comprehensive functional categorization revealed that those genes with functions related to signal transduction and cell-cell signaling were changed with the highest frequency (90 genes), followed by cellular transport and extracellular matrix (87 genes), transcription or translation (58 genes), development (29 genes) and metabolism (28 genes). Other important categories are related to stress response (14 genes), regulation of apoptosis (13 genes), protein folding (12 genes) and aging (10 genes) (Fig. 39). This trend might support neuronal viability or the defense mode response towards a mild toxic insult given by rotenone.

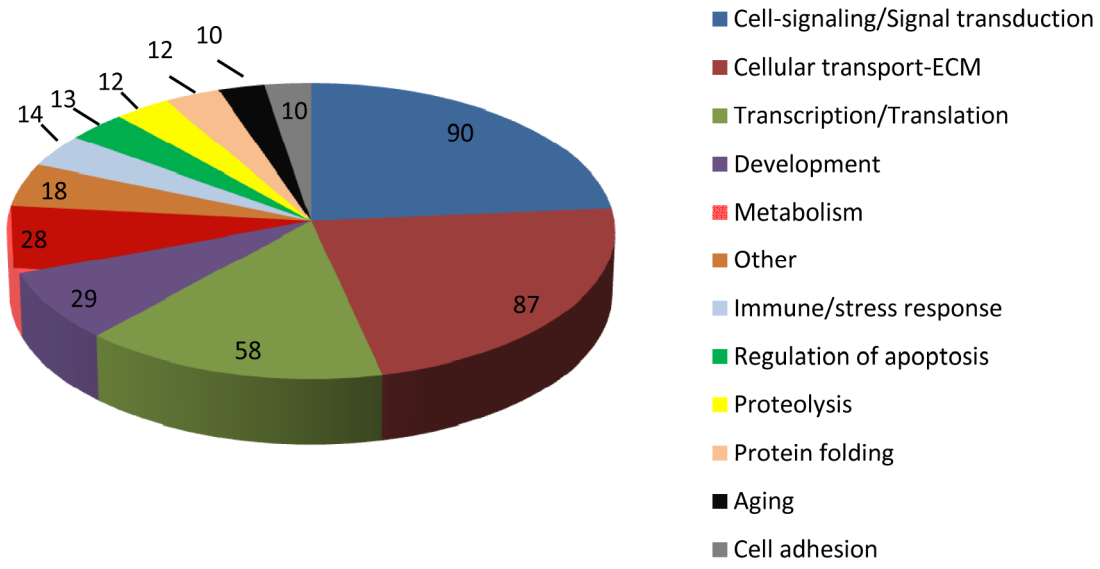

Figure 39: Functional categories of genes upregulated by rotenone. Given are the numbers of genes whose expression levels were increased during rotenone treatment in 3 days old male flies for three days. Clustering was achieved by DAVID and further manually sorted in 12 Gene Ontology categories after removal of duplications.

Likewise, a list of 176 downregulated genes was generated and clustered into 9 relevant functional categories (Fig. 40).

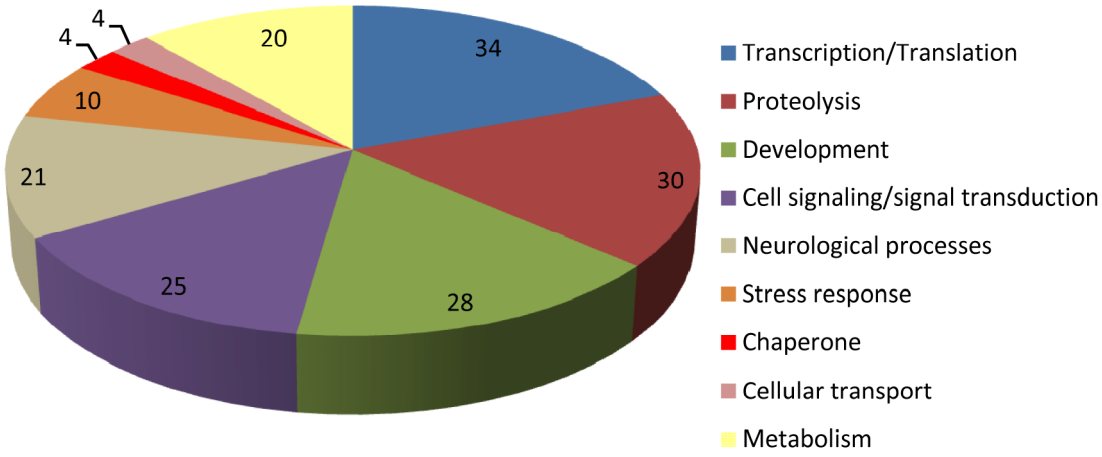

Figure 40: Functional categories of genes downregulated by rotenone. Given is the number of genes whose expression levels were decreased during rotenone treatment in 3 days old male flies for three days. Clustering was achieved by DAVID and further manually sorted in 9 Gene Ontology categories after removal of duplications.

Furthermore, the relevant clusters with high enrichment score and $p < 0.05$ and KEGG_pathways filtered by DAVID were selected and listed as shown in Table 7. For the sake of simplicity each of these pathways will be described separately below, while the clusters will be treated in one section.

Table 7: Enriched functional categories for genes differentially regulated by rotenone

Database identifier	Functional category (Enriched GO terms)	Number of changed genes	p-value <0.05
Upregulated genes			
GO:0032535	Regulation of cell size/Neurogenesis	13	0.022
GO:0042981	Apoptosis	10	0.030
GO:0007568	Aging	10	0.030
KEGG_PATHWAY	MAPK signaling pathway	6	
KEGG_PATHWAY	mTOR signaling pathway	4	
KEGG_PATHWAY	TGF-beta signaling pathway	5	
SM00034	CLECT C-type	6	0.040
GO:0007269	Cell-cell signaling/neurotransmitter secretion	15	0.040
GO:0000022	Motor activity	11	0.003
GO:0046146	Tetrahydrobiopterin metabolic process	4	0.012
Downregulated genes			
GO:0050877	Neurological system processes	20	0.014
KEGG_PATHWAY	Wnt signaling pathway	6	
GO:0010564	Regulation of cell cycle process	6	0.024
GO:0009310	Amine catabolic process	4	0.040

3.4.4.2 ROTENONE AFFECTS MAPK SIGNALING PATHWAY ASSOCIATED GENES

Interestingly, even at this early stage of disease development rotenone affects signaling pathways associated with the pathology of neurodegenerative diseases. This includes among others, the mitogen-activated protein kinases (MAPK) that induce a variety of cellular functions such as gene expression, mitosis and apoptosis through the phoshorylation of specific serine and/or threonine residues of target proteins (Thomas and Huganir, 2004, Nagai et al., 2007).

Six genes that were elevated by approximately 2-fold in rotenone treated flies (Table 8) are associated with the MAPK signaling pathway. Three genes, Epidermal growth factor receptor (*Egfr)*, Ras oncogen at 85D (*Ras85D)* and Ras GTPase activating protein 1 (*RasGAP1)* are depicted in the KEGG_PATHWAY map (Fig. 41).

Table 8: MAPK signaling pathway-associated genes upregulated by rotenone

Gene name	Symbol	Mean	SEM
Ras Oncogene at 85D	Ras85D	2.184	±0.145
Epidermal growth factor receptor	Egfr	1.837	±0.025
Ras GTPase activating protein 1	RasGAP1	1.892	±0.042
Rab14	Rab14	4.027	±0.325
Protein kinase at 92B	Pk92B or DASK1	2.053	±0.153
Death associated protein kinase related	Drak	1.966	±0.060

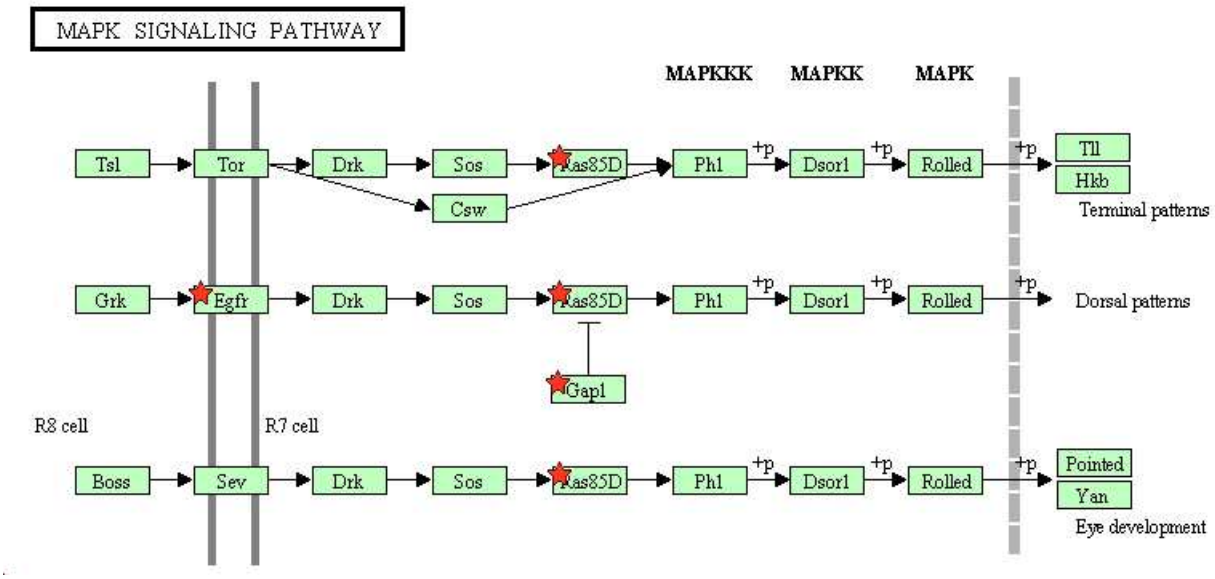

Figure 41: MAPK signaling pathway. Red stars indicate genes whose expression was affected by rotenone generated by KEGG_PATHWAY (http://david.abcc.ncifcrf.gov/).

The three other genes were Death associated protein kinase related *(Drak)*, *Rab14* and Protein kinase at 92B *(Pk92)* a.k.a *DASK1*. *DASK1* is an ortholog of *ASK1* (Apoptosis signal regulating kinase 1) in mammals that is activated by various types of stress such as reactive oxygen species (ROS), endoplasmic reticulum stress, calcium influx, tumor necrosis factor, lipopolysaccharides and selectively activates JNK and p38 MAPK pathways reviewed in (Nagai et al., 2007).

3.4.4.3 ROTENONE AFFECTS TGF-β SIGNALING PATHWAY ASSOCIATED GENES

The transforming growth factor beta (TGF-β) pathway is another signaling pathway, which was shown to be altered during early stages of PD phenotype development induced by rotenone in the flies. This pathway controls a plethora of cellular processes in both embryos and adult organisms such as cell growth, cell differentiation, apoptosis, cellular homeostasis and other cellular functions (Raftery and Sutherland, 1999, Bruce and Sapkota, 2012). Expression levels of *SkpF*, Daughters against dpp (*Dad)*, Smad anchor for receptor activation *(Sara)* and Rho-kinase A *(rok*) were altered during rotenone treatment (Table 9 and Fig. 42).

Table 9: TGF-β signaling pathway-associated genes regulated by rotenone

Gene name	Symbol	Mean	SEM
SkpF	skpF	2.261	±0.005
Daughters against dpp	Dad	1.842	±0.100
Smad anchor for receptor activation	Sara	1.364	±0.095
Rho-kinase A	rok	1.335	±0.060

3.4.4.4 ROTENONE AFFECTS mTOR SIGNALING PATHWAY ASSOCIATED GENES

Another signaling pathway whose genes were altered during rotenone treatment was the mTOR (mammalian target of rapamycin) pathway. This is a serine/threonine protein kinase that regulates cell proliferation, cell motility, cell survival, protein synthesis and transcription (Hay and Sonenberg, 2004, Lieberthal and Levine, 2012). In addition few important genes, which are involved in mTOR pathway were differentially regulated in rotenone treated flies. It includes, target of rapamycin (*Tor), Akt1,* and Eukaryotic initiation factor 4B (*eIF4B)* (Table 10 & Fig. 43).

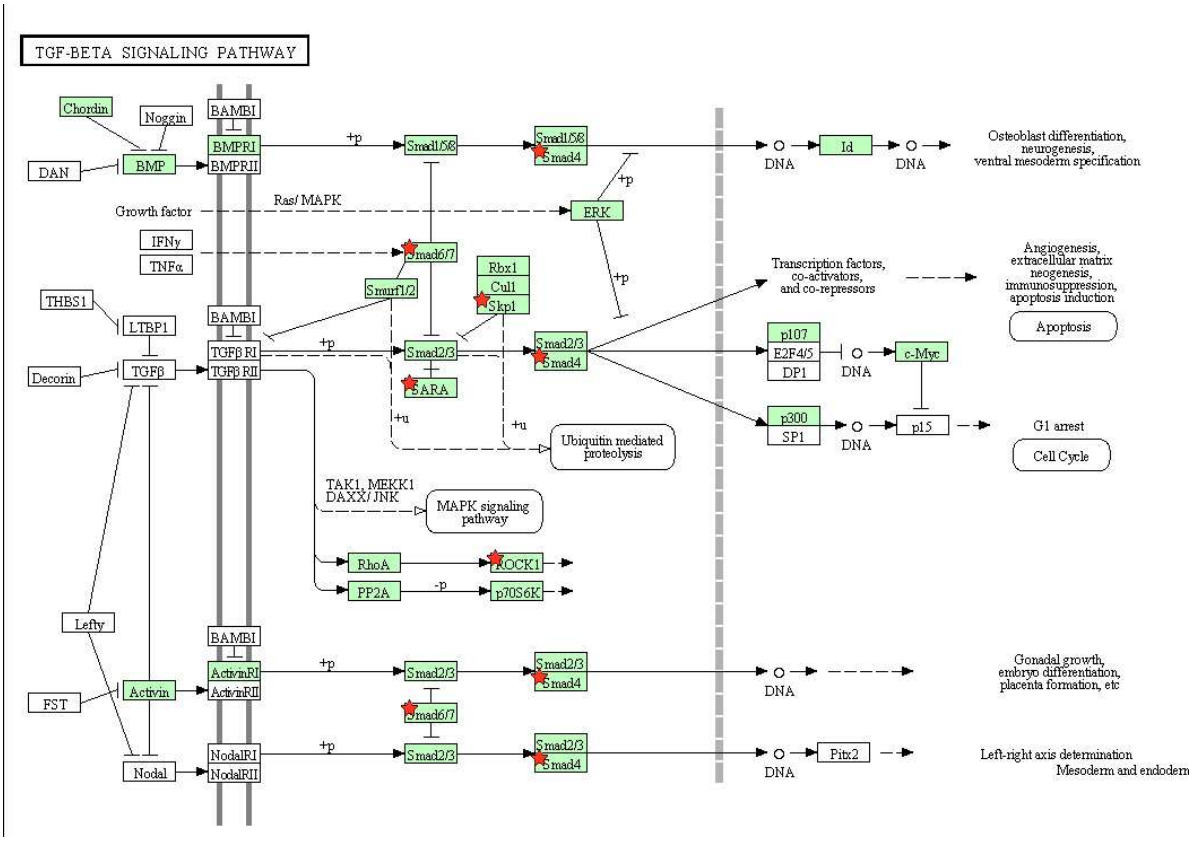

Figure 42: TGF-β signaling pathway. Red stars indicate genes whose expression was affected by rotenone generated by KEGG_PATHWAY (http://david.abcc.ncifcrf.gov/).

Table 10: mTOR signaling pathway-associated genes regulated by rotenone

Gene name	Symbol	Mean	SEM
Eukaryotic initiation factor 4B	eIF-4B	1.870	±0.185
Akt1	Akt1	1.409	±0.110
Target of rapamycin	Tor	2.228	±0.016

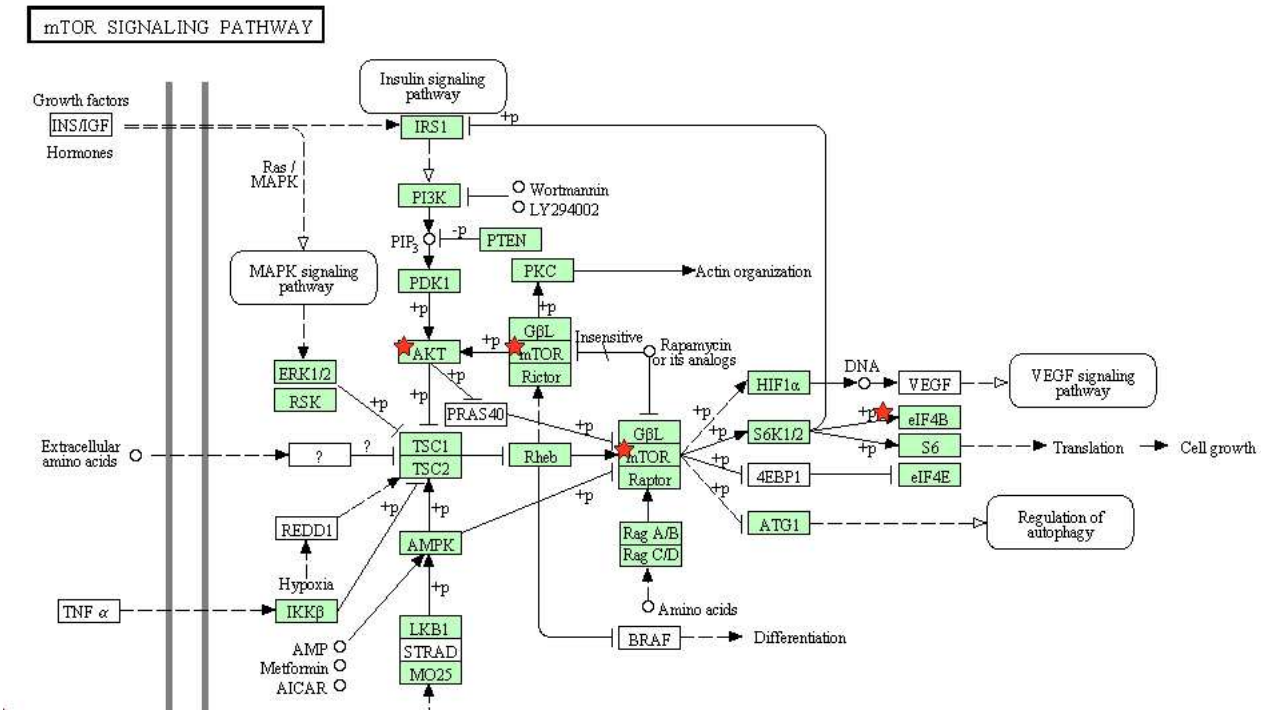

Figure 43: mTOR signaling pathway. Red stars indicate genes whose expression was affected by rotenone generated by KEGG_PATHWAY (http://david.abcc.ncifcrf.gov/).

3.4.4.5 ROTENONE AFFECTS Wnt SIGNALING PATHWAY ASSOCIATED GENES

Wnt signaling was also distinctively regulated. Five genes depicted in Figure 44 by KEGG_PATHWAY and listed in Table 11 were downregulated while one gene was upregulated.

Table 11: Wnt signaling pathway-associated genes regulated by rotenone

Gene name	Symbol	Mean	SEM
skpA	skpA	0.133	0.068
Calcineurin A1	CanA1	0.828	0.139
Smad on X	smox	0.545	0.035
Shaggy	sgg	0.665	0.229
CG32568	CG32568	0.070	0.084
Cyclin D	CycD	1.546	0.033

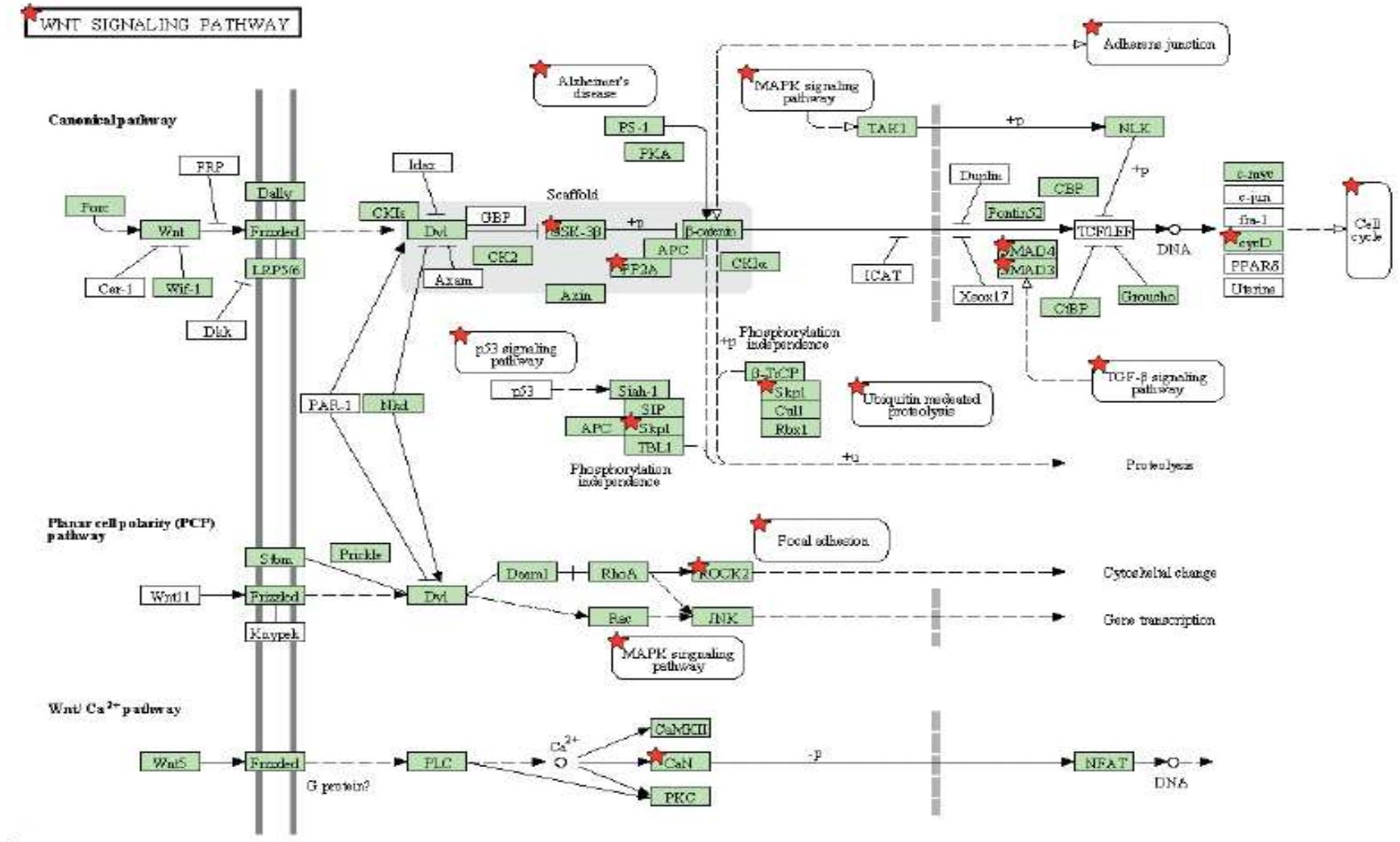

Figure 44: Wnt signaling pathway. Red stars indicate genes whose expression was affected by rotenone; generated by KEGG_PATHWAY (http://david.abcc.ncifcrf.gov/).

3.4.4.6 ROTENONE AFFECTS MULTIPLE CELLULAR AND BIOLOGICAL PROCESSES

Shown in Table 7 are assorted sets of differentially regulated genes from rotenone treated flies with significantly ($p < 0.05$) and highly enriched GO terms provided by DAVID. Most of these groups are connected to cell fate through neurogenesis, regulation of apoptosis, aging and regulation of cell cycle processes. Other relevant functional categories include neurotransmitter secretion/cell-cell signaling, stress response and oxidative phosphorylation, motor activity, amine metabolism, c-type lectins, and neurological processes (Fig. 45 & 46).

Apoptosis and aging are hallmarks of neurodegeneration. Surprisingly, even at this early stage of PD development, rotenone induced changes in genes involved in these processes. Among others it includes Death associated molecule related to Mch2 *(Damm),* Death caspase 1 *(Dcp-1),* Bax Inhibitor 1*(BI-1),* Thioredoxin peroxidase 2 *(Jafrac2)*, thread *(th)*, Programmed cell death 5 *(PDCD-5), Hsp60D,* Outsiders *(out) and* Sox box protein 15 *(sox15).* Relative expression changes of these genes are shown in Fig. 45 A & B.

Morover, significant functional categories whose genes were differentially regulated were neurogenesis and neurotransmitter secretion/cell-cell signaling. Because it is a long list of about 26 genes, the full names of these genes are only given in the figure legend (Fig. 45 C & D). The expression levels of the genes involved in stress response and oxidative phosphorylation processes were also altered by rotenone (Fig. 45E). Among seven altered genes, three were cytochrome P450 coding genes: *Cyp6a2*, *Cyp12a5,* which were upregulated whereas *Cyp12a4* was downregulated. Peroxiredoxin 2540-2 *(Prx2540-2),* and *Su(TpI)* are other stress response genes that were upregulated.

Furthermore, seven genes involved in motor activity/behavior were differentially expressed. Surprisingly, *Tau* was the highest upregulated gene in all categories. Its expression level was increased by 18 fold. Other genes that fall under this functional category were: Dynein heavy chain at 93AB *(Dhc93AB),* Dynein light chain 90F *(Dlc90F) Osm-1,* Chromosome bows (*chb),* Jaguar *(jar),* and Calmodulin *(cam)*.

Expression of the two genes Cryptochrome *(cry)* and Moladietz *(mol)* was repressed *(*Fig. 46F).

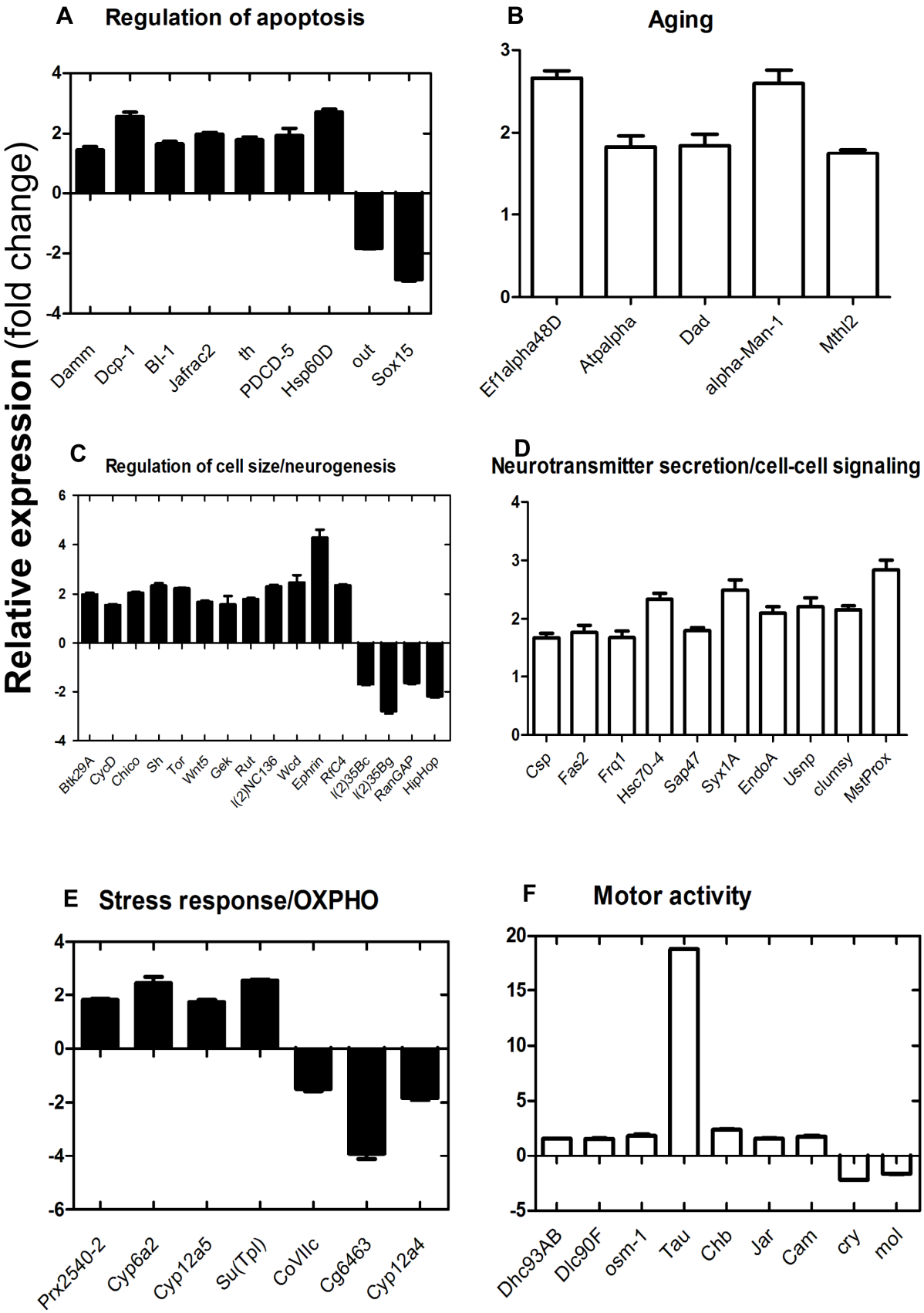
A
Regulation of apoptosis
Relative expression (fold change)
Damm
Dcp-1
Bl-1
Jafrac2
th
PDCD-5
Hsp60D
out
Sox15
B
Aging
Ef1alpha48D
Atpalpha
Dad
alpha-Man-1
Mthl2
C
Regulation of cell size/neurogenesis
Btk29A
CycD
Chico
Sh
Tor
Wnt5
Gek
Rut
l(2)NC136
Wcd
Ephrin
RfC4
l(2)35Bc
l(2)35Bg
RanGAP
HipHop
D
Neurotransmitter secretion/cell-cell signaling
Csp
Fas2
Frq1
Hsc70-4
Sap47
Syx1A
EndoA
Usnp
clumsy
MstProx
E
Stress response/OXPHO
Prx2540-2
Cyp6a2
Cyp12a5
Su(Tpl)
CoVIIc
Cg6463
Cyp12a4
F
Motor activity
Dhc93AB
Dlc90F
osm-1
Tau
Chb
Jar
Cam
cry
mol

Figure 45: Gene expression pattern changes in cellular processes affected by rotenone. Functional categories overrepresented in the lists of genes differentially expressed in rotenone treated flies identified by DAVID (http://david.abcc.ncifcrf.gov/), (Table 7, $p < 0.05$). (A) Fold changes for genes in regulation of apoptosis (B) Aging (C) Neurogenesis (D) Neurotransmitter secretion/cell-cell signaling (E) Stress response and (F) Motor activity. Error bars represent SEM. Btk29A (Btk family kinase at 29A), CycD (Cyclin D), chico, sh (Shaker), Tor (target of rapamycin), Wnt5 (Wnt oncogene analog 5), gek (Genghis khan), rut (Rutabaga), l(2)NC136 (lethal (2) NC136), wcd (wicked), Ephrin, RfC4 (Replication factor c subunit 4), l(2)35Bg (lethal (2) 35 Bg, RanGAP (Ran GTPase activating protein), HipHop (HP1-HOAP-interacting protein), Csp (Cysteine string protein), Fas2 (Fasciclin2), Frq1 (Frequenin 1), Hsc70-4 (Heat shock protein cognate 4), Sap47 (Synapse associated protein 47kD), Syx1A (Syntaxin 1A), EndoA (Endophilin A), Usnp (Ubisnap), clumsy, and MstProx.

Similarly, there was a significant differential expression of four genes involved in dopamine and other catecholamine metabolism. These include punch *(pu),* purple *(pr),* Sepiapterin reductase *(Sptr)* and Dopamine N acetyltransferase *(dat)* (Fig. 46A). Another functional category, which was highly enriched in GO terms provided by DAVID, was c-type lectin (carbohydrate binding). Relative expression levels of four genes were increased. These genes were; *lectin-46Cb, CG14500,* C-type lectin 27kD (*Clect27)* and Uninflatable *(uif)* (Fig. 46B).

Regulation of cell cycle and neurological processes were the other enriched functional categories. The expression levels of the genes controlling these processes were repressed. Some of these genes such as *Dat, CanA1, cry, sgg* and *mol* are already described in other categories above. Others include; *14-3-3 epsilon*, Darkener of apricot *(Doa)*, Odorant-binding protein 44a *(Obp44a)*, Guanylyl cyclase alpha-subunit at 99B *(Gycalpha 99B),* Gustatory receptor 39b *(Gr39b),* Gustatory receptor 59e *(Gr59e),* Gustatory receptor 93a *(Gr93a),* Microtubule-associated protein futsch *(futsch),* Nicotinamide mononucleotide adenylytransferase *(Nmnat),* Odorant binding protein 51a *(Obp51a),* Rhodopsin 2 *(Rh2)*, Syntaxin 5 *(Syx5),* Crinkled (*ck)*, Kurtz (*krz),* orange *(or),* SkpA associated protein *(Skap), skpA,* fascetto *(feo),* four way stop *(fws),* and missing oocyte *(mio)* (Fig. 46C & D). In addition, three immune response genes were more than 2 fold upregulated. These genes were Peptidoglycan recognition protein LA (*PGRP-LA)*, Drosomycin like 4 (*Drsl4)* and Immune induced molecule 1 (*Im1)* (Fig. 46C).

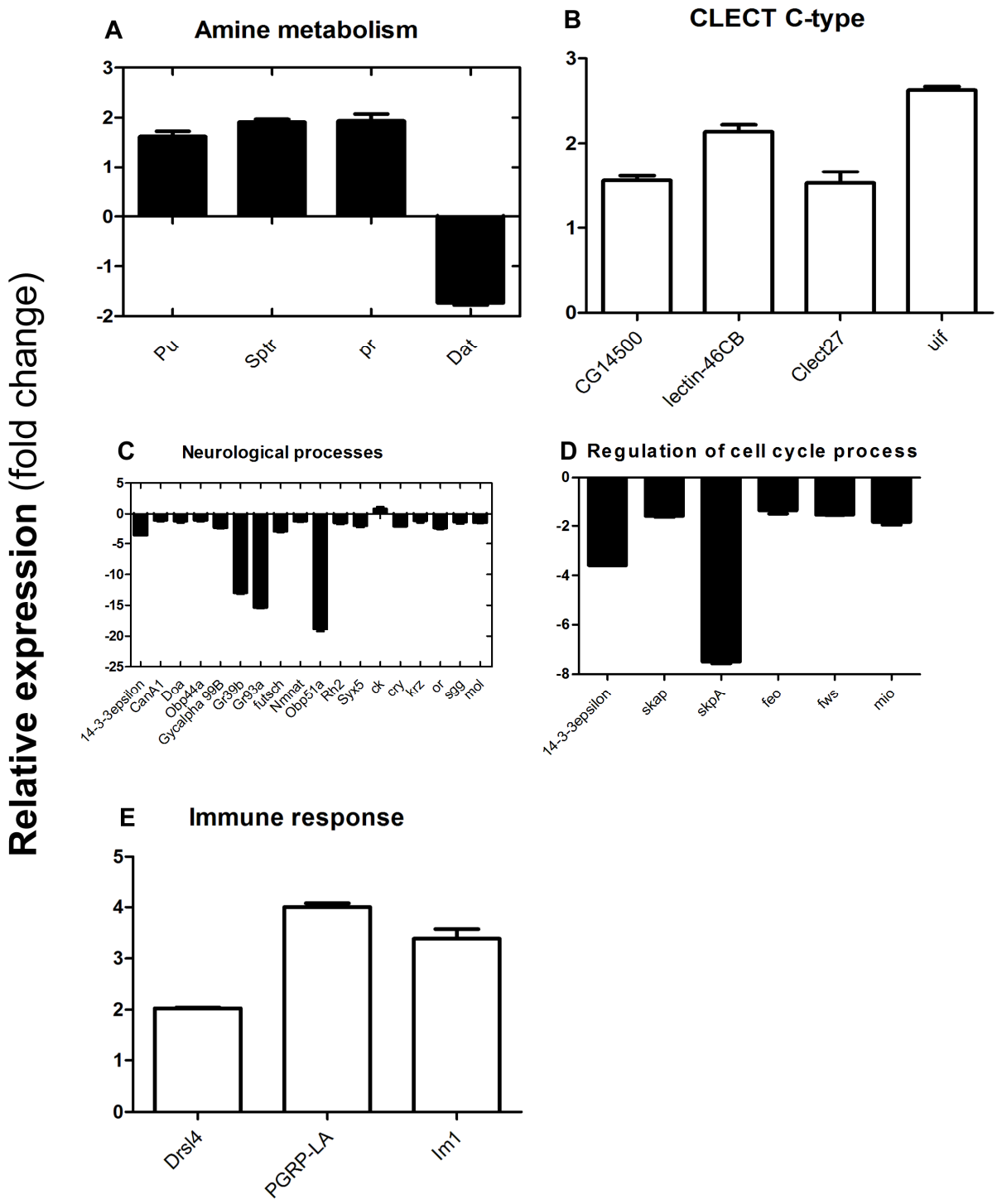

Figure 46: Gene expression pattern changes in cellular processes affected by rotenone. Functional categories overrepresented in the lists of genes differentially expressed in rotenone treated flies identified by DAVID (http://david.abcc.ncifcrf.gov/), (Table 7, $p < 0.05$). Fold changes for genes in regulation of (A) Amine metabolism, (B) c- type lectins and (C) Neurological processes, (D) Regulation of cell cycle processes (E) Immune response. Error bars represents SEM.

3.5 VALIDATION OF MICROARRAY DATA BY qRT-PCR

Quantitative Real Time PCR is one of the methods that are used to validate the accuracy of microarray data. The qRT-PCR was performed on magnetic sorted DA neurons from the 3 control samples and 3 rotenone treated samples. The total RNA samples are the ones, which were used for the microarray analysis. From the microarray analysis every gene that was deregulated seems to be important and relevant and that makes it hard to choose the genes for further analysis. Given the fact that pathway analysis is expected to provide more informative data than single gene analysis; (Ohnuki et al., 2010; pers. comm. K. Kallsen, FZB-Kiel), I chose the four deregulated pathways for qRT-PCR. For a respective pathway, a target gene, a key regulator or a key ligand was selected for analysis. For the MAPK/EGFR signaling pathway, a ligand spitz was chosen. Armadillo a homology of mammalian β-catenin, is a key regulatory component of Wnt signaling pathway. In case of TGFR-β and mTor signaling pathways, Dad and Ash2 target genes, respectively, were selected for qRT-PCR. In addition, three genes that represent three functional categories were chosen. These genes include; *l(2)NC136* that represents the neurogenesis category, *dat* represents genes involved in catecholamine metabolism and *Calmodulin* for motor activity category. The fold differences of relative gene expression in control versus rotenone treated samples were determine by the method described in (Pfaffl, 2001). This method takes into consideration the efficiencies of all the primers including the efficiency of the reference gene. The results from qRT-PCR experiments largely confirmed the results from the microarray (Fig. 47). However, I also observed some variability between samples particularly for Ash2 gene (data not shown).

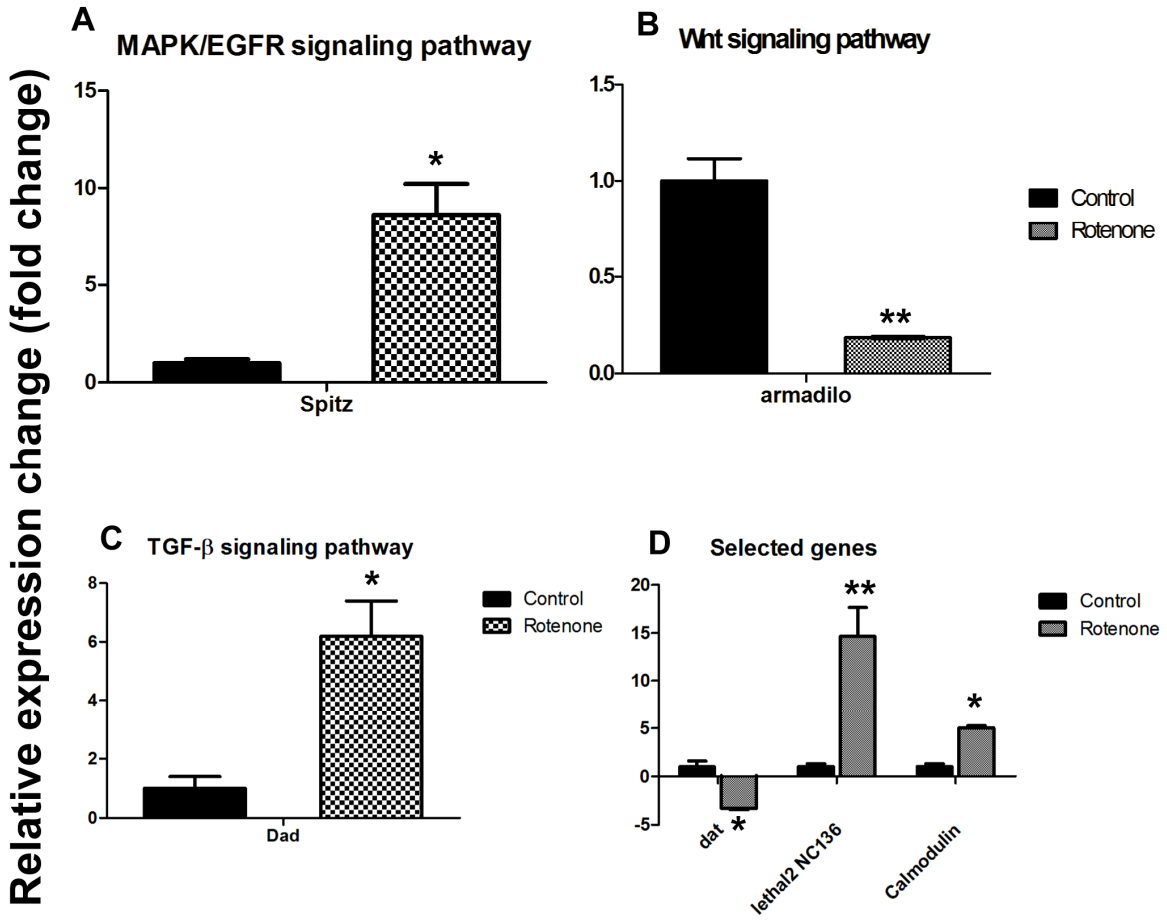

Figure 47: Validation of microarray data by qRT-PCR. (A-E) show the fold change in expression of genes selected for qRT-PCR experiments from three control samples versus three rotenone treated samples. (A) Shows increased expression of spitz gene, a key ligand of EGFR signaling pathway in the rotenone group while (B) shows the decreased expression of armadillo, a key regulatory component of Wnt signaling pathway. The increased expression of Dad, a target gene for TGFR-β signaling pathway is shown in (C). (D) shows decreased expression of dat and upregulation of lethal2NC136 and Calmodulin. Dad: Daughters against dpp, dat: Dopamine N acetyltransferase, EGFR: Epidermal Growth Factor Receptor, TGFR-β: Transforming Growth Factor Receptor-β. *p < 0.05, **p < 0.01, Student's t-test, n = 3 per group and error bars represent SEM.

3.6 MODULATION OF INTRACELLULAR SIGNALING IN DOPAMINE PRODUCING NEURONS

I have used *Drosophila* to test whether the increase or decrease of second messengers namely, cAMP and Ca^{2+} may be beneficial during rotenone-induced DA neuronal cell death. To obtain these transgenes, UAS-M1D1, UAS-M4D1, and UAS-M5Dbar were overexpressed in DA neurons by TH-GAL4 driver. As explained earlier in section 3.3.1 the UAS-M1D1 allows to induce increase of Ca^{2+} levels. Progenies from TH-GAL4 x UAS-M1D1 referred hereafter as, TH>M1D1 were subjected to four

different experimental conditions. First set of TH>M1D1, 3 day old male flies, were chronically fed 0.5 mM rotenone in 10 % glucose to induce the Parkinsonism phenotype. A second set of these flies was fed 1 mM CNO in 10 % glucose to activate the DREADD receptors. The third set of flies was fed CNO and rotenone and lastly, another set were fed glucose only as an experimental condition control. Concurrently, F1 flies from TH-GAL4 x w^{1118}, (TH> w^{1118}) were used as control group. For the period of 10 days treatment, no difference was observed in climbing ability measured by negative geotaxis assay for experimental and control flies when fed with glucose or CNO alone (Fig. 48 A & B). A dramatic climbing disability was observed in day 7 and 10 in those flies fed with rotenone alone and in day 7 for CNO + rotenone. The effect was similar in both TH>M1D1 and TH> w^{1118} flies whereby the majority of the flies did not climb above the height of 6 cm in 20 sec (Fig.48 C & D). The same effect was observed in TH>M4D1 flies which have decreased cAMP levels. For UAS-M5Dbar, which increases cAMP levels, F1 flies fed with CNO alone showed a decreased climbing ability on day 7 and 10, red line, (Fig. 48 B) compared to other tested flies. The effect was stronger for the flies fed with rotenone only and CNO + rotenone (Fig. 48 C&D). These flies seem to be more sensitive to CNO and rotenone compared to other experimental lines and the control line. Generally, these results indicate that the modulation of second messengers either enhance the toxicity of rotenone, or alternatively, CNO gives some stress to DA neurons as exemplified by the TH>M5Dbar and TH> w^{1118} flies.

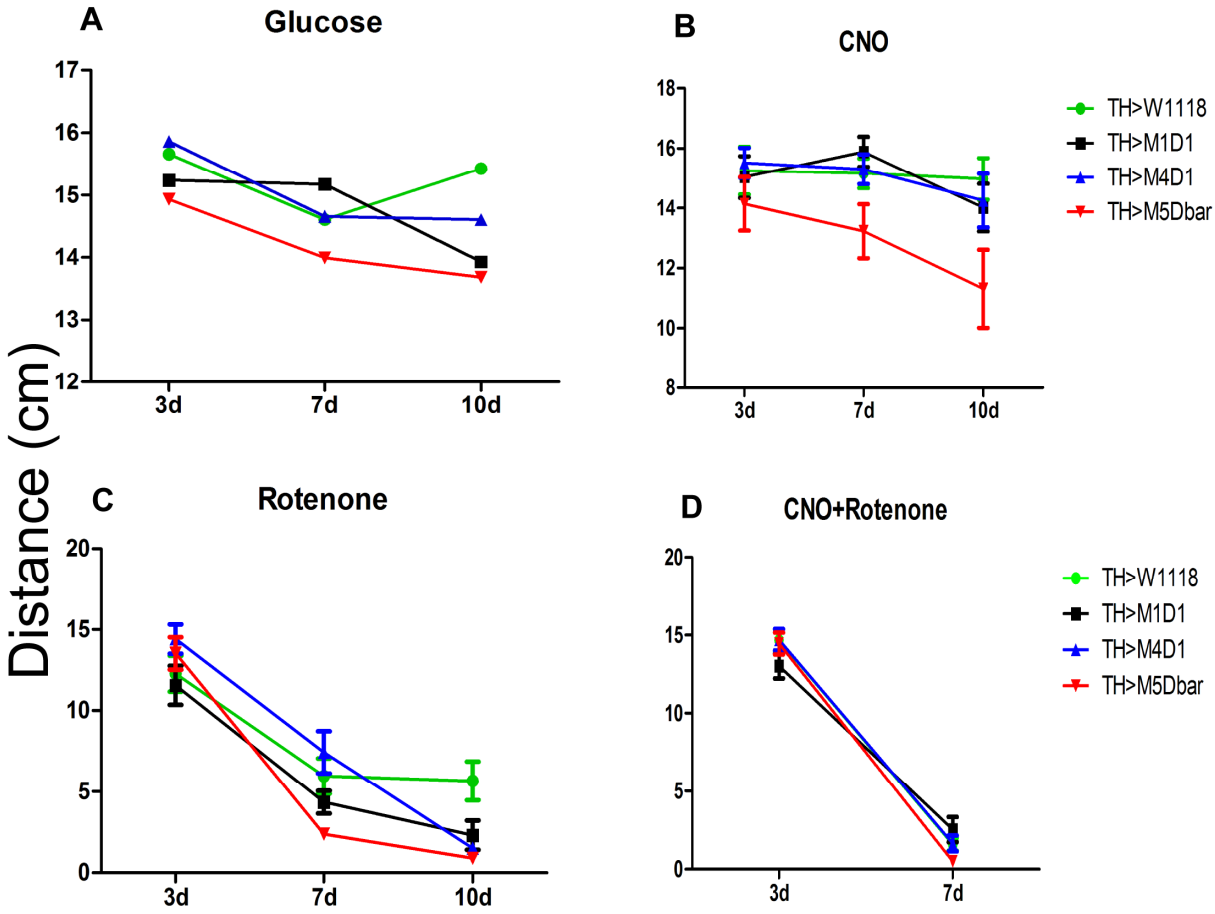

Figure 48: Overexpression of DREADD receptors to DA neurons did not rescue the climbing disability induced by rotenone. Climbing ability test measured at 3, 7 and 10 day, respectively. (A) Shows all genotypes tested fed with 10 % glucose alone, (B) 1 mM CNO in 10 % glucose, (C) 0.5 mM rotenone in 10 % glucose and (D) CNO and rotenone.

4 DISCUSSION

Dopamine is used as an intercellular messenger in both vertebrates and invertebrates (Cottrell, 1967). It is produced in cells of the nervous system, but also by those outside the CNS. The dopaminergic system comprises dopamine itself and all pathways and mechanisms required to synthesize and inactivate it, as well as of the specific dopamine receptors. Dopaminergic systems in mammals control several important physiological functions ranging from voluntary movement and reward to general aspects of hormonal regulation and the regulation of blood pressure to name only few. Surprisingly, the dopaminergic system in *Drosophila* is not well characterized. Emerging studies from the last decade have begun to elucidate the spatial expression patterns and functional roles of this system (Scholz et al., 2000, Strauss, 2002, Kim et al., 2003, Draper et al., 2007, Kim et al., 2007, Lebestky et al., 2009, Selcho et al., 2009, Inagaki et al., 2012a). Taking advantage of genetic tools available in *Drosophila*, such as the GAL4/UAS system (Brand and Perrimon, 1993), this study analyzed the distribution and physiological functions of the dopaminergic system in both CNS and digestive tract in detail. The system plays a central role in a number of important medical conditions, including Schizophrenia, Attention Deficit Hyperactivity Disorder, drug addiction and PD. For PD, despite of extensive studies, there is currently no cure or treatment that can stop disease progression and the precise pathologic mechanisms remain unclear. The fruit fly *Drosophila* shares many important molecular components with human, in particular the *Drosophila* genome encodes orthologs of the currently identified PD-related genes (PARK genes): *LRRK2/Dardarin, parkin, PINK1, Omi/HtrA2, DJ-1, UCH-L1, GIGYF2, PLA2G6, and GBA*, which makes it a suitable model to study PD. To gain insight into molecular mechanisms underlying PD pathogenesis, I performed trancriptome studies during the pre-symptomatic stage of rotenone induced Parkinsonism. In addition, I used a new approach that combines genetic and pharmacological manipulations (pharmocogenetic) to control neuronal signaling in *Drosophila*. In this, I tested whether modulation of intracellular signaling by overexpressing DREADD (Designer Receptors Exclusively Activated by Designer Drugs) receptors on DA-producing neurons during rotenone treatment might prevent development of the disease phenotype.

4.1 DOPAMINE RECEPTOR EXPRESSION IN THE BRAIN AND THE DIGESTIVE TRACT

The characterization of the dopaminergic system in normal flies to be able to manipulate this system was a basis of this study. The expression patterns of four dopamine receptors DopR (CG9652), DopR2 (CG18741), DopEcR (CG18318) and D2R (CG33517) were analyzed. The GAL4/UAS system was employed (Brand and Perrimon, 1993) to express the green fluorescent protein (GFP) under transcriptional control of receptor coding gene specific promoters. The analysis was carried out in both larval and adult flies focusing on the central nervous system and the digestive tract. The detailed localization of specific cell nuclei and structures were analyzed microscopically with tissue stained with specific antibodies. The results generated in this study give a good impression about the localization and provide insights into the roles played by these receptors in controlling different physiological functions and behaviors in the fruit fly.

Strikingly, this study showed clearly that two receptors, DopR and DopR2, are localized in l-LNvs, a subset of clock neurons that expresses the neuropeptide PDF (pigment dispersing factor). A previous transcriptomic study (Shang et al., 2011) showed that dopamine receptor mRNAs are present in purified l-LNvs neurons. Moreover, Renn and co-authors (Renn et al., 1999) reported earlier that there are ten l-LNvs (five on each side of the brain) that have related neurons nearby, the eight small LNvs (s-LNvs). Both l-LNvs and s-LNvs express the neuropeptide PDF. Neuropeptide PDF is a key transmitter in the circadian clock in *Drosophila*. Out of the 75 bilaterally organized pairs of circadian neurons, only l-LNvs and s-LNvs secrete PDF (Wulbeck et al., 2008, Choi et al., 2012). This result indicates the involvement of DopR and DopR2 receptors in controlling circadian rhythms in *Drosophila melanogaster*.

More importantly, this part of the study demonstrated the existence of DopR in dopamine producing cells, which suggests an auto-receptor function of this receptor at least in this subset of dopamine producing cells. This was approached with anti DDC (dopamine decarboxylase) antibodies and confirmed with a semi-quantitative reverse transcriptase analysis using sorted DA neurons. Since DDC encodes an enzyme catalyzing the biosynthesis of dopamine from its precursor L-DOPA, the

dopaminergic neurons will express DDC. To the best of my knowledge no evidence has been reported for the existence of dopamine autoreceptor in *Drosophila*. In mammals it is known that D2 receptors have a presynaptic location that inhibit neuronal firing, DA synthesis and release through negative feedback mechanisms in response to changes in extracellular neurotransmitter levels (Civelli et al., 1991, De Mei et al., 2009, Beaulieu and Gainetdinov, 2011).

The expression pattern of dopamine receptors in the digestive tract was also very striking. Notably, three dopamine receptors were expressed differently in the major cells present in the midgut. The DopR was found to be expressed in the mid-gut secretory enteroendocrine cells, while DopR2 was found to be expressed in the absorptive Enterocytes and D2R was expressed in the intestinal stem cells and enteroblasts. For the D2R, this study confirmed previous findings (Draper et al., 2007, El-Kholy PhD thesis, 2010) who reported the expression of D2R in the cell bodies located in the posterior midgut. In addition, this study showed that activation of DopR2 receptor localized in enterocytes triggered the action of PLC-β that leads to mobilization of intracellular Ca^{2+} *in vivo.* The concentration of dopamine agonist was within a pharmacologically relevant range (10^{-1}M to 10^{-9}M). This strongly supports the hypothesis that DopR2 receptors are present in enterocytes and that they play an important role in changing the physiological state of these cells. The wide distribution of dopamine receptors in neurons and non-neuronal tissues given by this study indicate that these receptors play various major physiological and behavioral roles in *Drosophila melanogaster.* Further studies should focus on dissecting the functions of the specific cell discussed above to gain a better knowledge of their functions with respect to dopamine signaling.

4.2 LOCOMOTOR ACTIVITY PATTERN

With the initial effort of dissecting the function of dopamine receptors in *Drosophila melanogaster*, I silenced the expression of endogenous DopRs mRNA by an RNAi approach. Flies carrying either the UAS-ds-DopR, UAS-ds-DopR2 or UAS-ds-D2R transgenes were crossed to the n-syb-Gal4 driver, which drives expression in all neurons. The daily locomotor activity was monitored by the DAM system. Results

obtained in this study showed that only D2R-RNAi flies showed substantially reduced locomotor activity counts per 24 hrs in comparison to control flies. This result suggests that D2R is necessary for controlling locomotor activity in *Drosophila*. This finding is consistent with previous RNAi studies (Draper et al., 2007) which showed that locomotor activity in *Drosophila* is regulated by D2-like receptor. Moreover, locomotor activity in flies reflects sleep-wake transitions. It has been shown that, dopamine controls this endogenously generated form of arousal through DopR (van Swinderen and Andretic, 2003). Further analysis of DopR receptor was carried out in this study by employing flies with a hypomorphic mutation in DopR, $DopR^{f02676}$. $DopR^{f02676}$ mutant flies showed a decreased activity pattern over a 24 hours period in comparison to control flies in LD. The phenotype was stronger in constant darkness (DD) conditions. Monitoring at one-hour intervals, $DopR^{f02676}$ flies showed considerably decreased activity in comparison to control flies during the night phase, the phenotype, which was rescued by overexpression of PDF. These results are consistent with previous findings from Lebestky and colleagues who reported that a loss-of-function mutation in DopR leads to a decrease in sleep-wake arousal (Lebestky et al., 2009). My findings provided an additional strong evidence of the involvement of DopR in controlling sleep-wake behavior in this species.

4.3 GENE EXPRESSION CHANGES INDICATE EARLY SIGNS OF NEURODEGENERATION IN A DROSOPHILA MODEL OF PARKINSON'S DISEASE

This study provides a genome-wide transcriptional analysis of changes associated with neurodegeneration in a *Drosophila* model of PD at a time point preceding DA cell death. Parkinson's disease in humans is a gradual progressive neurodegenerative disease that becomes clinically apparent after an estimated 70 % of vulnerable DA neurons in the *Substantia nigra* have already died (Fearnley and Lees, 1991). Moreover, molecular mechanisms underlying the degenerative process of these neurons remain elusive. Identifying the molecular pathways that contribute to the etiology of PD was the major aim of this study. The gene expression analysis carried out in this study is, to my knowledge, the first for rotenone-induced

Parkinsonism in *Drosophila* that was focused on DA neurons. Prior studies of gene expression in *Drosophila* models of neurodegenerative diseases have been limited to studies of homogenates of brain tissue (Scherzer et al., 2003, Shieh and Bonini, 2011). In human brain tissues, the laser capture microdissection (LCM) technique has recently been employed for capturing only DA neurons for transcriptional profiling studies (Cantuti-Castelvetri et al., 2007, Simunovic et al., 2009, Simunovic et al., 2010). As a major result of the current study, the power of cDNA microarray analysis in investigating this neurodegenerative disease revealed regulation of four major pathways in presymptomatic DA neurons; EGFR/MAPK, TGF-β, mTor and Wnt.

The downregulation of Wnt signaling pathways due to mild rotenone treatment in young adult flies was apparent in this study as depicted in Fig. 44. The term 'Wnt' is derived from a combination of the *Drosophila* wingless (*wg*) and the mouse homolog Int-1 proteins (Rijsewijk et al., 1987, Nusse et al., 1991). For the canonical Wnt pathway, Wnt signal to β-catenin, named armadillo in *Drosophila*, which enters the nucleus and activates transcription of Wnt target genes. Wnt signaling is also executed independently of β-catenin, in what is referred to as the non-canonical pathways; these include the planar cell polarity pathway (PCP pathway) and the Wnt-Ca^{2+} pathway. Wnt pathways are known to be involved in controlling diverse cellular processes including developing adult tissues including tissue differentiation, neuronal survival, axon extension, synapse formation and plasticity, neurotrophin transcription, neurogenesis and neuroprotection (Inestrosa and Arenas, 2010, Marchetti et al., 2013). Wnt signaling pathways are conserved throughout the animal kingdom (Liang-Wei, 2013). Moreover, deregulated Wnt signaling pathways are suggested to represent important pathomechanisms for a number of neurological conditions including Alzheimer's disease, PD and Schizophrenia (Inestrosa and Toledo, 2008, Berwick and Harvey, 2012). Thus Wnt cascades can be considered essential for the central nervous system at all stages of life. Several studies have shown the involvement of Wnt signaling pathways in midbrain DA neuron development and hippocampal neurogenesis through both canonical and non-canonical Wnt signaling pathways. The canonical Wnt/β-catenin signaling appears to be a key mechanism in controlling DA neuronal fate decision from neuronal stem cells or progenitors in the midbrain during embryonic development (Tang et al., 2009, Alves dos Santos and Smidt, 2011, Blakely et al., 2011, Liang-Wei, 2013). Notably, both GSK3-β inhibition

and β-catenin stabilization increased commitment into DA neurons of neural precursors in the ventral midbrain (Castelo-Branco et al., 2004). Interestingly, current studies illustrated the emerging role of Wnts in the adult nervous system (Inestrosa and Arenas, 2010). Importantly, current evidence points to dysregulation of Wnt signaling pathways associated with PD pathophysiology. Dysfunction of Wnt pathways signaling was shown to play a causal role in the pathophysiology of nigrostriatal DA neurons and in PD experimental models (Inestrosa and Arenas, 2010, Berwick and Harvey, 2012). Cantuti-Castelverti and colleagues reported the downregulation of β-catenin in DA neurons of the *Substantia nigra* in PD patients (Cantuti-Castelvetri et al., 2007). Interestingly, emerging evidences in animal models of PD indicate that proteins encoded by PARK genes can modify Wnt pathways (Berwick and Harvey, 2012). In particular, PARK8, encoding LRRK2 (leucine-rich repeat kinase 2), which constitute a major cause of familial PD (Zimprich et al., 2004) was linked to Wnt signaling (Berwick and Harvey, 2012, 2013). On the other hand, Parkin, an E3 ubiquitin ligase linked to familial PD, regulated β-catenin protein levels *in vivo* (Rawal et al., 2009). In MPTP (1-methyl-4-phenyl-1,2,3,6-tetrahydropyridine) mouse models of PD, contribution of Wnt/β-catenin signaling and interaction with reactive astrocytes in survival and protection of DA neurons (L'Episcopo et al., 2011a, Francesca et al., 2011b, Marchetti et al., 2013) has been reported. Moreover, gene expression profiling in progressively MPTP-lesioned macaques indicated downregulation of β-catenin and dysregulation of key components of Wnt signaling (Ohnuki et al., 2010). My findings are consistent with the above findings suggesting a role of Wnt signaling pathways in PD development. The fact that Wnt signaling pathways have a crucial role for DA neuronal survival, neurogenesis and repair may be attributed to the downregulation of these pathways observed at pre-symptomatic stages indicative for the early signs of neurodegeneration. Hence, these results indicate that manipulation of this pathway may be a therapeutic target for treatment of PD.

MAPK signal transduction pathways are evolutionarily conserved in eukaryotic cells and transduce signals in response to a variety of extracellular stimuli. MAPK is activated by serine and threonine phosphorylation catalyzed by a family of the dual-specificity protein kinase MAP2K. MAP2K is in turn activated by phosphorylation mediated by MAP3K. Cascades of MAPKs mediate responses such as cell

proliferation, differentiation, survival, and death. There are multiple MAPKs in eukaryotes. Three subgroups of the MAPK superfamily have been identified in mammals: ERK, JNK, and p38 (Kim and Choi, 2010). *Drosophila melanogaster* expresses all three subgroups of MAPKs: Rl (Rolled; ERK homolog), dJNK/Basket (*Drosophila* homolog of JNK), and dp38a and dp38b (*Drosophila* homologs of p38) (Tateno et al., 2000, Takeda et al., 2008). Deviation from the strict control of MAPK signaling pathways has been implicated in the development of many human diseases including Alzheimer's, PD and various types of cancers (Kim and Choi, 2010).

Strikingly, even at this early stage of disease development, expression of four genes associated with the MAPK signaling pathway was elevated by approximately 2-fold in rotenone treated flies. These genes are Ras oncogene at 85D (*Ras85D), Rab14* and Ras GTPase activating protein 1 (*RasGAP1),* which are all Ras proteins. All Ras protein family members belong to a class of protein called small GTPase, which are involved in cellular signal transduction. Another gene whose expression was increased was a receptor tyrosine kinase, namely the Epidermal growth factor receptor (*Egfr)*. Epidermal growth factor receptor signaling plays essential roles in development and maintenance of adult tissues including the brain by regulating cell proliferation, growth, differentiation, migration and survival (Wong and Guillaud, 2004, Wieduwilt and Moasser, 2008). Transgenic mice lacking the EGFR develop neurodegenerative diseases and die within the first month after birth (Wong and Guillaud, 2004). EGFR has been shown to be expressed in the subventricular zone only in adult rats and in hippocampal neurons (Tucker et al., 1993, Cameron et al., 1998). In neuronal culture models, EGF stimulated neurite outgrowth, increased dopamine uptake and enhanced long-term survival in cultured dopaminergic neurons (Yamada et al., 1997). Ectopic activation of ERK1/2 in rotenone rat models of PD protected dopamine neurons from cell death (Hsuan et al., 2006). Several evidences from mammalian studies indicate the involvement of MAPK cascade through activation of ERK in learning and memory (Thomas and Huganir, 2004). Moreover, reduced EGFR signaling in the CNS leads to impairment of olfactory learning in *Drosophila* larvae (Rahn et al., 2013). The increased expression of EGFR and Ras protein coding genes (Ras/MAPK or EGFR signaling) in rotenone induced Parkinsonism in *Drosophila* suggests that these neurons launch defensive

mechanisms due to stress given by rotenone. These findings support the view that EGFR signaling promotes cell survival also in the vulnerable DA neurons.

TGF-β controls a plethora of cellular processes in both embryos and adult organisms such as cell growth, cell differentiation, apoptosis, cellular homeostasis and other cellular functions (Raftery and Sutherland, 1999, Bruce and Sapkota, 2012). When components of the TGF-β pathway are compromised, numerous human diseases, including cancer and neurodegeneration result (Katsuno et al., 2011, Bruce and Sapkota, 2012). There is growing support for a role of TGF-β signaling in neuronal maintenance function and degeneration (Koh et al., 2004, Andrews et al., 2006, Tesseur et al., 2006, Katsuno et al., 2011).

As most of the other pathways mentioned above, the target of rapamycin (TOR) signaling pathway is evolutionary conserved. It regulates cell proliferation, cell motility, cell survival, protein synthesis and transcription (Hay and Sonenberg, 2004, Lieberthal and Levine, 2012). TOR is a serine/threonine protein kinase belonging to the phosphoinositide 3-kinase (PI3K) family. The major regulatory inputs for TOR are nutrients, growth factors, energy and stress. Mammalian TOR (mTOR) is implicated in diseases such as cancer, metabolic diseases and ageing (Zoncu et al., 2012). This pathway was also upregulated in flies treated with rotenone. This included the major key players of the pathway, TOR, Akt and the effector eIF4B, indicative for induction of survival mechanisms by increasing the rate of protein synthesis.

Collectively, the expression of several genes involved in the MAPK/EGFR, TGF-β and TOR signaling pathways were increased. The upregulation of these growth factors and stress activated pathways signify the neuroprotective role to DA neurons to counteract the stress and presumably the first phases of cell death. The downregulation of Wnt signaling pathways indicate early signs of neurodegeneration. Thus, this study has given insights for further investigation of these pathways that may help to identify potential targets for neuroprotective measures for PD at pre-clinical stages.

4.4 PREVENTION OF THE DISEASE PHENOTYPE INDUCED BY ROTENONE

I have used *Drosophila* to test whether the increase or decrease of second messengers namely, cAMP and Ca^{2+} may be beneficial during rotenone induced DA neuronal cell death. This was done by overexpressing DREADDs in DA neurons using the dopamine containing cell specific TH-GAL4 driver. DREADDs are modified muscarinic acetylcholine G-protein coupled receptors that are activated only by a synthetic ligand, namely by Clozapine-N-Oxide (CNO) (Armbruster et al., 2007). This is a new technology that combines genetic and pharmacology approaches to manipulate cellular signaling and control of behaviors (Nichols and Roth, 2009). The results indicated that neither decrease of cAMP nor increase of cAMP or of Ca^{2+} rescues the climbing disability phenotype elicited by rotenone. Conventional medical approaches for treatment of PD aim to replenish dopamine levels in the striatum. The classical pharmaceutical drug that is used to alleviate symptoms is L-DOPA, which has got debilitating side effects and often worsens the situation over time. There are several emerging alternative therapies including nicotine and caffeine. Epidemiological studies and animal models have begun to establish nicotine and caffeine as promising therapeutic candidates against PD (Chen et al., 2001, Ho, 2002, Hart et al., 2009, Seidl and Potashkin, 2011). Some toxin-induced *Drosophila* models of PD to assay the beneficial effects of certain compounds have been reported (Coulom and Birman, 2004, Hosamani and Muralidhara, 2010, Jimenez-Del-Rio et al., 2010). All the approaches performed above target the postsynaptic cells (dopamine and other receptors). I have carried out chronic exposure to rotenone of control flies and flies with reduced or increased levels of cAMP and increased level of Ca^{2+} targeting the dopamine producing cells (presynaptic cells) by overexpressing DREADD receptors. These receptors are predicted to mimic the dopamine release. In *Drosophila* the effect of rotenone becomes apparent after six to seven days of exposure (Coulom and Birman, 2004, Bayersdorfer et al., 2010). Rotenone acts as an inhibitor of mitochondrial respiratory complex I, leading to decrease in ATP levels, production of mitochondrial ROS and subsequent increase oxidative stress to DA neurons (Betarbet et al., 2000, Sherer et al., 2003), finally leading to activation of various cell death pathways (Gupta et al., 2008, Sonia Angeline et al., 2012). The overexpression of the M5Dbar, DREADD receptor that is positively coupled to AC and modulates the production of cAMP in DA neurons was predicted to mimic the

D1-like receptor signaling and hence control the locomotion behavior. Unexpectedly, results indicated that flies overexpressing the M5Dbar receptor had a lower performance as compared to control flies when treated with rotenone. One possible explanation could be that the cells are critically affected by oxidative stress from rotenone and they are not in a situation to cooperate for their own survival. They rather need help to run away from the oxidative stress such as antioxidants that will scavenge the free radicals and reduce their stress rather than involving themselves into the repairing or rescue mechanisms. Secondly, it might be due to increase of L-type calcium channels triggered by cAMP signaling.

Overexpression of the M1D1 receptor was predicted to mobilize Ca^{2+} from intracellular stores that will affect aspects of neuronal and muscle physiology. As for M5Dbar overexpression, results indicated that flies overexpressing the M1D1 receptor had a lower performance as compared to control flies when treated with rotenone. Basal cytosolic Ca^{2+} levels are controlled by an efficient interplay of calcium transport system from both surface plasma membrane and on the membrane of intracellular compartments such as endoplasmic reticulum. Also cytosolic Ca^{2+} levels depend on the presence of a number of Ca^{2+} binding proteins, which integrate changes with the downstream effectors. Given the fact that oxidative stress from rotenone interferes with the performance of the cells, it might contribute to impairment of such orchestrated systemic calcium signaling. Studies from genetic interaction screens have shown that mechanisms of maintaining Ca^{2+} homeostasis in *Drosophila* are cell specific (Chorna and Hasan, 2012). Moreover, it has been suggested that the vulnerability of DA neurons in PD may be related to unusual calcium ion-channel activity in the affected neuronal population, with increased calcium influx into the cell triggering neuronal dysfunction and cell death (Gupta et al., 2008). Application of calcium antagonists targeting L-type calcium channels in PD models (MPTP, rotenone, and 6-hydroxydopamine) demonstrated survival of dopaminergic *Substantia nigra* neurons (Chan et al., 2007). Epidemiological studies demonstrated that patients taking dihydropyridine-type calcium antagonists have a reduced incidence of PD (Surmeier, 2007).

Similarly, flies overexpressing M4D1 (TH>M4D1), showed a decreased climbing ability. The overexpression of M4D1 was predicted to mimic D2-like receptor

signaling by silencing neurons via decreasing AC activity and cAMP production and closing of membrane potassium channels via βγ-mediated effects (Neve et al., 2004, Beaulieu and Gainetdinov, 2011). Disruption of short term learning and memory behavior in flies overexpressing M4D1 in the mushroom bodies has been observed. Although the exact mechanism for this phenotype was not determined, it was postulated that the effect is likely to be either through the opening of potassium channels to produce hyper-polarization of the cell membrane or due to decrease in cAMP levels (pers. comm. CD Nichols, USA).

Transgenic mouse studies with all three DREADD receptors have demonstrated the utility of the DREADD technology. In particular, mice expressing M5Dbar in the hippocampus showed both increases in hippocampal neuronal activity and locomotor behaviors and seizures in a dose dependent fashion (Alexander et al., 2009). Other studies showed influences on feeding behaviors (Krashes et al., 2011) and the sleep/wakefulness state (Sasaki et al., 2011). However, the utility of this technology in *Drosophila* is at an infancy stage (pers. comm. CR Nichols, USA). Therefore, interpretation of the results from this study should be taken cautiously. It is assumed that CNO represents a “biologically inert synthetic ligand” that selectively activates the muscarinic receptor-based DREADD. In contrast, it has been reported that CNO has cell membrane permeability effects and can undergo redox cycling with clozapine (CNO/CN). Therefore CNO is biologically active and its conversion products are capable of undermining DREADD effects due to production of ROS/oxidative stress (Ray et al., 2011). This supports my findings, as all flies including control group die after day seven, suggesting a strong oxidative stress to the cells. To gain better insight of utility of this technology in *Drosophila*, future studies should focus first on testing basic behaviors (without manipulation with other chemicals) and/or measuring activity of certain specific neurons (cellular level), before moving to behaviors (systemic level). Taking together, the results obtained from this study did not confer the neuroprotective mechanism to DA neurons. Instead they support the current favored mechanisms for DA neuronal death in sporadic PD: mitochondrial dysfunction, calcium imbalance and oxidative stress (Gupta et al., 2008, Whitworth, 2011).

4.5 CONCLUSIONS AND OUTLOOK

One of the major aims of this study was to elucidate the expression patterns of dopamine receptors in the CNS and periphery system particulary, the digestive tract. This study provides comprehensive knowledge about the spatial distribution of dopamine receptors in the CNS and digestive tracts of *Drosophila melanogaster* both in larvae and adults. These findings provide insights into the roles played by these receptors in controlling different physiological functions and behaviors in the fruit fly. Taken together, the *Drosophila* dopaminergic systems seem to control diverse functions at both cellular and systemic levels, developing and adult stages as it happens in mammals. Further studies should focus on dissecting the roles played by the identified structures and specific cells to get better insights of their roles in the fruit fly with respect to dopamine signaling.

The second major aim of this stuy was to gain insight into the molecular mechanisms underlying PD pathogenesis, with a focus on pre-symptomatic stages of the disease. This study provides evidences that the outcome of various highly relevant signaling pathways is modified in the corresponding dopamine producing neurons. Amongst them are the Wnt-, MAPK/EGFR-, TGF-β-, and TOR-signaling pathways, which are known to be important for cell survival and/or cell death in the CNS. Further investigation of these pathways may provide new insights into the molecular events underlying pathogenesis and, hopefully, lead to the identification of new potential targets for neuroprotective measures for PD at pre-clinical stages.

Lastly, this study aimed at finding an alternative way for protection of DA neurons during induction of Parkinsonism in *Drosophila*. Overexpression of DREADD receptors in DA-producing neurons did not prevent development of the disease phenotype induced by rotenone in the *Drosophila* model of PD. Based on the sensitivity and vulnerability of DA neurons and the complexicity of the employed pharmocogenetic approach at the behavioral level, future studies should focus first on measuring the levels and activities of the cAMP and Ca^{2+} at the cellular level to get better insights of their mechanisms before moving to behavioral level and further employ complex manipulations.

References

Adams MD, Celniker SE, Holt RA, Evans CA, Gocayne JD, Amanatides PG, Scherer SE, Li PW, Hoskins RA, Galle RF, George RA, Lewis SE, Richards S, Ashburner M, Henderson SN, Sutton GG, Wortman JR, Yandell MD, Zhang Q, Chen LX, Brandon RC, Rogers YH, Blazej RG, Champe M, Pfeiffer BD, Wan KH, Doyle C, Baxter EG, Helt G, Nelson CR, Gabor GL, Abril JF, Agbayani A, An HJ, Andrews-Pfannkoch C, Baldwin D, Ballew RM, Basu A, Baxendale J, Bayraktaroglu L, Beasley EM, Beeson KY, Benos PV, Berman BP, Bhandari D, Bolshakov S, Borkova D, Botchan MR, Bouck J, Brokstein P, Brottier P, Burtis KC, Busam DA, Butler H, Cadieu E, Center A, Chandra I, Cherry JM, Cawley S, Dahlke C, Davenport LB, Davies P, de Pablos B, Delcher A, Deng Z, Mays AD, Dew I, Dietz SM, Dodson K, Doup LE, Downes M, Dugan-Rocha S, Dunkov BC, Dunn P, Durbin KJ, Evangelista CC, Ferraz C, Ferriera S, Fleischmann W, Fosler C, Gabrielian AE, Garg NS, Gelbart WM, Glasser K, Glodek A, Gong F, Gorrell JH, Gu Z, Guan P, Harris M, Harris NL, Harvey D, Heiman TJ, Hernandez JR, Houck J, Hostin D, Houston KA, Howland TJ, Wei MH, Ibegwam C, Jalali M, Kalush F, Karpen GH, Ke Z, Kennison JA, Ketchum KA, Kimmel BE, Kodira CD, Kraft C, Kravitz S, Kulp D, Lai Z, Lasko P, Lei Y, Levitsky AA, Li J, Li Z, Liang Y, Lin X, Liu X, Mattei B, McIntosh TC, McLeod MP, McPherson D, Merkulov G, Milshina NV, Mobarry C, Morris J, Moshrefi A, Mount SM, Moy M, Murphy B, Murphy L, Muzny DM, Nelson DL, Nelson DR, Nelson KA, Nixon K, Nusskern DR, Pacleb JM, Palazzolo M, Pittman GS, Pan S, Pollard J, Puri V, Reese MG, Reinert K, Remington K, Saunders RD, Scheeler F, Shen H, Shue BC, Siden-Kiamos I, Simpson M, Skupski MP, Smith T, Spier E, Spradling AC, Stapleton M, Strong R, Sun E, Svirskas R, Tector C, Turner R, Venter E, Wang AH, Wang X, Wang ZY, Wassarman DA, Weinstock GM, Weissenbach J, Williams SM, WoodageT, Worley KC, Wu D, Yang S, Yao QA, Ye J, Yeh RF, Zaveri JS, Zhan M, Zhang G, Zhao Q, Zheng L, Zheng XH, Zhong FN, Zhong W, Zhou X, Zhu S, Zhu X, Smith HO, Gibbs RA, Myers EW, Rubin GM, Venter JC (2000) The genome sequence of Drosophila melanogaster. Science 287:2185-2195.

Adams MD, Sekelsky JJ (2002) From sequence to phenotype: reverse genetics in Drosophila melanogaster. Nat Rev Genet 3:189-198.

Alexander GM, Rogan SC, Abbas AI, Armbruster BN, Pei Y, Allen JA, Nonneman RJ, Hartmann J, Moy SS, Nicolelis MA, McNamara JO, Roth BL (2009) Remote control of neuronal activity in transgenic mice expressing evolved G protein-coupled receptors. Neuron 63:27-39.

Alves dos Santos MT, Smidt MP (2011) En1 and Wnt signaling in midbrain dopaminergic neuronal development. Neural Dev 6:23.

Andrews ZB, Zhao H, Frugier T, Meguro R, Grattan DR, Koishi K, McLennan IS (2006) Transforming growth factor beta2 haploinsufficient mice develop age-related nigrostriatal dopamine deficits. Neurobiol Dis 21:568-575.

Aperia AC (2000) Intrarenal dopamine: a key signal in the interactive regulation of sodium metabolism. Annu Rev Physiol 62:621-647.

Armbruster BN, Li X, Pausch MH, Herlitze S, Roth BL (2007) Evolving the lock to fit the key to create a family of G protein-coupled receptors potently activated by an inert ligand. Proceedings of the National Academy of Sciences 104:5163-5168.

Bang S, Hyun S, Hong S-T, Kang J, Jeong K, Park J-J, Choe J, Chung J (2011) Dopamine Signalling in Mushroom Bodies Regulates Temperature-Preference Behaviour in Drosophila. PLoS Genet 7:e1001346.

Bayersdorfer F, Voigt A, Schneuwly S, Botella JA (2010) Dopamine-dependent neurodegeneration in Drosophila models of familial and sporadic Parkinson's disease. Neurobiol Dis 40:113-119.

Beaulieu J-M, Gainetdinov RR (2011) The Physiology, Signaling, and Pharmacology of Dopamine Receptors. Pharmacological Reviews 63:182-217.

Bellen HJ, Tong C, Tsuda H (2010) 100 years of Drosophila research and its impact on vertebrate neuroscience: a history lesson for the future. Nat Rev Neurosci 11:514-522.

Berwick DC, Harvey K (2012) The importance of Wnt signalling for neurodegeneration in Parkinson's disease. Biochem Soc Trans 40:1123-1128.

Berwick DC, Harvey K (2013) LRRK2: an eminence grise of Wnt-mediated neurogenesis? Front Cell Neurosci 7:82.

Betarbet R, Sherer TB, MacKenzie G, Garcia-Osuna M, Panov AV, Greenamyre JT (2000) Chronic systemic pesticide exposure reproduces features of Parkinson's disease. Nat Neurosci 3:1301-1306.

Bibb JA, Snyder GL, Nishi A, Yan Z, Meijer L, Fienberg AA, Tsai LH, Kwon YT, Girault JA, Czernik AJ, Huganir RL, Hemmings HC, Jr., Nairn AC, Greengard P (1999) Phosphorylation of DARPP-32 by Cdk5 modulates dopamine signalling in neurons. Nature 402:669-671.

Bier E (2005) Drosophila, the golden bug, emerges as a tool for human genetics. Nat Rev Genet 6:9-23.

Bilen J, Bonini NM (2005) Drosophila as a model for human neurodegenerative disease. Annu Rev Genet 39:153-171.

Blakely BD, Bye CR, Fernando CV, Horne MK, Macheda ML, Stacker SA, Arenas E, Parish CL (2011) Wnt5a regulates midbrain dopaminergic axon growth and guidance. PLoS ONE 6:e18373.

Blum K, Chen AL, Giordano J, Borsten J, Chen TJ, Hauser M, Simpatico T, Femino J, Braverman ER, Barh D (2012) The addictive brain: all roads lead to dopamine. J Psychoactive Drugs 44:134-143.

Brand AH, Perrimon N (1993) Targeted gene expression as a means of altering cell fates and generating dominant phenotypes. Development 118:401-415.

Bruce DL, Sapkota GP (2012) Phosphatases in SMAD regulation. FEBS Lett 586:1897-1905.

Busch S, Selcho M, Ito K, Tanimoto H (2009) A map of octopaminergic neurons in the Drosophila brain. The Journal of Comparative Neurology 513:643-667.

Cameron HA, Hazel TG, McKay RD (1998) Regulation of neurogenesis by growth factors and neurotransmitters. J Neurobiol 36:287-306.

Cantuti-Castelvetri I, Keller-McGandy C, Bouzou B, Asteris G, Clark TW, Frosch MP, Standaert DG (2007) Effects of gender on nigral gene expression and parkinson disease. Neurobiol Dis 26:606-614.

Castelo-Branco G, Rawal N, Arenas E (2004) GSK-3beta inhibition/beta-catenin stabilization in ventral midbrain precursors increases differentiation into dopamine neurons. J Cell Sci 117:5731-5737.

Chan CS, Guzman JN, Ilijic E, Mercer JN, Rick C, Tkatch T, Meredith GE, Surmeier DJ (2007) 'Rejuvenation' protects neurons in mouse models of Parkinson's disease. Nature 447:1081-1086.

Chen JF, Xu K, Petzer JP, Staal R, Xu YH, Beilstein M, Sonsalla PK, Castagnoli K, Castagnoli N, Jr., Schwarzschild MA (2001) Neuroprotection by caffeine and A(2A) adenosine receptor inactivation in a model of Parkinson's disease. J Neurosci 21:RC143.

Chiang A-S, Lin C-Y, Chuang C-C, Chang H-M, Hsieh C-H, Yeh C-W, Shih C-T, Wu J-J, Wang G-T, Chen Y-C, Wu C-C, Chen G-Y, Ching Y-T, Lee P-C, Lin C-Y, Lin H-H, Wu C-C, Hsu H-W, Huang Y-A, Chen J-Y, Chiang H-J, Lu C-F, Ni R-F, Yeh C-Y, Hwang J-K (2011) Three-Dimensional Reconstruction of Brain-wide Wiring Networks in Drosophila at Single-Cell Resolution. Current biology : CB 21:1-11.

Choi C, Cao G, Tanenhaus AK, McCarthy EV, Jung M, Schleyer W, Shang Y, Rosbash M, Yin JC, Nitabach MN (2012) Autoreceptor control of peptide/neurotransmitter corelease from PDF neurons determines allocation of circadian activity in drosophila. Cell Rep 2:332-344.

Chorna T, Hasan G (2012) The genetics of calcium signaling in Drosophila melanogaster. Biochim Biophys Acta 1820:1269-1282.

Civelli O, Bunzow JR, Grandy DK, Zhou Q-Y, Van Tol HHM (1991) Molecular biology of the dopamine receptors. European Journal of Pharmacology: Molecular Pharmacology 207:277-286.

Cottrell GA (1967) Occurrence of dopamine and noradrenaline in the nervous tissue of some invertebrate species. Br J Pharmacol Chemother 29:63-69.

Coulom H, Birman S (2004) Chronic exposure to rotenone models sporadic Parkinson's disease in Drosophila melanogaster. J Neurosci 24:10993-10998.

Dawson TM, Ko HS, Dawson VL (2010) Genetic animal models of Parkinson's disease. Neuron 66:646-661.

De Mei C, Ramos M, Iitaka C, Borrelli E (2009) Getting specialized: presynaptic and postsynaptic dopamine D2 receptors. Curr Opin Pharmacol 9:53-58.

de Rooij J, Zwartkruis FJ, Verheijen MH, Cool RH, Nijman SM, Wittinghofer A, Bos JL (1998) Epac is a Rap1 guanine-nucleotide-exchange factor directly activated by cyclic AMP. Nature 396:474-477.

Diegelmann S, Fiala A, Leibold C, Spall T, Buchner E (2002) Transgenic flies expressing the fluorescence calcium sensor cameleon 2.1 under UAS control. genesis 34:95-98.

Draper I, Kurshan PT, McBride E, Jackson FR, Kopin AS (2007) Locomotor activity is regulated by D2-like receptors in Drosophila: An anatomic and functional analysis. Developmental Neurobiology 67:378-393.

El-kholy EGS (2010) Bioamine receptors of the fruit fly Drosophila melanogaster as targets for insecticides. PhD Thesis, CAU-Kiel.

Feany MB, Bender WW (2000) A Drosophila model of Parkinson's disease. Nature 404:394-398.

Fearnley JM, Lees AJ (1991) Ageing and Parkinson's disease: substantia nigra regional selectivity. Brain 114 (Pt 5):2283-2301.

Feng G, Hannan F, Reale V, Hon YY, Kousky CT, Evans PD, Hall LM (1996) Cloning and functional characterization of a novel dopamine receptor from Drosophila melanogaster. J Neurosci 16:3925-3933.

Forno LS (1996) Neuropathology of Parkinson's disease. J Neuropathol Exp Neurol 55:259-272.

Francesca LE, Maria FS, Cataldo T, Nunzio T, Salvatore C, Maria CM, Stefano P, Bianca M (2011b) A Wnt1 regulated Frizzled-1/Î²-Catenin signaling pathway as a candidate regulatory circuit controlling mesencephalic dopaminergic neuron-astrocyte crosstalk: Therapeutical relevance for neuron survival and neuroprotection. Molecular Neurodegeneration 6:49-49.

Friggi-Grelin F, Coulom H, Meller M, Gomez D, Hirsh J, Birman S (2003) Targeted gene expression in Drosophila dopaminergic cells using regulatory sequences from tyrosine hydroxylase. J Neurobiol 54:618-627.

Gerfen CR (2003) D1 dopamine receptor supersensitivity in the dopamine-depleted striatum animal model of Parkinson's disease. Neuroscientist 9:455-462.

Giros B, Sokoloff P, Martres MP, Riou JF, Emorine LJ, Schwartz JC (1989) Alternative splicing directs the expression of two D2 dopamine receptor isoforms. Nature 342:923-926.

Gotzes F, Balfanz S, Baumann A (1994) Primary structure and functional characterization of a Drosophila dopamine receptor with high homology to human D1/5 receptors. Receptors Channels 2:131-141.

Guo M (2012) Drosophila as a model to study mitochondrial dysfunction in Parkinson's disease. Cold Spring Harb Perspect Med 2.

Gupta A, Dawson VL, Dawson TM (2008) What causes cell death in Parkinson's disease? Ann Neurol 64 Suppl 2:S3-15.

Han KA, Millar NS, Grotewiel MS, Davis RL (1996) DAMB, a novel dopamine receptor expressed specifically in Drosophila mushroom bodies. Neuron 16:1127-1135.

Hart RG, Pearce LA, Ravina BM, Yaltho TC, Marler JR (2009) Neuroprotection trials in Parkinson's disease: systematic review. Mov Disord 24:647-654.

Hay N, Sonenberg N (2004) Upstream and downstream of mTOR. Genes Dev 18:1926-1945.

Hearn MG, Ren Y, McBride EW, Reveillaud I, Beinborn M, Kopin AS (2002) A Drosophila dopamine 2-like receptor: Molecular characterization and identification of multiple alternatively spliced variants. Proc Natl Acad Sci U S A 99:14554-14559.

Herve D, Levi-Strauss M, Marey-Semper I, Verney C, Tassin JP, Glowinski J, Girault JA (1993) G(olf) and Gs in rat basal ganglia: possible involvement of G(olf) in the coupling of dopamine D1 receptor with adenylyl cyclase. J Neurosci 13:2237-2248.

Ho A (2002) Two Wrongs Make A Right: Nicotine and Caffeine as Defensive Agents Against Parkinson's Disease. Nutrition Bytes 8.

Hosamani R, Muralidhara (2010) Prophylactic treatment with Bacopa monnieri leaf powder mitigates paraquat-induced oxidative perturbations and lethality in Drosophila melanogaster. Indian J Biochem Biophys 47:75-82.

Hsuan SL, Klintworth HM, Xia Z (2006) Basic fibroblast growth factor protects against rotenone-induced dopaminergic cell death through activation of extracellular signal-regulated kinases 1/2 and phosphatidylinositol-3 kinase pathways. J Neurosci 26:4481-4491.

Huang da W, Sherman BT, Lempicki RA (2009) Systematic and integrative analysis of large gene lists using DAVID bioinformatics resources. Nat Protoc 4:44-57.

Inagaki Hidehiko K, Ben-Tabou de-Leon S, Wong AM, Jagadish S, Ishimoto H, Barnea G, Kitamoto T, Axel R, Anderson David J (2012b) Visualizing Neuromodulation In Vivo: TANGO-Mapping of Dopamine Signaling Reveals Appetite Control of Sugar Sensing. Cell 148:583-595.

Inestrosa NC, Arenas E (2010) Emerging roles of Wnts in the adult nervous system. Nat Rev Neurosci 11:77-86.

Inestrosa NC, Toledo EM (2008) The role of Wnt signaling in neuronal dysfunction in Alzheimer's Disease. Mol Neurodegener 3:9.

Iversen SD, Iversen LL (2007) Dopamine: 50 years in perspective. Trends Neurosci 30:188-193.

Iyer EPR, Iyer SC, Sulkowski MJ, Cox DN (2009) Isolation and Purification of Drosophila Peripheral Neurons by Magnetic Bead Sorting. J Vis Exp e1599.

Jimenez-Del-Rio M, Guzman-Martinez C, Velez-Pardo C (2010) The effects of polyphenols on survival and locomotor activity in Drosophila melanogaster exposed to iron and paraquat. Neurochem Res 35:227-238.

Kalidas S, Smith DP (2002) Novel genomic cDNA hybrids produce effective RNA interference in adult Drosophila. Neuron 33:177-184.

Kallsen K. pers. comm., Forschungszentrum Borstel-Kiel, Germany.

Katsuno M, Banno H, Suzuki K, Adachi H, Tanaka F, Sobue G (2011) TGF-beta signaling in neurodegenerative diseases]. Rinsho Shinkeigaku 51:982-985.

Kebabian JW, Calne DB (1979) Multiple receptors for dopamine. Nature 277:93-96.

Kebabian JW, Greengard P (1971) Dopamine-sensitive adenyl cyclase: possible role in synaptic transmission. Science 174:1346-1349.

Kim EK, Choi EJ (2010) Pathological roles of MAPK signaling pathways in human diseases. Biochim Biophys Acta 1802:396-405.

Kim Y-C, Lee H-G, Seong C-S, Han K-A (2003) Expression of a D1 dopamine receptor dDA1/DmDOP1 in the central nervous system of Drosophila melanogaster. Gene Expression Patterns 3:237-245.

Kim YC, Lee HG, Han KA (2007) D1 dopamine receptor dDA1 is required in the mushroom body neurons for aversive and appetitive learning in Drosophila. J Neurosci 27:7640-7647.

Koh YH, Rehfeld K, Ganetzky B (2004) A Drosophila model of early onset torsion dystonia suggests impairment in TGF-beta signaling. Hum Mol Genet 13:2019-2030.

Kong EC, Allouche L, Chapot PA, Vranizan K, Moore MS, Heberlein U, Wolf FW (2010) Ethanol-regulated genes that contribute to ethanol sensitivity and rapid tolerance in Drosophila. Alcohol Clin Exp Res 34:302-316.

Krashes MJ, Koda S, Ye C, Rogan SC, Adams AC, Cusher DS, Maratos-Flier E, Roth BL, Lowell BB (2011) Rapid, reversible activation of AgRP neurons drives feeding behavior in mice. J Clin Invest 121:1424-1428.

L'Episcopo F, Tirolo C, Testa N, Caniglia S, Morale MC, Cossetti C, D'Adamo P, Zardini E, Andreoni L, Ihekwaba AE, Serra PA, Franciotta D, Martino G, Pluchino S, Marchetti B (2011a) Reactive astrocytes and Wnt/beta-catenin signaling link nigrostriatal injury to repair in 1-methyl-4-phenyl-1,2,3,6-tetrahydropyridine model of Parkinson's disease. Neurobiol Dis 41:508-527.

Le Bourg E, Lints FA (1992) Hypergravity and aging in Drosophila melanogaster. 4. Climbing activity. Gerontology 38:59-64.

Lebestky T, Chang JS, Dankert H, Zelnik L, Kim YC, Han KA, Wolf FW, Perona P, Anderson DJ (2009) Two different forms of arousal in Drosophila are oppositely regulated by the dopamine D1 receptor ortholog DopR via distinct neural circuits. Neuron 64:522-536.

Lefkowitz RJ, Shenoy SK (2005) Transduction of Receptor Signals by ÃŸ-Arrestins. Science 308:512-517.

Lessing D, Bonini NM (2009) Maintaining the brain: insight into human neurodegeneration from Drosophila melanogaster mutants. Nat Rev Genet 10:359-370.

Li ZS, Schmauss C, Cuenca A, Ratcliffe E, Gershon MD (2006) Physiological modulation of intestinal motility by enteric dopaminergic neurons and the D2 receptor: analysis of dopamine receptor expression, location, development, and function in wild-type and knock-out mice. J Neurosci 26:2798-2807.

Liang-Wei C (2013) Roles of Wnt/Î²-Catenin Signaling in Controlling the Dopaminergic Neuronal Cell Commitment of Midbrain and Therapeutic Application for Parkinsonâ€™s Disease.

Lieberthal W, Levine JS (2012) Mammalian target of rapamycin and the kidney. I. The signaling pathway. Am J Physiol Renal Physiol 303:F1-10.

Mao Z, Davis RL (2009) Eight different types of dopaminergic neurons innervate the Drosophila mushroom body neuropil: anatomical and physiological heterogeneity. Front Neural Circuits 3:5.

Marchetti B, L'Episcopo F, Morale MC, Tirolo C, Testa N, Caniglia S, Serapide MF, Pluchino S (2013) Uncovering novel actors in astrocyte–neuron crosstalk in Parkinson's disease: the Wnt/β-catenin signaling cascade as the common final pathway for neuroprotection and self-repair. European Journal of Neuroscience 37:1550-1563.

Missale C, Nash RS, Robinson SW, Jaber M, Caron MG (1998) Dopamine Receptors: From Structure to Function. Physiological Reviews 78:189-225.

Monsma FJ, McVittie LD, Gerfen CR, Mahan LC, Sibley DR (1989) Multiple D2 dopamine receptors produced by alternative RNA splicing. Nature 342:926-929.

Nagai H, Noguchi T, Takeda K, Ichijo H (2007) Pathophysiological roles of ASK1-MAP kinase signaling pathways. J Biochem Mol Biol 40:1-6.

Nassel DR, Elekes K (1992) Aminergic neurons in the brain of blowflies and Drosophila: dopamine- and tyrosine hydroxylase-immunoreactive neurons and their relationship with putative histaminergic neurons. Cell Tissue Res 267:147-167.

Neve KA, Seamans JK, Trantham-Davidson H (2004) Dopamine Receptor Signaling. Journal of Receptors and Signal Transduction 24:165-205.

Nichols CD, Roth BL (2009) Engineered G-protein Coupled Receptors are Powerful Tools to Investigate Biological Processes and Behaviors. Front Mol Neurosci 2:16.

Nichols CD, pers. comm., Louisiana State University Health Sciences Center, New Orleans, LA, USA.

Nusse R, Brown A, Papkoff J, Scambler P, Shackleford G, McMahon A, Moon R, Varmus H (1991) A new nomenclature for int-1 and related genes: the Wnt gene family. Cell 64:231.

Ohlstein B, Spradling A (2006) The adult Drosophila posterior midgut is maintained by pluripotent stem cells. Nature 439:470-474.

Ohnuki T, Nakamura A, Okuyama S, Nakamura S (2010) Gene expression profiling in progressively MPTP-lesioned macaques reveals molecular pathways associated with sporadic Parkinson's disease. Brain Res 1346:26-42.

Pfaffl MW (2001) A new mathematical model for relative quantification in real-time RT-PCR. Nucleic Acids Res 29:e45.

Pfeiffer BD, Ngo TT, Hibbard KL, Murphy C, Jenett A, Truman JW, Rubin GM (2010) Refinement of tools for targeted gene expression in Drosophila. Genetics 186:735-755.

Raftery LA, Sutherland DJ (1999) TGF-beta family signal transduction in Drosophila development: from Mad to Smads. Dev Biol 210:251-268.

Rahn T, Leippe M, Roeder T, Fedders H (2013) EGFR signaling in the brain is necessary for olfactory learning in Drosophila larvae. Learn Mem 20:194-200.

Rawal N, Corti O, Sacchetti P, Ardilla-Osorio H, Sehat B, Brice A, Arenas E (2009) Parkin protects dopaminergic neurons from excessive Wnt/beta-catenin signaling. Biochem Biophys Res Commun 388:473-478.

Ray RS, Corcoran AE, Brust RD, Kim JC, Richerson GB, Nattie E, Dymecki SM (2011) Impaired Respiratory and Body Temperature Control Upon Acute Serotonergic Neuron Inhibition. Science 333:637-642.

Renn SC, Park JH, Rosbash M, Hall JC, Taghert PH (1999) A pdf neuropeptide gene mutation and ablation of PDF neurons each cause severe abnormalities of behavioral circadian rhythms in Drosophila. Cell 99:791-802.

Rijsewijk F, Schuermann M, Wagenaar E, Parren P, Weigel D, Nusse R (1987) The Drosophila homolog of the mouse mammary oncogene int-1 is identical to the segment polarity gene wingless. Cell 50:649-657.

Rondou P, Haegeman G, Van Craenenbroeck K (2010) The dopamine D4 receptor: biochemical and signalling properties. Cell Mol Life Sci 67:1971-1986.

Rubin GM, Spradling AC (1982) Genetic transformation of Drosophila with transposable element vectors. Science 218:348-353.

Rulifson EJ, Kim SK, Nusse R (2002) Ablation of Insulin-Producing Neurons in Flies: Growth and Diabetic Phenotypes. Science 296:1118-1120.

Sasaki K, Suzuki M, Mieda M, Tsujino N, Roth B, Sakurai T (2011) Pharmacogenetic modulation of orexin neurons alters sleep/wakefulness states in mice. PLoS ONE 6:e20360.

Scherzer CR, Jensen RV, Gullans SR, Feany MB (2003) Gene expression changes presage neurodegeneration in a Drosophila model of Parkinson's disease. Hum Mol Genet 12:2457-2466.

Scholz H, Ramond J, Singh CM, Heberlein U (2000) Functional ethanol tolerance in Drosophila. Neuron 28:261-271.

Seidl SE, Potashkin JA (2011) The promise of neuroprotective agents in Parkinson's disease. Front Neurol 2:68.

Selcho M, Pauls D, Han KA, Stocker RF, Thum AS (2009) The role of dopamine in Drosophila larval classical olfactory conditioning. PLoS ONE 4.

Shang Y, Haynes P, Pirez N, Harrington KI, Guo F, Pollack J, Hong P, Griffith LC, Rosbash M (2011) Imaging analysis of clock neurons reveals light buffers the wake-promoting effect of dopamine. Nat Neurosci 14:889-895.

Sherer TB, Betarbet R, Testa CM, Seo BB, Richardson JR, Kim JH, Miller GW, Yagi T, Matsuno-Yagi A, Greenamyre JT (2003) Mechanism of toxicity in rotenone models of Parkinson's disease. J Neurosci 23:10756-10764.

Shieh S-Y, Bonini NM (2011) Genes and pathways affected by CAG-repeat RNA-based toxicity in Drosophila. Human Molecular Genetics.

Simunovic F, Yi M, Wang Y, Macey L, Brown LT, Krichevsky AM, Andersen SL, Stephens RM, Benes FM, Sonntag KC (2009) Gene expression profiling of substantia nigra dopamine neurons: further insights into Parkinson's disease pathology. Brain 132:1795-1809.

Simunovic F, Yi M, Wang Y, Stephens R, Sonntag KC (2010) Evidence for Gender-Specific Transcriptional Profiles of Nigral Dopamine Neurons in Parkinson Disease. PLoS ONE 5:e8856.

Snell GD, Reed S (1993) William Ernest Castle, pioneer mammalian geneticist. Genetics 133:751.

Sokoloff P, Diaz J, Le Foll B, Guillin O, Leriche L, Bezard E, Gross C (2006) The dopamine D3 receptor: a therapeutic target for the treatment of neuropsychiatric disorders. CNS Neurol Disord Drug Targets 5:25-43.

Sonia Angeline M, Chaterjee P, Anand K, Ambasta RK, Kumar P (2012) Rotenone-induced parkinsonism elicits behavioral impairments and differential expression of parkin, heat shock proteins and caspases in the rat. Neuroscience 220:291-301.

Srivastava DP, Yu EJ, Kennedy K, Chatwin H, Reale V, Hamon M, Smith T, Evans PD (2005) Rapid, nongenomic responses to ecdysteroids and catecholamines mediated by a novel Drosophila G-protein-coupled receptor. J Neurosci 25:6145-6155.

Strauss R (2002) The central complex and the genetic dissection of locomotor behaviour. Curr Opin Neurobiol 12:633-638.

Sugamori KS, Demchyshyn LL, McConkey F, Forte MA, Niznik HB (1995) A primordial dopamine D1-like adenylyl cyclase-linked receptor from Drosophila melanogaster displaying poor affinity for benzazepines. FEBS Letters 362:131-138.

Surmeier DJ (2007) Calcium, ageing, and neuronal vulnerability in Parkinson's disease. The Lancet Neurology 6:933-938.

Takeda K, Noguchi T, Naguro I, Ichijo H (2008) Apoptosis signal-regulating kinase 1 in stress and immune response. Annu Rev Pharmacol Toxicol 48:199-225.

Tanaka NK, Tanimoto H, Ito K (2008) Neuronal assemblies of the Drosophila mushroom body. J Comp Neurol 508:711-755.

Tang M, Miyamoto Y, Huang EJ (2009) Multiple roles of beta-catenin in controlling the neurogenic niche for midbrain dopamine neurons. Development 136:2027-2038.

Tateno M, Nishida Y, Adachi-Yamada T (2000) Regulation of JNK by Src During Drosophila Development. Science 287:324-327.

Tesseur I, Zou K, Esposito L, Bard F, Berber E, Can JV, Lin AH, Crews L, Tremblay P, Mathews P, Mucke L, Masliah E, Wyss-Coray T (2006) Deficiency in neuronal TGF-beta signaling promotes neurodegeneration and Alzheimer's pathology. J Clin Invest 116:3060-3069.

Thomas GM, Huganir RL (2004) MAPK cascade signalling and synaptic plasticity. Nat Rev Neurosci 5:173-183.

Tucker MS, Khan I, Fuchs-Young R, Price S, Steininger TL, Greene G, Wainer BH, Rosner MR (1993) Localization of immunoreactive epidermal growth factor receptor in neonatal and adult rat hippocampus. Brain Res 631:65-71.

Vallone D, Picetti R, Borrelli E (2000) Structure and function of dopamine receptors. Neuroscience & Biobehavioral Reviews 24:125-132.

van Swinderen B, Andretic R (2003) Arousal in Drosophila. Behav Processes 64:133-144.

Venken KJ, Bellen HJ (2007) Transgenesis upgrades for Drosophila melanogaster. Development 134:3571-3584.

Venken KJT, Bellen HJ (2005) Emerging technologies for gene manipulation in Drosophila melanogaster. Nat Rev Genet 6:167-178.

Whitworth AJ (2011) Drosophila models of Parkinson's disease. Adv Genet 73:1-50.

Whitworth AJ, Wes PD, Pallanck LJ (2006) Drosophila models pioneer a new approach to drug discovery for Parkinson's disease. Drug Discov Today 11:119-126.

Wieduwilt MJ, Moasser MM (2008) The epidermal growth factor receptor family: biology driving targeted therapeutics. Cell Mol Life Sci 65:1566-1584.

Witkovsky P (2004) Dopamine and retinal function. Documenta Ophthalmologica 108:17-39.

Wong RW, Guillaud L (2004) The role of epidermal growth factor and its receptors in mammalian CNS. Cytokine Growth Factor Rev 15:147-156.

Wulbeck C, Grieshaber E, Helfrich-Forster C (2008) Pigment-dispersing factor (PDF) has different effects on Drosophila's circadian clocks in the accessory medulla and in the dorsal brain. J Biol Rhythms 23:409-424.

Xu Y, Yan J, Zhou P, Li J, Gao H, Xia Y, Wang Q (2012) Neurotransmitter receptors and cognitive dysfunction in Alzheimer's disease and Parkinson's disease. Prog Neurobiol 97:1-13.

Yamada M, Ikeuchi T, Hatanaka H (1997) The neurotrophic action and signalling of epidermal growth factor. Prog Neurobiol 51:19-37.

Zhen X, Uryu K, Wang HY, Friedman E (1998) D1 dopamine receptor agonists mediate activation of p38 mitogen-activated protein kinase and c-Jun amino-terminal kinase by a protein kinase A-dependent mechanism in SK-N-MC human neuroblastoma cells. Mol Pharmacol 54:453-458.

Zimprich A, Biskup S, Leitner P, Lichtner P, Farrer M, Lincoln S, Kachergus J, Hulihan M, Uitti RJ, Calne DB, Stoessl AJ, Pfeiffer RF, Patenge N, Carbajal IC, Vieregge P, Asmus F, Muller-Myhsok B, Dickson DW, Meitinger T, Strom TM, Wszolek ZK, Gasser T (2004) Mutations in LRRK2 cause autosomal-dominant parkinsonism with pleomorphic pathology. Neuron 44:601-607.

Zoghbi HY, Warren ST (2010) Neurogenetics: advancing the "next-generation" of brain research. Neuron 68:165-173.

Zoncu R, Efeyan A, Sabatini DM (2012) mTOR: from growth signal integration to cancer, diabetes and ageing. Nat Rev Mol Cell Biol 12:21-35.

ACKNOWLEDGEMENTS

First and foremost, I owe my deepest gratitude to my supervisor, Prof. Dr. Thomas Roeder for his guidance and support throughout the program. This thesis would not have been possible without his valuable ideas and encouragement that made me to understand the subject of my research and remained motivated.

The financial support provided by World Bank project CIBI of the College of Natural and Applied Sciences, University of Dar es Salaam, Tanzania is greatly acknowledged.

I thank Britta Laubenstein for her assistance in the laboratory, particularly, quantitative real time PCR technique. Also special thank to Dr. Kim Kallsen (Research Centre Borstel), who kindly provided some of the primers used in this study. The support of Dr. Christine Fink, Dr. Julia Hoffmann, Dr. Huajiang Xiong, and Li Yong in handling the transcriptomic data is highly appreciated. Special thank to Dr. Julia Hoffmann for the German version of the summary of this thesis. My cordial thanks also go to the Department of Zoophysiology I and II members for the friendly working environment.

Last but not least, I am deeply indebted to my husband Dr. Nelson Boniface for his love, encouragement and more importantly for his patience especially all this time, which I was away from home. Taking good care of two children without a mother around was not an easy task for you, but you never complained. You are a wonderful husband and a father. I am also heartily indebted to my lovely children, Kennedy and Elizabeth for missing mother's care. You were, are and will always be my motivator. I also thank my parents, my siblings, my relatives and my in-laws for the encouragement and prayers. I also thank all who in one way or another help me academically or socially to make all this possible.

CURRICULUM VITAE

Personal information

Name: Flora

Surname: Stephano

Date of birth: 6.10.1976

Place of birth: Ileje-Mbeya, Tanzania.

Nationality: Tanzanian

Marital status: Married

Academic qualifications

October 2009-date: PhD student at the Institute of Zoophysiology II, Christian–Albrechts University, Kiel, Germany. Title of my thesis: Manipulation of the dopaminergic system in the fruit fly *Drosophila melanogaster* as a tool to model Parkinson's disease

October 2002-June 2006: Master of Science (Zoology) University of Dar es Salaam, Tanzania. Investigations on the development of the myelencephalon in the clawed-frog, *Xenopus muelleri.*

October 1998-September 2002: Bachelor of Science General majoring in Zoology & Wildlife Ecology & Management University of Dar es Salaam**,** Tanzania.

Work experience

June 2006-date: Assistant Lecturer University of Dar es Salaam, Department of Zoology and Wildlife Conservation, Dar es Salaam, Tanzania.

Workshops, Scientific Conferences and other trainings

June 12-17, 2013: 11th Society of Neuroscientists of Africa (SONA) International Conference Rabat, Morocco**.** Poster presentation with the title: Transcriptome analysis indicates early signs of neurodegeneration in *Drosophila* model of Parkinson's disease

July 28-29, 2011: 22nd Neurobiology PhD student Workshop**.** Department of Zoology University of Bonn, Germany. Poster presentation with the title: Dopamine receptors in the Central Nervous System of the fruit fly *Drosophila melanogaster.*

January–May 2009: spring semester –Graduate courses in Neuroscience at Brown University Providence, USA. (Academic exchange program between University of Dar es Salaam and Brown University).

August 2003: Workshop on Genes, Genomics and Development of Behavior**:** the development of function in the Nervous system ICTP, Trieste, Italy

September 2002: 3rd IBRO Neuroscience School: Techniques in structure and functions of vertebrate Nervous systems, Nairobi, Kenya

DECLARATION

I here declare that this work is my own work apart from supervisor's guidance and acknowledged assistances. This dissertation has not been submitted for the award of doctoral degree to another examining body and was prepared according to the Rules of Good Scientific Practice of the German Research Foundation.

Part of this thesis was presented as posters:

Flora Stephano and Thomas Roeder (2013). Transcriptome analysis indicates early signs of neurodegeneration in *Drosophila* model of Parkinson's disease. **11th International Conference of the Society of Neuroscientists of Africa,** Rabat, Morocco.

Flora Stephano, Samar El-Kholy and Thomas Roeder (2011) Dopamine receptors in the Central Nervous System of the fruit fly *Drosophila melanogaster.* **22nd Neurobiology PhD student Workshop.** Department of Zoology University of Bonn, Germany.

The three dopamine receptor GAL4 lines DopR (CG9652), DopR2 (CG18741), and D2R (CG33517) were generated in Prof. Dr. Thomas Roeder's laboratory and BestGene Inc services by Samar Elkoly, PHD thesis (2010).

Date, place

Signature

APPENDICES

Appendix 1: Immunofluorescence of larval midgut cells.

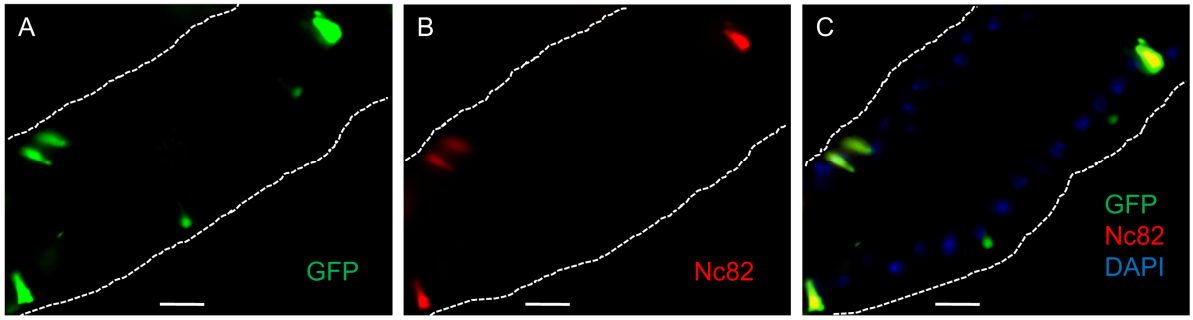

Fig A1 DopR is expressed in the Enteroendocrine cells (EEs). (A) Enhancement of GFP reporter for DopR-Gal4 expression in EEs by anti-GFP antibody (green). (B) Nc 82 positive cells (red). (C) Co-localization of fluorescent signals, yellow, and a DNA/nuclei marker, DAPI (blue). Scale bars: 20 µm

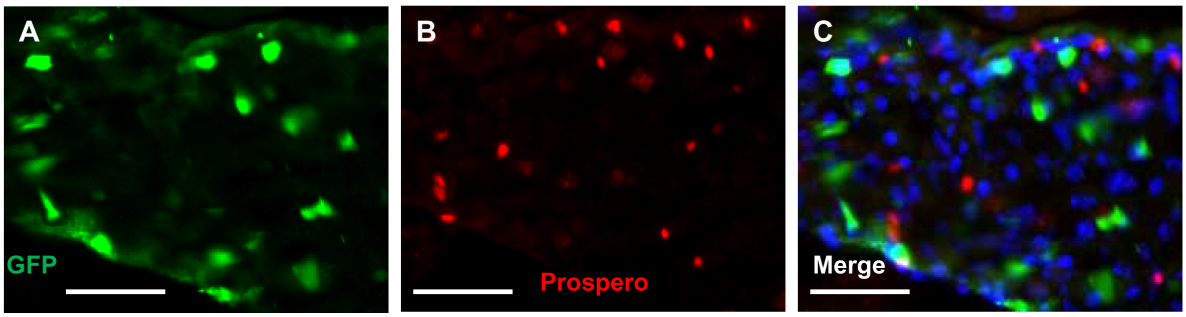

Fig A2 D2R is not expressed in the Enteroendocrine cells (EEs). (A) Enhancement of GFP reporter for D2R-Gal4 expression in EEs by anti-GFP antibody (green). (B) Prospero positive cells (red). (C) No co-localization of fluorescent signals between green and red is seen. DNA/nuclei marker, DAPI (blue). Scale bars: 20 µm

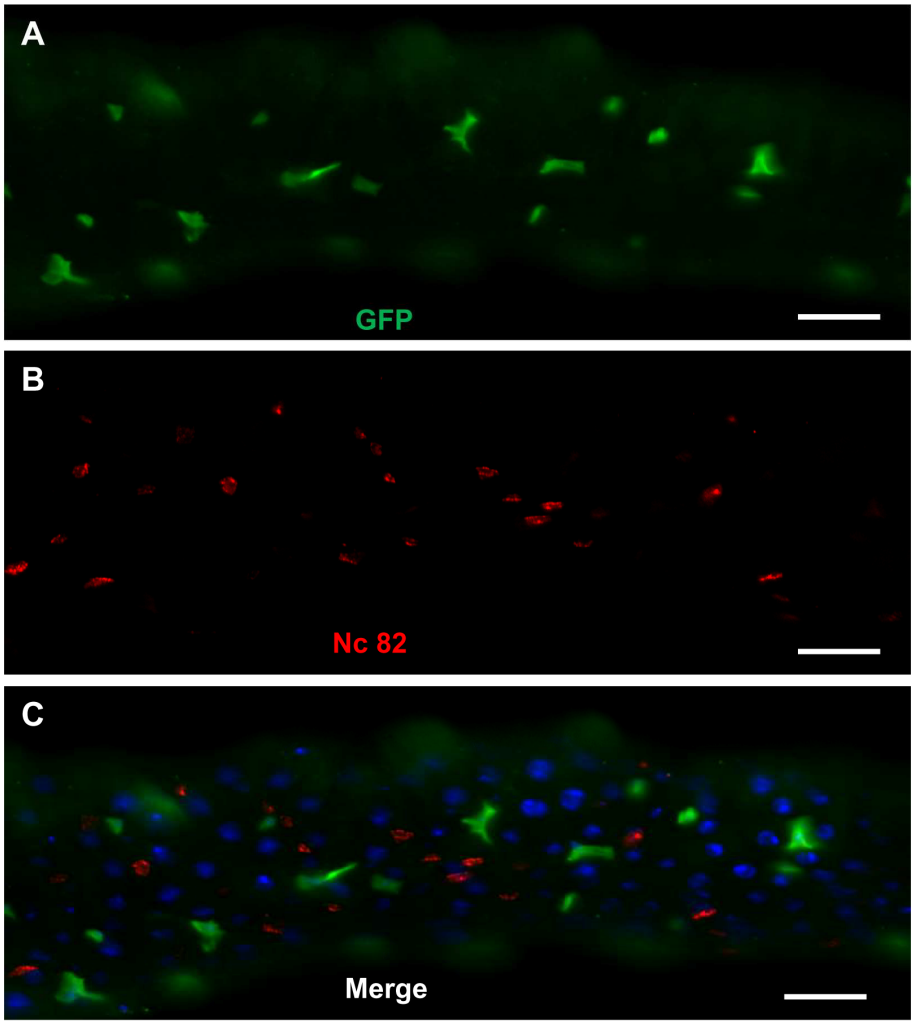

Fig A3 D2R is not expressed in the Enteroendocrine cells (EEs). (A) Enhancement of GFP reporter for D2R-Gal4 expression in EEs by anti-GFP antibody (green). (B) Nc 82 positive cells (red). (C) No co-localization of fluorescent signals between green and red is seen. DNA/nuclei marker, DAPI (blue). Scale bars: 20 µm

Table A2. List of upregulated genes upon rotenone treatment

id	Symbol	Mean	SEM
CG100435	CG100435	1,942	0.085
CG10045	GstD1	1,869	0.025
CG10059	MAGE	1,365	0.191
CG10079	Egfr	1,837	0.025
CG10107	velo	1,566	0.174
CG10119	LamC	1,355	0.073
CG10134	beat-Va	1,901	0.054
CG10158	CG10158	1,858	0.113
CG10215	Ercc1	1,731	0.012
CG10243	Cyp6a19	1,084	0.291
CG10261	aPKC	2,220	0.070
CG10264	CG10264	1,335	0.120
CG10281	TfIIFalpha	2,005	0.043
CG10303	Osi4	2,121	0.089
CG10332	CG10332	1,667	0.057
CG10333	CG10333	1,355	0.444
CG10379	mbc	1,910	0.193
CG10419	Gem2	1,286	0.191
CG10428	CG10428	1,502	0.076
CG10474	CG10474	1,658	0.014
CG10477	CG10477	1,770	0.172
CG10489	Pole2	1,575	0.018
CG1056	5-HT2	2,083	0.107
CG10560	CG10560	2,709	0.372
CG10572	Cdk8	1,849	0.206
CG10575	Ppat-Dpck	1,359	0.066
CG10581	CG10581	1,598	0.055
CG10669	CG10669	1,588	0.116
CG10686	tral	2,289	0.134
CG10747	CG10747	2,280	0.073
CG10772	Fur1	1,655	0.006
CG1079	Fie	1,710	0.074
CG10801	CG10801	1,488	0.022
CG10811	eIF4G	1,157	0.292
CG10822	CG10822	1,620	0.069
CG10837	eIF-4B	1,870	0.186
CG10845	CG10845	1,052	0.182
CG10849	Sc2	1,104	0.151
CG10895	lok	1,390	0.154
CG10933	CG10933	1,867	0.070

CG10952	eag	0.992	0.256
CG110270	CG110270	1,768	0.174
CG11035	CG11035	1,766	0.013
CG11061	GM130	1,751	0.077
CG11071	mamo	1,915	0.058
CG11091	CG11091	3,235	0.141
CG11141	CG11141	2,231	0.114
CG1115	CG1115	1,106	0.145
CG11151	CG11151	1,306	0.157
CG11166	Eaf	1,156	0.184
CG11173	usnp	2,209	0.152
CG11183	Dcp1	1,717	0.008
CG11206	Liprin-gamma	1,958	0.002
CG11280	trn	1,898	0.076
CG11303	TM4SF	1,828	0.087
CG11314	Npc2g	1,612	0.113
CG11348	nAcRbeta-64B	1,600	0.012
CG11376	Zir	2,067	0.026
CG11409	CG11409	2,409	0.020
CG11423	CG11423	2,437	0.077
CG114731	CG114731	1,810	0.014
CG11474	CG11474	1,874	0.023
CG1148	Osi2	1,951	0.012
CG11488	mRpL10	1,932	0.020
CG11489	srpk79D	2,018	0.064
CG1149	MstProx	2,840	0.165
CG11522	RpL6	2,389	0.036
CG11585	CG11585	1,529	0.113
CG11692	CG11692	1,312	0.068
CG11765	Prx2540-2	1,810	0.042
CG11771	CG11771	1,516	0.117
CG11785	bai	1,597	0.066
CG11807	CG11807	2,748	0.159
CG11821	Cyp12a5	1,734	0.077
CG11837	CG11837	1,553	0.032
CG11893	CG11893	1,306	0.177
CG11901	Ef1gamma	1,912	0.017
CG11905	CG11905	3,067	0.257
CG12056	CG12056	1,711	0.060
CG12057	CG12057	1,227	0.222
CG12081	CG12081	1,993	0.027
CG12117	Sptr	1,910	0.057
CG12141	Aats-lys	1,683	0.141
CG12161	Prosbeta2R2	2,774	0.096
CG12220	mRpL32	3,055	0.488

CG12227	skpF	2,261	0.005
CG12231	CG12231	2,737	0.180
CG12263	CG12263	1,549	0.131
CG12284	th	1,799	0.089
CG1233	CG1233	1,873	0.040
CG12342	dgo	1,774	0.032
CG12348	Sh	2,342	0.087
CG12358	Paip2	2,284	0.087
CG12363	Dlc90F	1,581	0.047
CG12372	spt4	1,699	0.050
CG12384	CG12384	2,391	0.065
CG12391	CG12391	1,350	0.094
CG12403	Vha68-1	2,362	0.112
CG12418	CG12418	2,220	0.171
CG12420	CG12420	1,734	0.082
CG12661	CG12661	2,022	0.137
CG12691	CG12691	2,512	0.015
CG12729	CG12729	1,991	0.072
CG1274	Jafrac2	1,986	0.053
CG12768	CG12768	1,930	0.074
CG12796	CG12796	2,633	0.528
CG12817	CG12817	1,585	0.071
CG12846	Tsp42Ed	3,071	0.135
CG12853	CG12853	4,414	0.219
CG12854	CG42254	1,682	0.039
CG12860	CG12860	1,897	0.010
CG12861	CG12861	1,490	0.104
CG12883	CG12883	1,772	0.120
CG12896	CG12896	2,109	0.088
CG12905	Obp46a	2,805	0.106
CG12911	CG12911	1,676	0.001
CG12913	CG12913	1,401	0.144
CG13070	CG13070	2,183	0.076
CG13072	PDCD-5	1,937	0.242
CG13073	CG13073	1,280	0.178
CG13085	CG13085	1,481	0.061
CG13120	CG44152	1,583	0.094
CG13126	CG13126	1,437	0.093
CG13157	CG13157	1,391	0.161
CG13186	CG13186	1,543	0.040
CG13260	CG42389	1,841	0.051
CG13365	CG13365	1,416	0.115
CG13389	RpS13	1,993	0.016
CG13390	CG13390	2,107	0.125
CG13397	CG13397	1,797	0.064

CG13415	Cby	1,525	0.008
CG13420	CG42335	1,685	0.018
CG13625	CG13625	2,060	0.143
CG13631	CG13631	1,920	0.081
CG13634	CG13634	1,967	0.066
CG13720	CG13720	2,302	0.099
CG13758	Pdfr	1,883	0.178
CG13779	CG13779	1,586	0.046
CG13786	CG13786	1,619	0.141
CG13809	osm-1	1,847	0.137
CG13826	cnc	1,812	0.136
CG13843	CG13843	1,955	0.242
CG13869	CG13869	1,714	0.066
CG1387	CG1387	2,886	0.227
CG13880	mRpL17	1,299	0.229
CG13893	CG13893	1,897	0.147
CG13913	mwh	1,524	0.100
CG13939	Obp50e	2,028	0.142
CG13964	sick	2,112	0.128
CG13996	CG13996	1,596	0.133
CG14033	CR14033	1,208	0.193
CG1404	Ran	1,396	0.094
CG1412	RhoGAP19D	2,036	0.002
CG14122	CG14212	1,534	0.049
CG14129	CG34420	2,369	0.186
CG14186	CG14186	1,715	0.059
CG14223	CG14223	1,865	0.161
CG1429	Mef2	1,660	0.026
CG14296	endoA	2,099	0.109
CG14321	CG14321	1,090	0.161
CG14330	CG14330	1,679	0.121
CG14332	CG14332	2,011	0.001
CG14442	CG14442	2,134	0.081
CG14443	CG14443	1,675	0.020
CG14469	dpr12	1,942	0.106
CG14481	CG42561	1,507	0.130
CG14497	CG34386	1,607	0.135
CG14500	CG14500	1,557	0.057
CG14560	msopa	2,630	0.053
CG14646	CG14646	2,787	0.289
CG14647	CG14647	2,575	0.077
CG14680	Cyp12e1	2,203	0.165
CG14691	CG14691	2,064	0.087
CG14760	CG14760	1,730	0.126
CG14780	CG14780	1,737	0.094

CG14788	ns3	1,560	0.162
CG14895	Pak3	1,470	0.145
CG14904	Scp2	1,509	0.046
CG14905	CG14905	1,535	0.140
CG14910	CG42747	2,022	0.061
CG14960	CG14960	1,858	0.075
CG14989	CG14989	1,661	0.024
CG14997	CG14997	1,521	0.123
CG14999	RfC4	2,344	0.034
CG15004	Teh2	1,677	0.024
CG15020	CG15020	2,096	0.040
CG15067	CG15067	1,363	0.185
CG1507	Pur-alpha	1,401	0.154
CG15107	CG15107	1,413	0.048
CG15141	CG15141	1,604	0.022
CG15145	CG15145	1,639	0.020
CG15180	glob2	2,321	0.161
CG15191	e(y)2	1,078	0.237
CG15200	CG15200	1,432	0.091
CG15233	CG15233	1,830	0.059
CG15282	CG15282	2,650	0.014
CG15286	CG15286	1,344	0.275
CG15347	CG15347	2,463	0.170
CG1550	CG1550	2,502	0.033
CG15523	CG15523	1,676	0.113
CG15529	CG15529	1,899	0.007
CG15530	CG15530	1,849	0.036
CG15534	CG15534	1,574	0.069
CG15536	CG15536	1,728	0.126
CG15541	CG34433	1,762	0.028
CG15592	Osi9	1,805	0.009
CG15625	CG15625	2,382	0.144
CG15667	Sara	1,364	0.095
CG15676	FoxP	4,908	0.048
CG1569	rod	1,169	0.217
CG15697	RpS30	1,548	0.005
CG15747	CG15747	1,656	0.032
CG15785	CG42749	2,706	0.315
CG158488	CG158488	1,534	0.087
CG15881	CG15881	2,108	0.166
CG15893	CG15893	2,004	0.286
CG15899	Ca-alpha1T	2,012	0.104
CG1591	REG	1,639	0.212
CG15922	CG15922	2,218	0.223
CG1602	CG1602	1,591	0.066

CG16245	CG16245	1,540	0.004
CG1652	lectin-46Cb	2,136	0.084
CG16700	CG16700	1,452	0.036
CG16716	CG16716	1,187	0.128
CG16771	CG16771	2,268	0.164
CG16784	pr	1,934	0.141
CG16786	CG16786	1,777	0.090
CG16793	brv2	1,876	0.092
CG16812	CG16812	2,024	0.031
CG16827	ItgalphaPS4	5,261	603.331
CG16848	CG16848	1,668	0.220
CG16857	CG16857	1,646	0.152
CG16899	FoxP	2,864	629.312
CG16902	Hr4	1,720	0.107
CG16903	CG16903	1,661	0.023
CG16954	Hsp60D	2,717	0.091
CG16963	Cry	1,655	0.029
CG16964	CG16964	2,580	0.181
CG16974	CG16974	2,424	0.114
CG16987	daw	1,804	0.117
CG17024	CR17024	1,559	0.209
CG17029	CG17029	1,496	0.127
CG17045	yellow-e3	2,550	0.049
CG1707	CG1707	1,025	0.268
CG17108	CG17108	2,251	0.106
CG17136	Rbp1	2,442	0.281
CG172287	CG172287	2,010	0.058
CG17255	nocte	2,065	0.105
CG17267	CG17267	2,060	0.053
CG17283	CG17283	1,920	0.039
CG17290	CG17290	1,592	0.042
CG17295	Rcd4	1,622	0.093
CG17331	Prosbeta4	1,828	0.044
CG17332	VhaSFD	1,372	0.116
CG17349	CG17349	1,701	0.022
CG17404	CG17404	1,586	0.064
CG17514	CG17514	2,005	0.030
CG17515	Rab21	2,269	0.054
CG17523	GstE2	1,457	0.030
CG17525	GstE4	1,331	0.166
CG17544	CG17544	1,076	0.180
CG17569	gry	1,598	0.113
CG17611	eIF6	1,311	0.083
CG176973	CG176973	2,054	0.102
CG17738	CG17738	1,628	0.040

CG1774	CG1774	1,317	0.199
CG1775	Med	1,320	0.177
CG17777	CG17777	1,150	0.185
CG17781	CG17781	1,617	0.068
CG17795	mthl2	1,745	0.046
CG17834	CG17834	1,309	0.248
CG17870	14-3-3zeta	1,653	0.154
CG17922	CG17922	1,624	0.117
CG17928	CG17928	1,303	0.205
CG17952	LBR	1,312	0.140
CG17957	Sry-alpha	2,082	0.059
CG18081	CG18081	1,357	0.110
CG18088	CG18088	4,008	0.217
CG18108	IM1	3,387	0.187
CG18132	CG18132	2,160	0.166
CG18136	CG18136	2,243	0.076
CG18171	CG18171	1,618	0.030
CG18188	Damm	1,455	0.107
CG18193	CG18193	1,839	0.075
CG18212	alt	1,659	0.234
CG18231	CG18231	1,449	0.097
CG1827	CG1827	1,543	0.114
CG183433	CG183433	1,708	0.006
CG18368	CG18368	2,261	0.005
CG18420	CG18420	2,013	0.007
CG18468	Lhr	1,343	0.124
CG18497	spen	2,360	0.055
CG18539	CG18539	1,477	0.121
CG18555	CG44002	1,607	0.021
CG18581	CG18581	1,631	0.147
CG1862	Ephrin	4,281	0.324
CG18627	betaggt-II	1,418	0.089
CG18641	CG18641	1,353	0.084
CG1865	Spn43Ab	1,857	0.069
CG18660	Nckx30C	1,813	0.040
CG1867	Or98b	2,310	0.078
CG18809	CG18809	1,500	0.109
CG18817	Tsp42Ea	2,159	0.040
CG1916	Wnt2	1,309	0.085
CG19215	CG19215	1,763	0.051
CG1938	Dlic	1,914	0.028
CG2021	CG2021	1,833	0.134
CG20823	CG20823	2,384	0.038
CG2146	didum	1,393	0.107
CG2227	Gip	1,570	0.136

CG2252	fs(1)h	1,147	0.186
CG2469	CG2469	1,647	0.016
CG2533	CG2533	2,034	0.087
CG2701	CG2701	1,939	0.055
CG2715	Syx4	1,321	0.103
CG2720	Hop	2,055	0.107
CG2819	Pph13	1,581	0.095
CG2839	CG2839	1,242	0.111
CG2861	CG2861	1,495	0.090
CG2924	CG2924	1,648	0.115
CG2947	HIP-R	2,757	0.150
CG2952	proPO59	1,668	0.133
CG2958	lectin-24Db	1,391	0.073
CG2986	RpS21	1,316	0.174
CG3001	Hex-A	1,795	0.048
CG30011	gem	2,101	0.059
CG30015	CG30015	1,744	0.070
CG30021	metro	1,766	0.030
CG30035	Tret1-1	1,502	0.088
CG30094	CG30094	2,465	0.088
CG30100	CG30100	2,594	0.040
CG30125	Ir56a	1,466	0.096
CG30142	Obp57b	1,648	0.232
CG30151	CG30151	1,410	0.184
CG30171	Unc-89	1,354	0.073
CG30291	CG30291	1,775	0.181
CG30376	CG30376	1,723	0.073
CG30395	CG30395	1,523	0.004
CG30430	CG30430	1,399	0.105
CG30440	CG30440	1,507	0.115
CG3081	CG3081	2,090	0.048
CG31038	CG31038	1,437	0.086
CG31057	tau	18,793	0.017
CG31060	Gr98c	1,840	0.039
CG31136	Syx1A	2,491	0.179
CG31141	CG31141	2,332	0.101
CG31145	CG31145	1,520	0.038
CG31183	CG31183	3,520	0.156
CG31198	CG31198	1,700	0.188
CG3126	C3G	1,794	677.232
CG31347	CG31347	2,079	0.068
CG31550	CG31550	1,937	0.070
CG31595	CG31595	2,016	0.057
CG31637	CG31637	1,895	0.148
CG31663	CG31663	1,473	0.148

CG31665	wry	2,189	0.080
CG31708	CG31708	1,451	0.119
CG3174	Fmo-2	1,913	0.043
CG31764	vir-1	2,865	0.079
CG31769	CG31769	2,005	0.099
CG31779	Acp24A4	1,769	0.193
CG31828	CG31828	2,266	0.062
CG31898	CG31898	2,326	0.120
CG31922	CG31922	1,290	0.180
CG31955	CG31955	2,483	0.116
CG319907	CG319907	2,056	0.115
CG32031	Argk	1,920	0.133
CG32042	PGRP-LA	4,003	0.076
CG32114	CG32114	2,342	0.159
CG32208	825-Oak	1,751	0.150
CG32217	Su(Tpl)	2,559	0.036
CG32264	CG32264	2,732	0.112
CG32278	CG32278	2,367	0.032
CG32280	CG32280	1,609	0.111
CG32282	Drsl4	2,025	0.017
CG32353	CG43078	2,524	0.100
CG32368	CG32368	1,438	0.200
CG32394	dikar	2,362	0.071
CG32401	Or65a	1,660	0.006
CG3242	sob	1,975	0.131
CG32435	chb	2,421	0.046
CG3244	Clect27	1,528	0.136
CG32453	CG32453	1,644	0.061
CG32483	CG32483	1,645	0.135
CG32487	CG32487	2,088	0.147
CG325295	CG325295	1,567	0.074
CG32543	CG42450	1,913	0.068
CG32551	CG32551	2,419	0.079
CG32556	chas	2,003	0.062
CG3259	CG3259	1,410	0.038
CG32614	CG32614	1,895	0.126
CG32642	CG32642	1,997	0.064
CG32666	Drak	1,966	0.060
CG32668	CG32668	2,617	0.069
CG32682	alpha-Man-I	2,595	0.165
CG32695	CG32695	1,984	0.065
CG3274	Bap170	1,628	0.001
CG32755	CG32755	2,053	0.018
CG3277	CG3277	2,287	0.007
CG3281	CG3281	1,633	0.003

CG32835	CR32835	2,150	0.080
CG3285	CG3285	1,853	0.039
CG32852	Csk	1,794	0.095
CG32859	eIF4E-7	1,702	0.117
CG3295	CG3295	2,172	0.029
CG3299	Vinc	2,044	0.073
CG33057	CG33057	1,458	0.212
CG33083	Gr97a	1,496	0.120
CG33110	CG33110	1,546	0.112
CG331262	CG331262	1,627	0.038
CG331290	CG331290	2,267	0.222
CG332170	CG332170	1,877	0.024
CG3322	LanB2	1,881	0.081
CG33298	CG33298	1,476	0.050
CG33482	CG42685	2,898	0.423
CG3351	mRpL11	1,790	0.026
CG34970	CG34970	1,725	0.029
CG3527	CG3527	1,924	0.195
CG3542	CG3542	1,926	0.173
CG3589	CG3589	1,130	0.180
CG3631	CG3631	1,442	0.087
CG3665	Fas2	1,770	0.120
CG3675	Art2	1,376	0.055
CG3705	aay	1,974	0.010
CG3717	bcn92	2,057	0.025
CG3723	Dhc93AB	1,595	0.011
CG3776	CG3776	1,769	0.008
CG3788	CG3788	2,107	0.016
CG3796	ac	1,618	0.008
CG3849	Lasp	1,515	0.139
CG3853	Glut3	1,940	0.071
CG3871	Six4	2,130	0.105
CG3896	Nox	1,451	0.089
CG3906	CG3906	1,732	0.118
CG3924	Chi	1,594	0.036
CG3945	Rad9	1,483	0.084
CG3949	hoip	1,359	0.091
CG3955	CG3955	1,126	0.206
CG3967	CG3967	1,608	0.099
CG3991	TppII	1,633	0.062
CG3994	ZnT35C	1,901	0.001
CG4004	CG4004	2,588	0.368
CG40049	mRpS5	1,332	0.142
CG4006	Akt1	1,409	0.119
CG4012	gek	1,568	0.344

CG40128	CG40128	2,206	0.158
CG40221	CG40221	1,500	0.047
CG40244	CG40244	2,121	0.084
CG404522	CG404522	2,005	0.095
CG4046	RpS16	1,772	0.005
CG4054	Fili	2,190	0.032
CG4064	CG42699	1,705	0.005
CG4090	Mur89F	1,719	0.150
CG41050	CG41050	1,484	0.098
CG41074	CG41074	1,881	0.104
CG41123	CG41123	1,724	0.005
CG4162	lace	1,356	0.134
CG4184	MED15	1,705	0.150
CG4185	NC2beta	3,231	0.317
CG4212	Rab14	4,027	0.326
CG4216	term	1,628	0.053
CG4249	c(2)M	1,492	0.064
CG42571	CG42571	1,819	0.028
CG4261	Hel89B	1,556	0.006
CG4264	Hsc70-4	2,338	0.099
CG4265	Uch	2,054	0.081
CG4270	CG4270	1,948	0.036
CG4287	CG4287	2,203	0.091
CG4302	CG4302	2,297	0.005
CG4313	CG4313	1,858	0.028
CG4318	CG4318	1,424	0.047
CG4326	mRpS17	2,025	0.078
CG4341	CG4341	1,312	0.092
CG4349	Fer3HCH	1,663	0.052
CG4406	CG4406	1,799	0.210
CG4428	Atg4	1,661	0.119
CG4447	CG4447	1,644	0.051
CG4455	CG4455	2,068	0.031
CG4471	Tsp42Ep	1,618	0.077
CG4481	GluRIB	1,798	0.031
CG4497	CG4497	1,847	0.034
CG4510	Surf6	2,018	0.087
CG4542	CG4542	2,103	0.082
CG4560	Arpc3A	1,479	0.101
CG4577	CG4577	1,817	0.053
CG4610	CG4610	3,243	0.139
CG4661	CG4661	1,689	0.068
CG4680	Grp	1,867	0.012
CG4716	CG4716	1,866	0.051
CG4720	Pk92B	2,053	0.154

CG4785	CG4785	1,807	0.084
CG4797	CG4797	2,201	0.172
CG4802	CG4802	1,757	0.069
CG4821	Tequila	1,630	0.011
CG4863	RpL3	1,410	0.124
CG4869	betaTub97EF	1,788	0.195
CG4891	CG4891	1,448	0.057
CG4938	Aats-ser	2,200	0.055
CG4952	dac	2,190	0.009
CG4994	Mpcp	2,223	0.091
CG4996	CG4996	1,910	0.047
CG5005	HLH54F	1,634	0.050
CG5057	MED10	1,858	0.114
CG5059	CG5059	1,589	0.130
CG5070	CG5070	2,049	0.020
CG5081	Syx7	1,221	0.150
CG5092	Tor	2,228	0.017
CG5103	CG5103	2,057	0.006
CG5161	l(3)72Dh	1,248	0.133
CG5169	GckIII	1,612	0.050
CG5171	CG5171	1,803	0.143
CG5178	Act88F	1,772	0.050
CG5186	slim	2,041	0.017
CG5191	CG5191	1,644	0.140
CG5201	Dad	1,842	0.140
CG5242	mRpL40	2,044	0.041
CG5252	Ranbp9	1,897	0.064
CG5261	CG5261	1,786	0.055
CG5300	Klp31E	2,813	0.089
CG5346	CG5346	1,887	0.030
CG5370	Dcp-1	2,568	0.144
CG5385	CG5385	2,315	0.061
CG5399	CG5399	1,575	0.150
CG5407	Sur-8	2,038	0.185
CG5473	SP2637	1,705	0.168
CG5501	Myo95E	1,716	0.191
CG5505	scny	1,650	0.072
CG5506	CG5506	1,780	0.073
CG5517	Ide	1,535	0.131
CG55183	CG55183	1,650	0.043
CG5541	CG5541	1,341	0.106
CG5577	CG5577	1,286	0.111
CG5596	Mlc1	1,941	0.079
CG5625	Vps35	1,804	0.018
CG5654	yps	1,693	0.121

CG5670	Atpalpha	1,827	0.135
CG5675	X11L	1,975	0.117
CG5676	CG5676	2,256	0.183
CG5686	chico	2,035	0.039
CG5695	jar	1,598	0.055
CG5714	ecd	2,102	0.042
CG5727	CG5727	2,585	0.140
CG5735	orb2	1,876	0.091
CG5738	lolal	1,550	0.093
CG5741	orb2	1,559	0.043
CG5742	CG5742	1,955	0.058
CG5744	Frq1	1,678	0.113
CG5778	CG5778	2,317	0.144
CG5793	CG5793	1,539	0.146
CG5809	CaBP1	1,424	0.068
CG5835	CG5835	1,519	0.122
CG5848	cact	1,635	0.069
CG5869	CG5869	2,346	0.125
CG5874	Nelf-A	2,300	0.029
CG5886	CG5886	1,341	0.133
CG5915	Rab7	1,941	0.226
CG5969	CG5969	1,458	0.042
CG6004	Muc68D	2,244	0.154
CG6015	CG6015	1,473	0.067
CG6022	Cchl	1,651	0.118
CG6024	CG6024	1,849	0.054
CG6026	CG6026	1,421	0.083
CG6139	Vmat	1,265	0.174
CG6143	Pep	1,919	0.050
CG6185	Ir68a	1,387	0.196
CG6208	CG6208	1,754	0.043
CG6211	gce	1,053	0.260
CG6214	MRP	1,716	0.176
CG6315	fl(2)d	1,689	0.033
CG6329	CG6329	1,863	0.036
CG6332	CG6332	1,467	0.159
CG6347	CG6347	1,285	0.075
CG6354	Rb97D	1,689	0.155
CG6362	CG6362	1,803	0.276
CG6382	Elf	2,129	0.005
CG6395	Csp	1,675	0.077
CG6407	Wnt5	1,667	0.050
CG6418	CG6418	2,630	0.155
CG6425	CG6425	1,817	0.039
CG6431	CG6431	2,432	0.089

CG6447	TwdlL	2,064	0.055
CG6455	CG6455	1,670	0.029
CG6477	RhoGAP54D	1,391	0.089
CG6480	CG6480	1,343	0.088
CG6483	Jon65Aiii	1,718	0.041
CG6488	CG6488	2,384	0.149
CG6492	Ucp4A	1,588	0.103
CG6541	Mst33A	1,501	0.092
CG6625	Snap	1,283	0.231
CG6642	a10	1,717	0.088
CG6646	DJ-1alpha	2,083	0.090
CG6673	GstO2	1,375	0.142
CG6700	CG6700	1,938	0.007
CG6720	UbcD2	1,794	0.099
CG6721	RasGAP1	1,892	0.049
CG6757	SH3PX1	1,571	0.049
CG6768	DNApol-epsilon	2,641	0.037
CG6769	CG6769	1,999	0.081
CG6778	Aats-gly	3,046	0.132
CG6793	CG6793	1,914	0.006
CG6817	foi	1,558	0.007
CG6834	CG6834	2,229	0.068
CG6846	RpL26	1,397	0.113
CG6878	CG6878	1,566	0.059
CG6883	trh	1,482	0.062
CG6889	tara	1,513	0.040
CG6900	CR6900	2,109	0.109
CG6912	CG6912	1,674	0.083
CG6985	CG6985	1,402	0.226
CG7011	CG7011	1,777	0.115
CG7051	Dic61B	1,630	0.206
CG7075	Ntl	1,731	0.096
CG7091	CG7091	1,719	0.046
CG7098	dik	2,028	0.072
CG71295	CG71295	1,726	0.029
CG7188	BI-1	1,659	0.083
CG7189	Gr66a	1,569	0.042
CG7206	CG7206	1,888	0.074
CG7228	pes	2,220	0.065
CG7236	CG7236	1,688	0.024
CG7245	eys	1,408	0.106
CG7269	Hel25E	2,737	0.207
CG7293	Klp68D	1,371	0.163
CG7313	CheA75a	1,470	0.181
CG73255	CG73255	1,561	0.118

CG7333	CG7333	1,488	0.101
CG7407	CG7407	1,562	0.110
CG7408	CG7408	1,435	0.113
CG7519	CG7519	1,942	0.121
CG7523	CG7523	1,741	0.066
CG7532	l(2)34Fc	1,927	0.035
CG7548	CG7548	2,103	0.084
CG7557	CG7557	2,024	0.077
CG7565	CG7565	1,842	0.057
CG7570	hale	2,720	0.132
CG7582	CG7582	1,556	0.084
CG7604	Eig71Ee	2,437	0.115
CG7619	Rpn10	1,783	0.009
CG7628	CG42575	2,082	0.044
CG7638	CG7638	1,819	0.198
CG7653	CG7653	1,954	0.140
CG7668	CG7668	2,513	0.094
CG7772	CG7772	1,985	0.055
CG7787	CG7787	1,562	0.005
CG7825	Rad17	2,798	0.328
CG7851	Scgalpha	1,853	0.051
CG7876	Muc18B	1,452	0.098
CG7893	Vav	1,930	0.089
CG7902	bap	2,193	0.090
CG7912	CG7912	1,360	0.087
CG7937	C15	1,842	0.027
CG7972	mus301	1,431	0.034
CG7989	wcd	2,458	0.302
CG7990	CG7990	2,086	0.053
CG8023	eIF4E-3	1,424	0.156
CG8044	HP4	1,793	0.084
CG8049	Btk29A	1,979	0.058
CG8058	Hydr1	1,512	0.025
CG8063	yellow-f2	2,239	0.100
CG8067	CG8067	1,474	0.070
CG8119	CG8119	3,497	0.057
CG8128	CG8128	1,878	0.003
CG8176	CG8176	3,227	0.005
CG8186	Vha36-1	1,696	0.006
CG8198	l(1)G0136	1,781	0.137
CG8210	Vha14-1	1,485	0.074
CG8222	Pvr	1,902	0.054
CG8226	Tom7	1,897	0.098
CG8256	Gpo-1	1,679	0.085
CG8268	Srp9	1,421	0.063

CG8280	Ef1alpha48D	2,662	0.089
CG8282	Snx6	1,653	0.087
CG8287	Rab8	2,096	0.025
CG8322	ATPCL	1,425	0.109
CG8417	CG8417	2,410	0.156
CG8426	l(2)NC136	2,299	0.068
CG8441	CG8441	3,024	0.442
CG8443	clu	2,127	0.159
CG8448	mrj	1,718	0.096
CG8472	Cam	1,774	0.089
CG8481	CG8481	1,754	0.091
CG8511	Cpr49Ag	1,797	0.016
CG8523	Mdr50	1,625	0.017
CG8526	CG8526	1,663	0.012
CG8534	CG8534	1,412	0.152
CG8553	SelD	1,985	0.031
CG8562	CG8562	1,595	0.067
CG8568	CG8568	2,348	0.152
CG8589	tej	1,806	0.109
CG8591	CTCF	2,167	0.053
CG8622	Acp53Ea	2,562	0.032
CG8669	crc	1,568	0.024
CG8681	clumsy	2,155	0.069
CG8725	CSN4	1,612	0.049
CG8734	beta3GalTII	1,472	0.150
CG8772	CG42708	1,520	0.009
CG8877	Prp8	1,420	0.150
CG8884	Sap47	1,800	0.053
CG8885	Scox	2,284	0.016
CG8922	RpS5a	1,987	0.005
CG8924	CG8924	1,875	0.012
CG8927	CG8927	2,083	0.094
CG8928	Rrp47	2,306	0.028
CG89295	CG89295	1,535	0.018
CG8967	otk	1,814	0.064
CG8974	CG8974	2,050	0.010
CG8975	RnrS	1,476	0.102
CG9004	CG9004	1,391	0.130
CG90093	CG90093	1,864	0.116
CG9014	CG9014	1,961	0.021
CG9044	CG9044	1,469	0.023
CG9072	CG9072	1,533	0.217
CG9080	Listericin	1,580	0.046
CG9096	CycD	1,546	0.033
CG9128	Sac1	2,074	0.115

CG9138	uif	2,629	0.043
CG9198	shtd	1,865	0.118
CG9222	CG9222	2,126	0.073
CG9231	CG9231	2,188	0.132
CG9238	CG9238	1,498	0.070
CG9263	CG9263	1,735	0.114
CG9286	CG9286	1,615	0.017
CG9294	CG9294	1,555	0.062
CG9307	Cht5	1,187	0.197
CG9316	CG9316	1,687	0.085
CG9333	Oseg5	1,657	0.096
CG9345	Adgf-C	1,856	0.082
CG9350	CG9350	1,146	0.135
CG9354	RpL34b	1,710	0.068
CG9364	Treh	1,791	0.102
CG9375	Ras85D	2,184	0.145
CG9391	CG9391	1,953	0.117
CG9412	rin	1,739	0.114
CG9438	Cyp6a2	2,467	0.227
CG9441	Pu	1,624	0.102
CG9473	MED6	1,422	0.176
CG9528	retm	1,676	0.192
CG9533	rut	1,780	0.054
CG9539	Sec61alpha	1,633	0.135
CG9554	eya	2,972	0.071
CG9581	CG9581	1,796	0.044
CG9582	CG9582	1,248	0.189
CG9589	CG9589	1,700	0.035
CG9610	Poxm	1,299	0.084
CG9632	CG9632	2,341	0.113
CG9640	CG9640	1,642	0.094
CG9673	CG9673	1,194	0.144
CG9676	CG9676	1,946	0.087
CG9688	mRpS18C	1,319	0.158
CG9717	CG9717	1,382	0.119
CG97390	CG97390	2,838	0.189
CG9745	D1	1,409	0.159
CG9746	ird1	0.907	0.364
CG9761	Nep2	1,305	0.146
CG9774	rok	1,335	0.064
CG9837	CG9837	1,638	0.157
CG9843	CG9843	1,960	0.008
CG9862	Rae1	1,539	0.064
CG9863	CG9863	1,677	0.068
CG9882	Art7	1,742	0.053

CG9935	CG9935	3,267	0.327
CG9970	CG9970	2,093	0.155
CG9986	CG9986	1,707	0.038
CG9989	CG9989	3,012	0.266
CG6308	CG6308	3,249	0.132

Table A3 List of downregulated genes upon rotenone treatment

id	Symbol	Mean	SEM
CG10035	CG10035	0.427	0.222
CG10361	CG10361	0.450	0.118
CG10513	CG10513	0.269	0.103
CG10516	CG10516	0.449	0.100
CG10535	Elp1	0.259	0.099
CG10536	cbx	0.677	0.157
CG105399	CG105399	0.400	0.008
CG10706	SK	0.553	0.009
CG10749	CG10749	0.075	0.140
CG10814	CG10814	0.589	0.099
CG10858	CG10858	0.092	0.139
CG10868	orb	0.232	0.118
CG10897	tou	0.115	0.041
CG11159	CG11159	0.672	0.084
CG11181	cup	0.427	0.193
CG11207	feo	0.749	0.130
CG11242	TBCB	0.746	0.111
CG11266	CG11266	0.670	0.143
CG11282	caps	0.410	0.106
CG11317	CG11317	0.632	0.061
CG11320	CG11320	0.697	0.094
CG11330	cort	0.484	0.070
CG11378	CG11378	0.472	0.675
CG11379	CG11379	0.396	0.036
CG11391	CG11391	0.612	0.275
CG11438	CG11438	0.537	0.099
CG11577	CG11577	0.276	0.001
CG11601	CG11601	0.126	0.129
CG11793	Sod	0.835	0.145
CG11798	chn	0.325	0.177
CG11912	CG11912	0.635	0.005
CG11963	skap	0.635	0.048
CG11968	RagA-B	0.572	0.053
CG12025	CG12025	0.601	0.030
CG121426	CG121426	0.508	0.056
CG12159	CG12159	0.758	0.104
CG12256	CG12256	0.524	0.074
CG12367	Hen1	0.428	0.009
CG12379	CG12379	0.449	0.054
CG12424	ckn	0.375	0.171
CG12436	CG43373	0.531	0.035

CG12492	CG34355	0.500	0.084
CG12519	CG12519	0.336	0.097
CG125761	CG125761	0.661	0.139
CG12656	CG12656	0.071	0.109
CG12701	vfl	0.326	0.111
CG12728	CG12728	0.099	0.267
CG12821	CG12821	0.641	0.092
CG12822	CG12822	0.314	0.211
CG12840	Tsp42El	0.521	0.032
CG12923	CG12923	0.179	0.044
CG12993	p-cup	0.076	0.161
CG13102	CG13102	0.557	0.060
CG13111	Shawl	0.645	0.084
CG13290	CG33993	0.808	0.177
CG13320	Sans	0.479	0.085
CG13391	Aats-ala	0.333	0.191
CG13417	Gr93a	0.065	0.113
CG13645	Nmnat	0.754	0.083
CG13705	CG13705	0.470	0.201
CG13868	CG13868	0.502	0.061
CG13924	CG13924	0.118	0.097
CG13936	CG13936	0.175	0.141
CG13980	CG42534	0.062	0.134
CG14014	CG14014	0.040	0.211
CG1402	CG1402	0.124	0.236
CG14032	Cyp4ac1	0.178	0.141
CG14070	CG14070	0.365	0.110
CG14096	CG14096	0.037	0.190
CG14182	CG14182	0.425	0.151
CG14191	CG14191	0.232	0.117
CG14298	CG14298	0.706	0.095
CG14380	CG14380	0.318	0.385
CG14401	CG14401	0.554	0.027
CG14532	CG14532	0.482	0.053
CG1455	CanA1	0.823	0.139
CG14614	CG14614	0.502	0.002
CG1462	Aph-4	0.544	0.082
CG14792	sta	0.433	0.250
CG14841	CG14841	0.119	0.159
CG1487	krz	0.773	0.267
CG14957	CG14957	0.345	0.241
CG14995	CG14995	0.099	0.061
CG15088	List	0.129	0.032
CG15202	CG15202	0.352	0.120

CG15203	CG15203	0.845	0.202
CG15280	CR15280	0.512	0.197
CG1529	CG1529	0.277	0.070
CG15479	CG15479	0.202	0.155
CG15483	CG15483	0.340	0.036
CG15727	Aven	0.666	0.163
CG15749	dmrt11E	0.609	0.023
CG1629	yellow-h	0.540	0.032
CG1637	CG1637	0.545	0.041
CG16705	SPE	0.501	0.018
CG16740	Rh2	0.608	0.167
CG16894	CG16894	0.145	0.185
CG16979	CG16979	0.818	0.159
CG16983	skpA	0.133	0.068
CG17010	CG17010	0.852	0.193
CG17034	CG42321	0.533	0.075
CG1710	Hcf	0.020	0.774
CG17107	CG17107	0.737	0.167
CG17146	Adk1	0.678	0.096
CG17148	Est-P	0.064	0.187
CG17187	CG17187	0.493	0.015
CG17200	Ugt86Dg	0.172	0.077
CG17208	Gfrl	0.117	0.088
CG17224	CG17224	0.541	0.134
CG17361	CG17361	0.610	0.014
CG17436	vtd	0.470	0.105
CG17601	CG17601	0.444	0.022
CG17726	CG17726	0.451	0.124
CG17746	CG17746	0.381	0.061
CG17785	Golgin84	0.041	0.104
CG17816	CG17816	0.583	0.021
CG17820	fit	0.384	0.249
CG17829	CG17829	0.404	0.139
CG17883	CG17883	0.501	0.199
CG17919	CG17919	0.374	0.136
CG17921	HmgZ	0.549	0.058
CG17935	Mst84Dd	0.519	0.024
CG17944	CG17944	0.303	0.069
CG18094	CG18094	0.609	0.090
CG18112	Vps16B	0.521	0.182
CG18144	Hand	0.701	0.108
CG18178	CG18178	0.403	0.065
CG18271	slx1	0.122	0.268
CG18348	Cpr67Fb	0.734	0.156

CG18416	CG18416	0.510	0.251
CG1851	Ady43A	0.412	0.057
CG18536	CG18536	0.339	0.031
CG18557	CG18557	0.606	0.147
CG18619	CG18619	0.273	0.081
CG18676	Teh3	0.208	0.009
CG18678	CG43795	0.629	0.196
CG18743	Hsp70Ab	0.768	0.166
CG187699	CG187699	0.675	0.108
CG1912	Gycalpha99B	0.421	0.095
CG2009	bip2	0.674	0.036
CG2038	CSN7	0.696	0.050
CG2102	cas	0.376	0.227
CG2165	PMCA	0.613	0.000
CG2221	l(1)G0289	0.767	0.090
CG2229	Jon99Fii	0.814	0.107
CG2249	CoVIIc	0.673	0.080
CG2262	Smox	0.545	0.035
CG2297	Obp44a	0.824	0.166
CG2316	CG2316	0.615	0.018
CG2621	sgg	0.665	0.229
CG26372	CG26372	0.301	0.031
CG2684	lds	0.339	0.010
CG2746	RpL19	0.470	0.042
CG27742	CG27742	0.235	0.007
CG2808	CG34340	0.504	0.163
CG2890	PPP4R2r	0.354	0.096
CG2998	RpS28b	0.751	0.238
CG30028	gammaTry	0.934	0.238
CG30051	CG30051	0.638	0.214
CG30071	CG30071	0.187	0.013
CG3011	CG3011	0.207	0.005
CG30160	CG30160	0.756	0.142
CG30192	CG30192	0.278	0.240
CG3027	pyd3	0.866	0.152
CG30286	CG30286	0.454	0.094
CG3029	or	0.407	0.159
CG30322	Sema-2b	0.401	0.008
CG30353	CG30353	0.042	0.142
CG30381	CG30381	0.570	0.036
CG30428	CG30428	0.550	0.008
CG30473	Obp51a	0.053	0.341
CG3064	futsch	0.340	0.102
CG3069	Taf10b	0.087	0.336

CG3083	Prx6005	0.547	0.008
CG31013	CG31013	0.323	0.038
CG31032	CR31032	0.333	0.114
CG3107	CG3107	0.104	0.081
CG31161	CG31161	0.491	0.023
CG31196	14-3-3epsilon	0.272	0.001
CG31202	CG31202	0.341	0.122
CG31308	CG31308	0.545	0.072
CG31314	Meltrin	0.146	0.147
CG31348	Octbeta3R	0.621	0.023
CG31364	l(3)neo38	0.534	0.160
CG31389	CG31389	0.079	0.009
CG31484	CG31484	0.699	0.138
CG31526	CG31526	0.216	0.275
CG31542	CG31542	0.827	0.132
CG31546	CG31546	0.524	0.208
CG31605	Bsg	0.327	0.161
CG31620	Gr39b	0.077	0.170
CG31626	CG31626	0.090	0.146
CG31798	CG31798	0.401	0.112
CG31937	CG31937	0.571	0.088
CG32013	CG32013	0.517	0.165
CG32044	CG42268	0.112	0.277
CG32083	CG32083	0.292	0.062
CG32250	CG32250	0.203	0.101
CG32444	CG32444	0.308	0.081
CG32532	CG32532	0.699	0.074
CG32568	CG32568	0.070	0.084
CG32582	CG32582	0.431	0.292
CG32633	CG32633	0.387	0.124
CG32662	CG43154	0.691	0.102
CG3267	CG3267	0.083	0.272
CG3288	CG3288	0.491	0.043
CG32954	Adhr	0.491	0.072
CG32956	Chrac-14	0.589	0.046
CG33007	Ack-like	0.387	0.122
CG3301	CG3301	0.547	0.085
CG33044	CG33044	0.383	0.082
CG330452	CG330452	0.623	0.130
CG331167	CG331167	0.131	0.149
CG33151	Gr59e	0.473	0.123
CG33169	CG33169	0.446	0.102
CG3318	Dat	0.579	0.051
CG33204	Doa	0.741	0.205

CG33255	CG33255	0.628	0.094
CG33276	CG33276	0.440	0.182
CG33486	asparagine-synthetase	0.830	0.158
CG3523	CG3523	0.392	0.266
CG3605	CG3605	0.392	0.071
CG3613	qkr58E-1	0.503	0.073
CG3624	babos	0.351	0.050
CG3772	cry	0.457	0.016
CG3773	CG3773	0.460	0.078
CG3805	CG34126	0.340	0.206
CG3812	CG3812	0.211	0.051
CG3948	zetaCOP	0.796	0.165
CG39540	CG39540	0.740	0.084
CG40002	CG40002	0.528	0.100
CG40182	CR40182	0.459	0.113
CG40274	CG40274	0.601	0.114
CG4103	l(2)35Bc	0.588	0.036
CG4180	l(2)35Bg	0.357	0.089
CG4214	Syx5	0.478	0.208
CG4291	CG4291	0.519	0.055
CG4293	CG4293	0.484	0.089
CG4306	CG4306	0.253	0.049
CG4457	Srp19	0.595	0.053
CG4482	mol	0.624	0.048
CG4648	CG42399	0.472	0.106
CG4669	CG4669	0.276	0.022
CG4699	wah	0.096	0.147
CG4804	Spn31A	0.688	0.095
CG4921	Rab4	0.531	0.038
CG5079	CG5079	0.226	0.218
CG5084	CG5084	0.568	0.012
CG5085	Sirt2	0.413	0.039
CG5108	mRpS7	0.793	0.118
CG5168	CG5168	0.619	0.027
CG5185	Tom	0.434	0.083
CG52270	CG52270	0.092	0.077
CG5262	CG5262	0.230	0.238
CG5315	CG5315	0.462	0.200
CG5327	CG5327	0.303	0.020
CG5334	CG5334	0.260	0.021
CG5390	CG5390	0.365	0.226
CG5428	St1	0.325	0.036
CG5435	CG5435	0.233	0.163
CG5476	TwdlN	0.047	0.260

CG5494	Cpr92F	0.565	0.028
CG5618	CG5618	0.317	0.229
CG5652	drd	0.230	0.058
CG5922	Ir40a	0.402	0.095
CG5954	l(3)mbt	0.867	0.179
CG5970	cbc	0.521	0.039
CG5994	Nelf-E	0.770	0.092
CG6038	crim	0.568	0.037
CG6042	Cyp12a4	0.547	0.066
CG6094	CG6094	0.684	0.066
CG6181	Ge-1	0.792	0.163
CG62248	CG62248	0.497	0.010
CG6289	Spn77Bc	0.680	0.110
CG6340	CG6340	0.164	0.016
CG6375	pit	1,264	0.501
CG6415	CG6415	0.514	0.293
CG6416	Zasp66	0.563	0.021
CG6449	NijA	0.842	0.167
CG6459	P32	0.515	0.084
CG6463	CG6463	0.255	0.195
CG6475	CG6475	0.609	0.242
CG6545	lbe	0.229	0.283
CG6549	fws	0.656	0.008
CG6579	atilla	0.569	0.100
CG6620	ial	0.034	0.538
CG6634	mid	0.248	0.128
CG6661	CG6661	0.750	0.282
CG6709	CG6709	0.387	0.021
CG6724	CG6724	0.661	0.234
CG6733	CG6733	0.710	0.230
CG6766	CG6766	0.431	0.091
CG6775	rg	0.494	0.204
CG6813	CG6813	0.451	0.004
CG6874	HipHop	0.447	0.042
CG6891	CG6891	0.084	0.187
CG6932	CSN6	0.468	0.099
CG70188	CG70188	0.678	0.245
CG7074	mio	0.543	0.124
CG7105	Proct	0.327	0.024
CG7112	GAPcenA	0.634	0.016
CG7118	Jon66Ci	0.708	0.281
CG7130	CG7130	0.793	0.203
CG7158	CG7158	0.660	0.111
CG7227	CG7227	0.454	0.100

CG7260	byn	0.593	0.013
CG7324	CG7324	0.578	0.115
CG7382	CG7382	0.774	0.115
CG7429	CG7429	0.696	0.166
CG7595	ck	1,257	0.324
CG7704	Taf5	0.876	0.173
CG7749	kug	0.694	0.169
CG7779	Cng	0.710	0.135
CG7781	CG7781	0.636	0.042
CG7791	CG7791	0.255	0.128
CG8042	CG8042	0.635	0.124
CG8053	eIF-1A	0.641	0.068
CG8062	out	0.545	0.009
CG8190	eIF2B-gamma	0.726	0.227
CG8195	CG8195	0.711	0.078
CG8254	exex	0.136	0.087
CG8300	CG8300	0.521	0.048
CG8311	CG8311	0.395	0.109
CG8320	CG8320	0.665	0.100
CG8328	E(spl)mdelta-HLH	0.230	0.196
CG8333	E(spl)mgamma-HLH	0.293	0.300
CG8404	Sox15	0.349	0.048
CG8431	Aats-cys	0.614	0.010
CG8476	CG8476	0.740	0.170
CG8627	Dbi	0.427	0.000
CG8760	dysc	0.455	0.023
CG8806	prel	0.620	0.014
CG8977	Cctgamma	0.548	0.005
CG8979	Pl31	0.678	0.151
CG9000	ste24a	0.722	0.080
CG9033	Tsp47F	0.082	0.192
CG9093	Tsp26A	0.937	0.186
CG9106	CG9106	0.455	0.002
CG9186	CG9186	0.105	0.020
CG9335	CG9335	0.493	0.036
CG9372	CG9372	0.373	0.082
CG9373	rump	0.446	0.110
CG9386	CG9386	0.306	0.043
CG9426	CG9426	0.708	0.088
CG9427	CG9427	0.647	0.122
CG9449	CG9449	0.578	0.044
CG9456	Spn42Dd	0.561	0.048
CG9590	CG9590	0.617	0.003
CG9669	CG9669	0.974	0.188

CG9677	Int6	0.301	0.128
CG9682	CG9682	0.536	0.058
CG9684	CG9684	0.913	0.169
CG9790	Cks85A	0.782	0.094
CG9804	CG9804	0.347	0.108
CG9822	CG9822	0.520	0.057
CG9850	CG9850	0.563	0.036
CG9999	RanGAP	0.601	0.030